Measurement of inclusive and differential cross sections in the $H \to ZZ^* \to 4\ell$ decay channel in pp collisions at $\sqrt{s} = 13$ TeV with the ATLAS detector

JHEP10(2017)132

The ATLAS collaboration

E-mail: atlas.publications@cern.ch

ABSTRACT: Inclusive and differential fiducial cross sections of Higgs boson production in proton-proton collisions are measured in the $H \to ZZ^* \to 4\ell$ decay channel. The proton-proton collision data were produced at the Large Hadron Collider at a centre-of-mass energy of 13 TeV and recorded by the ATLAS detector in 2015 and 2016, corresponding to an integrated luminosity of 36.1 fb^{-1}. The inclusive fiducial cross section in the $H \to ZZ^* \to 4\ell$ decay channel is measured to be 3.62 ± 0.50 (stat) $^{+0.25}_{-0.20}$ (sys) fb, in agreement with the Standard Model prediction of 2.91 ± 0.13 fb. The cross section is also extrapolated to the total phase space including all Standard Model Higgs boson decays. Several differential fiducial cross sections are measured for observables sensitive to the Higgs boson production and decay, including kinematic distributions of jets produced in association with the Higgs boson. Good agreement is found between data and Standard Model predictions. The results are used to put constraints on anomalous Higgs boson interactions with Standard Model particles, using the pseudo-observable extension to the kappa-framework.

https://doi.org/10.1007/JHEP10(2017)132

Contents

1 Introduction

The ATLAS and CMS Collaborations at the Large Hadron Collider (LHC) have performed extensive studies of the Higgs boson properties in the past few years. The Higgs boson mass has been measured to be $m_H = 125.09 \pm 0.24\,\mathrm{GeV}$ [1] and no significant deviations from Standard Model (SM) predictions have been found in the cross sections measured per production mode, the branching ratios [2], or spin and parity quantum numbers [3–6]. Furthermore, inclusive and differential fiducial cross sections of Higgs boson production, defined as background-subtracted event yields corrected for the detector response, have been measured in proton-proton (pp) collisions at a centre-of-mass energy of $\sqrt{s} = 8\,\mathrm{TeV}$, using the 4ℓ ($\ell = e, \mu$), $\gamma\gamma$, and $e\nu\mu\nu$ final states [7–12]. The measured differential cross sections are also in good agreement with the SM predictions.

This paper presents a measurement of inclusive and differential fiducial cross sections in the $H \to ZZ^* \to 4\ell$ decay channel using pp collisions at $\sqrt{s} = 13\,\mathrm{TeV}$ recorded with the ATLAS detector. The combined effect of a higher centre-of-mass energy and an integrated luminosity of $36.1\,\mathrm{fb}^{-1}$ is expected to increase the number of Higgs boson events by a factor

of almost four compared to the previous analysis at $\sqrt{s} = 8\,\text{TeV}$. Significantly larger gains are expected in the regions of the differential distributions that probe higher momentum scales due to increased parton-parton luminosities. The differential cross sections presented in this paper are measured in a fiducial phase space to avoid model-dependent extrapolations. The observed distributions are corrected for detector inefficiency and resolution.

Fiducial cross sections are presented both inclusively and separately for each of the final states of the $H \to ZZ^* \to 4\ell$ decay (4μ, $2e2\mu$, $2\mu2e$, $4e$). Differential fiducial cross sections are presented for various observables that describe Higgs boson production and decay in pp collisions. They are inclusive in the different final states and Higgs boson production mechanisms, such as gluon-gluon fusion (ggF) or vector-boson fusion (VBF). The Higgs boson transverse momentum[1] $p_{\text{T},4\ell}$ can be used to test perturbative QCD calculations, especially when separated into exclusive jet multiplicities. This variable is also sensitive to the Lagrangian structure of the Higgs boson interactions [13]. The Higgs boson rapidity distribution $|y_{4\ell}|$ is sensitive to the parton distribution functions (PDFs) of the colliding protons. The decay variables $|\cos\theta^*|$ and m_{34} test the spin and parity of the Higgs boson. The variable $|\cos\theta^*|$ is defined as the magnitude of the cosine of the decay angle of the leading lepton pair in the four-lepton rest frame with respect to the beam axis. The variables m_{12} and m_{34} refer to the invariant masses of the leading and subleading lepton pairs and correspond to the invariant masses of the on-shell and off-shell Z bosons produced in the Higgs boson decay. The number of jets N_{jets} produced in association with the Higgs boson and the transverse momentum $p_{\text{T}}^{\text{lead.jet}}$ of the leading jet both provide sensitivity to the theoretical modelling of high-p_{T} quark and gluon emission. The invariant mass m_{jj} of the two leading jets in the event is sensitive to different production mechanisms. The signed angle between the two leading jets in the transverse plane[2] $\Delta\phi_{\text{jj}}$ is another observable that tests the spin and parity of the Higgs boson [14].

Providing fiducial cross sections simplifies the testing of theoretical models with $H \to ZZ^* \to 4\ell$ final states since the response of the detector has been corrected for. As an example, the cross section in the m_{12} vs m_{34} observable plane is interpreted in the framework of pseudo-observables [15], which are derived from on-shell decay amplitudes and provide a generalization of the kappa-framework [16]. Limits are set on parameters describing anomalous Higgs boson interactions with leptons and Z bosons.

2 ATLAS detector

The ATLAS detector [17] is a multi-purpose detector with a forward-backward symmetric cylindrical geometry. At small radii, the inner detector (ID), immersed in a 2 T magnetic field produced by a thin superconducting solenoid located in front of the calorimeter,

---

[1]ATLAS uses a right-handed coordinate system with its origin at the nominal interaction point (IP) in the centre of the detector and the z-axis along the beam pipe. The x-axis points from the IP to the centre of the LHC ring, and the y-axis points upward. Cylindrical coordinates (r, ϕ) are used in the transverse plane, ϕ being the azimuthal angle around the z-axis. The pseudorapidity is defined in terms of the polar angle θ as $\eta = -\ln\tan(\theta/2)$.

[2]$\Delta\phi_{\text{jj}}$ is defined as $\Delta\phi_{\text{jj}} = \phi_{j1} - \phi_{j2}$, if $\eta_{j1} > \eta_{j2}$, otherwise $\Delta\phi_{\text{jj}} = \phi_{j2} - \phi_{j1}$, where $j1$ is the leading and $j2$ the subleading jet.

is made up of a fine-granularity pixel detector, including the newly installed insertable B-layer [18, 19], a microstrip detector, as well as a straw-tube tracking detector. The silicon-based detectors cover the pseudorapidity range $|\eta| < 2.5$. The gas-filled straw-tube transition radiation tracker complements the silicon tracker at larger radii up to $|\eta| < 2$ and also provides electron identification capabilities based on transition radiation. The electromagnetic (EM) calorimeter is a lead/liquid-argon sampling calorimeter with accordion geometry. The calorimeter is divided into a barrel section covering $|\eta| < 1.475$ and two end-cap sections covering $1.375 < |\eta| < 3.2$. For $|\eta| < 2.5$ it is divided into three layers in depth, which are finely segmented in η and ϕ. A thin presampler layer, covering $|\eta| < 1.8$, is used to correct for fluctuations in upstream energy losses. A hadronic calorimeter in the region $|\eta| < 1.7$ uses steel absorbers and scintillator tiles as the active medium. A liquid-argon calorimeter with copper absorbers is used in the hadronic end-cap calorimeters, which covers the region $1.5 < |\eta| < 3.2$. A forward calorimeter using copper or tungsten absorbers with liquid argon completes the calorimeter coverage up to $|\eta| = 4.9$. The muon spectrometer (MS) measures the deflection of muon trajectories within $|\eta| < 2.7$, using three layers of precision drift tube chambers, with cathode strip chambers in the innermost layer for $|\eta| > 2.0$. The deflection is provided by a toroidal magnetic field from air-core superconducting magnets. The field integral of the toroids ranges between 2.0 and 6.0 T·m across most of the detector. The muon spectrometer is instrumented with trigger chambers covering $|\eta| < 2.4$. Events are selected using a first-level trigger implemented in custom electronics, which reduces the event rate to a maximum of 100 kHz using a subset of detector information. Software algorithms with access to the full detector information are then used in the high-level trigger to yield a recorded event rate of about 1 kHz [20].

3 Theoretical predictions and event simulation

The Higgs boson production cross sections and decay branching ratios, as well as their uncertainties, are taken from refs. [16, 21–23], and are referred to as LHCXSWG. The cross section for Higgs boson production via ggF is available at next-to-next-to-next-to-leading order (N3LO) in QCD and has next-to-leading-order (NLO) electroweak (EW) corrections applied [24–37]. The cross section for the VBF process is calculated with full NLO QCD and EW corrections [38–40], and approximate next-to-next-to-leading-order (NNLO) QCD corrections are applied [41]. The cross sections for the production of an electroweak boson in association with a Higgs boson, VH ($V = W, Z$), are calculated at NNLO accuracy in QCD [42, 43] and NLO EW radiative corrections [44] are applied. The cross section for the associated production of a Higgs boson with a $t\bar{t}$ pair, $t\bar{t}H$, is calculated at NLO accuracy in QCD [45–48]. The cross section for the $b\bar{b}H$ process is calculated by the Santander matching of the five-flavour scheme (NNLO in QCD) and four-flavour scheme (NLO in QCD) [49]. The composition of the different production modes in the SM is 87.3% (ggF), 6.8% (VBF), 4.1% (VH), 0.9% ($t\bar{t}H$), 0.9% ($b\bar{b}H$).

The Higgs boson decay branching ratio to the four-lepton final state ($\ell = e, \mu$) for $m_H = 125\,\text{GeV}$ is predicted to be 0.0124% [50] in the SM using PROPHECY4F [51, 52],

which includes the complete NLO QCD and EW corrections, and the interference effects between identical final-state fermions. Due to the latter, the expected branching ratios of the $4e$ and 4μ final states are about 10% higher than the branching ratios to $2e2\mu$ and $2\mu2e$ final states.

The POWHEG-BOX v2 Monte Carlo (MC) event generator [53–55] is used to simulate ggF [56], VBF [57] and VH [58] processes, using the PDF4LHC NLO PDF set [59]. The ggF Higgs boson production is accurate to NNLO in QCD, using the POWHEG method for merging the NLO Higgs boson plus jet cross section with the parton shower, and the MiNLO method [60, 61] to simultaneously achieve NLO accuracy for inclusive Higgs boson production. Furthermore, a reweighting procedure is performed using the HNNLO program [62–64] to achieve full NNLO accuracy [65]. This sample is referred to as NNLOPS. The VBF and VH samples are produced at NLO accuracy in QCD. For VH, the MiNLO method is used to merge zero- and one-jet events. For Higgs boson production in association with a heavy quark pair, events are simulated at NLO with MadGraph5_aMC@NLO (v.2.2.3 for $t\bar{t}H$ and v.2.3.3 for $b\bar{b}H$ [66]) [67], using the CT10nlo PDF set [68] for $t\bar{t}H$ and the NNPDF23 PDF set [69] for $b\bar{b}H$. For the ggF, VBF, VH, and $b\bar{b}H$ production mechanisms, PYTHIA 8 [70, 71] is used for the $H \to ZZ^* \to 4\ell$ decay as well as for parton showering, hadronization, and multiple partonic interactions using the AZNLO parameter set [72]. For the $t\bar{t}H$ production mechanism, HERWIG++ [73, 74] is used with the UEEE5 parameter set [75].

The measured event yields and the differential fiducial cross-section measurements are compared to a SM prediction constructed from the MC predictions presented above, after normalizing each sample using the corresponding LHCXSWG prediction. All samples are generated with $m_H = 125\,\text{GeV}$.

An alternative prediction for ggF SM Higgs boson production is generated using Mad-Graph5_aMC@NLO v.2.3.3 at NLO accuracy in QCD for zero, one, two additional jets, merged with the FxFx scheme [67, 76], using the NNPDF30_nlo_as_0118 PDF set [77]. This MG5_aMC@NLO_FxFx sample is interfaced to PYTHIA 8 for Higgs boson decay, parton showering, hadronization and multiple partonic interactions using the A14 parameter set [78]. The data are also compared to ggF SM Higgs boson production in the 4ℓ decay channel simulated with HRes v2.3 [64, 79], using the MSTW2008 NNLO PDF set [80]. The HRes program computes fixed-order cross sections for ggF SM Higgs boson production up to NNLO in QCD and describes the $p_{\text{T},4\ell}$ distribution at NLO. All-order resummation of soft-gluon effects at small transverse momenta is consistently included up to next-to-next-to-leading logarithmic order (NNLL) in QCD, using dynamic factorization and resummation scales (the central scales are chosen to be $m_H/2$). The program implements top quark and bottom quark mass dependence up to next-to-leading logarithmic order (NNL) + NLO in QCD. At NNLL + NNLO accuracy only the top quark contribution is considered. HRes does not perform parton showering and QED final-state radiation effects are not included. Both the MG5_aMC@NLO_FxFx and the HRes predictions are normalized using the LHCXSWG cross section.

A ggF sample used to study deviations from the SM predictions within the pseudo-observable framework [15, 81] is generated with MadGraph5 at LO using FeynRules 2 [82]

and the NN23PDF PDF set. The sample is interfaced to Pythia 8 using the A14 parameter set. It is normalized using the LHCXSWG cross section.

The $ZZ^{(*)}$ continuum background from quark-antiquark annihilation is simulated with Sherpa 2.2 [83–85], using the NNPDF3.0 NNLO PDF set. NLO accuracy is achieved in the matrix element calculation for zero- and one-jet final states and LO accuracy for two- and three-jet final states. The merging is performed with the Sherpa parton shower [86] using the MePs@NLO prescription [87]. NLO EW corrections are applied as a function of the invariant mass of the ZZ^* system m_{ZZ^*} [88, 89]. The gluon-induced ZZ^* production is modelled with gg2VV [90] at leading order in QCD. The K-factor accounting for missing higher-order QCD effects in the calculation of the $gg \rightarrow ZZ^*$ continuum is taken to be 1.7 ± 1.0 [91–96].

Sherpa 2.2 is also used to generate samples of the Z+jets background at NLO accuracy for zero-, one- and two-jet final states and LO accuracy for three- and four-jet final states. In this measurement, the Z+jets background is normalized using control samples from data. For comparisons with simulation, the QCD NNLO Fewz [97, 98] and Mcfm cross-section calculations are used for inclusive Z boson and $Z + b\bar{b}$ production, respectively. Samples for the $t\bar{t}$ background are produced with Powheg-Box interfaced to Pythia 6 [70] for parton showering and hadronization, to Photos [99] for QED radiative corrections, to Tauola [100, 101] for the simulation of τ lepton decays and to EvtGen v.1.2.0 [102] for the simulation of b-hadron decays. For this sample, the Perugia 2012 parameter set [103] is used. The WZ background is modelled using Powheg-Box+Pythia 8 and the AZNLO parameter set. The triboson backgrounds ZZZ, WZZ, and WWZ with four or more leptons originating from the hard scatter are produced with Sherpa 2.1. MadGraph, interfaced to Pythia 8 with the A14 parameter set is used to simulate the all-leptonic $t\bar{t} + Z$ as well as the $t\bar{t} + W$ processes.

The particle-level events produced by each event generator are passed through the Geant4 [104] simulation of the ATLAS detector [105] and reconstructed in the same way as the data. Additional pp interactions in the same and nearby bunch crossings (pile-up) are simulated using inelastic pp collisions generated using Pythia 8 (with the A2 MSTW2008LO parameter set) and overlaid on the simulated events discussed above. The MC events are weighted to reproduce the distribution of the average number of interactions per bunch crossing observed in the data.

4 Event selection

Events with at least four leptons are selected with single-lepton, dilepton and trilepton triggers. The trigger selection requirements, e.g. the minimum transverse energy E_{T}/transverse momentum p_{T}, the identification and the isolation requirements, were tightened periodically during the data-taking to maintain a maximum overall trigger rate as the instantaneous luminosity increased. For example, the E_{T} threshold changed from 24 to 26 GeV for the single-electron trigger. The multilepton triggers have lower E_{T} or p_{T} requirements and more relaxed identification requirements. The combined trigger efficiency in this analysis is about 98%. The data are subjected to quality requirements to reject events in which

detector components were not operating correctly. Events are required to have at least one vertex with two associated tracks with $p_T > 400$ MeV, and the primary vertex is chosen to be the reconstructed vertex with the largest $\sum p_T^2$ of reconstructed tracks.

Electrons are reconstructed using tracks in the ID and energy clusters in the EM calorimeter [106]. They are required to satisfy loose identification criteria based on tracking and calorimeter information. Muons are reconstructed as tracks in the ID and the MS [107] if they lie in the region $0.1 < |\eta| < 2.5$. In the region $|\eta| < 0.1$, the MS has reduced coverage, and muons are reconstructed from ID tracks and identified by either a minimal energy deposit in the calorimeter or hits in the MS. For $2.5 < |\eta| < 2.7$, only the MS can be used. For events with four muons, at least three muons are required to be reconstructed by combining ID and MS tracks. Each muon (electron) must have transverse momentum $p_T > 5\,\text{GeV}$ ($E_T > 7\,\text{GeV}$), within the pseudorapidity range $|\eta| < 2.7$ (2.47) and with a longitudinal impact parameter $|z_0 \sin(\theta)| < 0.5$ mm. Muons originating from cosmic rays are removed with the transverse impact parameter requirement $|d_0| < 1$ mm. Jets are reconstructed from topological clusters of calorimeter cells using the anti-k_t algorithm [108, 109] with the radius parameter $R = 0.4$. Jets are corrected for detector response and pile-up contamination [110, 111] and required to have $p_T > 30\,\text{GeV}$, and $|\eta| < 4.5$. In order to avoid double counting of electrons also reconstructed as jets, jets are removed if $\Delta R(\text{jet}, e) = \sqrt{\Delta\phi(\text{jet}, e)^2 + \Delta\eta(\text{jet}, e)^2} < 0.2$. This overlap removal is also applied to jets close to muons if the jet has fewer than three tracks and the energy and momentum differences between the muon and the jet are small ($p_{T,\mu} > 0.5\ p_{T,\text{jet}}$ and $p_{T,\mu} > 0.7\ p_{T,\text{jet,tracks}}$), or if $\Delta R(\text{jet}, \mu) < 0.1$.

Higgs boson candidates are formed by selecting two same-flavour opposite-sign (SFOS) lepton pairs, called a lepton quadruplet. The analysis selection proceeds in parallel for the four final states (4μ, $2e2\mu$, $2\mu2e$, $4e$, where the first two leptons refer to the leading lepton pair). The leading pair is defined as the SFOS pair with the mass m_{12} closest to the Z boson mass and the subleading pair is defined as the SFOS pair with the mass m_{34} second closest to the Z boson mass. Mispairing within a quadruplet occurs for about 1% of the selected events for the 4μ or $4e$ final states. Furthermore, a quadruplet can be formed with an extra lepton originating from the W/Z for VH or $t\bar{t}H$ production, moving $m_{4\ell}$ away from m_H. The expected rate for VH or $t\bar{t}H$ with leptonic decays is about 0.3% of all Higgs events in the full $m_{4\ell}$ range after the event selection. For each final state, a quadruplet is chosen in which the three leading leptons pass p_T (E_T) $>$ 20, 15, 10 GeV. In addition to the dilepton mass, lepton separation and J/ψ veto requirements (given in table 1), loose calorimeter- and track-based isolation as well as impact parameter requirements are imposed on the leptons. For the track-based isolation, the sum of the p_T of the tracks lying within a cone of size $\Delta R = \min[0.3, 10\,\text{GeV}/p_T]$ ($\min[0.2, 10\,\text{GeV}/E_T]$) around the muon (electron) is required to be smaller than 15% of the lepton p_T (E_T). Similarly, the sum of the calorimeter E_T deposits in a cone of size $\Delta R = 0.2$ around the muon (electron) is required to be smaller than 30% (20%) of the lepton p_T (E_T). As the four leptons should originate from a common vertex, a requirement on the χ^2 value of a common vertex fit is applied, corresponding to a signal efficiency of 99.5% for all decay channels. If more than one quadruplet passes all requirements, e.g. for VH or $t\bar{t}H$, the channel with the
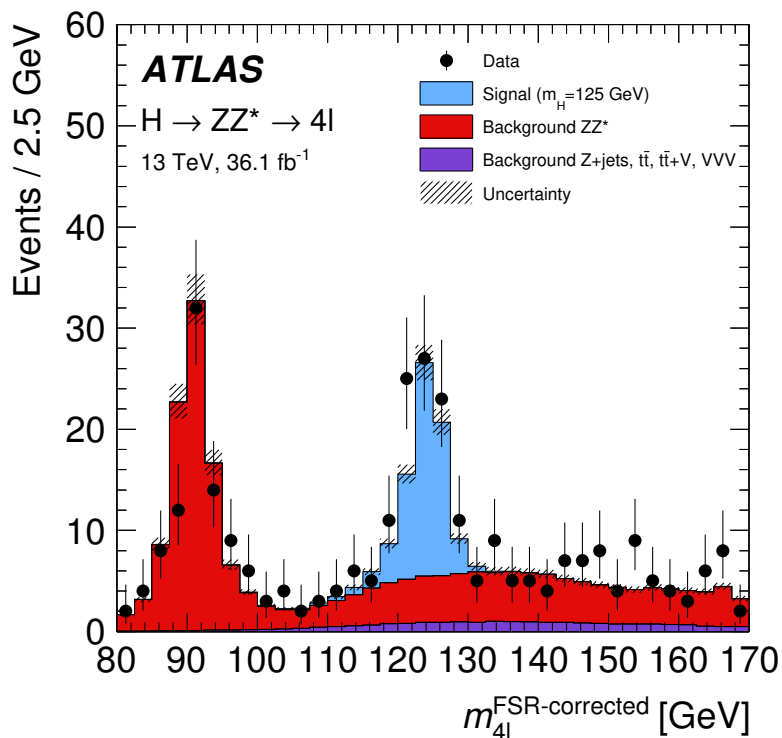
Figure 1. Four-lepton invariant mass distribution of the selected events before the $m_{4\ell}$ requirement, corrected for final-state radiation (FSR). The error bars on the data points indicate the statistical uncertainty. The SM Higgs boson signal prediction is obtained from the samples discussed in section 3. The backgrounds are determined following the description in section 6. The uncertainty in the prediction is shown by the hatched band, calculated as described in section 9.

highest expected signal rate after reconstruction and event selection is selected, in the order: 4μ, $2e2\mu$, $2\mu2e$ and $4e$. In order to improve the four-lepton mass reconstruction, the reconstructed final-state radiation (FSR) photons in Z boson decays are accounted for using the same strategy as in the Run-1 data analysis [112]. The invariant mass distribution of the four leptons of the selected events is shown in figure 1. Only events with a four-lepton invariant mass in the range 115–130 GeV are used in the extraction of the signal.

The selected events are divided into bins of the variables of interest. The bin boundaries are chosen such that each bin has an expected signal significance greater than 2σ (where the significance is calculated from the number of signal events S and the number of background events B as $S/\sqrt{S+B}$) and that there are minimal migrations between bins, which reduces the model dependence of the correction for the detector response.

5 Fiducial phase space

The fiducial cross sections are defined at particle level using the selection requirements outlined in table 1, which are chosen to closely match those in the detector-level analysis in order to minimize model-dependent acceptance extrapolations.

Leptons and jets	
Muons:	$p_{\mathrm{T}} > 5$ GeV, $|\eta| < 2.7$
Electrons:	$p_{\mathrm{T}} > 7$ GeV, $|\eta| < 2.47$
Jets:	$p_{\mathrm{T}} > 30$ GeV, $|y| < 4.4$
Jet-lepton overlap removal:	$\Delta R(\mathrm{jet}, \ell) > 0.1\,(0.2)$ for muons (electrons)
Lepton selection and pairing	
Lepton kinematics:	$p_{\mathrm{T}} > 20, 15, 10$ GeV
Leading pair (m_{12}):	SFOS lepton pair with smallest $|m_Z - m_{\ell\ell}|$
Subleading pair (m_{34}):	remaining SFOS lepton pair with smallest $|m_Z - m_{\ell\ell}|$
Event selection (at most one quadruplet per channel)	
Mass requirements:	50 GeV$< m_{12} < 106$ GeV and 12 GeV$< m_{34} < 115$ GeV
Lepton separation:	$\Delta R(\ell_i, \ell_j) > 0.1\,(0.2)$ for same- (different-)flavour leptons
J/ψ veto:	$m(\ell_i, \ell_j) > 5$ GeV for all SFOS lepton pairs
Mass window:	115 GeV$< m_{4\ell} < 130$ GeV

Table 1. List of event selection requirements which define the fiducial phase space of the cross-section measurement. SFOS lepton pairs are same-flavour opposite-sign lepton pairs.

The fiducial selection is applied to final-state[3] electrons and muons that do not originate from hadrons or τ decays. The leptons are "dressed", i.e. the four-momenta of photons within a cone of size $\Delta R = 0.1$ are added to the lepton four-momentum, requiring the photons to not originate from hadron decays. Particle-level jets are reconstructed from final-state particles using the anti-k_t algorithm with radius parameter $R = 0.4$. Electrons, muons, neutrinos (if they are not from hadron decays) and photons used to dress leptons, are excluded from the jet clustering. Jets are removed if they are within a cone of size $\Delta R = 0.1\,(0.2)$ around a selected muon (electron).

Quadruplets are formed with the selected dressed leptons. Using the same procedure as for reconstructed events reproduces the mispairing of the leptons from Higgs boson decays when assigning them to the leading and subleading Z bosons and the inclusion of leptons originating from vector bosons produced in association with the Higgs boson. The variables used in the differential cross-section measurement are calculated using the dressed leptons in the quadruplets.

The acceptance of the fiducial selection (with respect to the full phase space of $H \rightarrow ZZ^* \rightarrow 2\ell2\ell'$, where $\ell, \ell' = e$ or μ) is 42% for a SM Higgs boson with $m_H = 125$ GeV. The ratio of the number of events passing the detector-level event selection to those passing the particle-level selection is 53%. Due to resolution effects, about 2% of the events which pass the detector-level selection fail the particle-level selection.

---

[3]Final-state particles are defined as particles with a lifetime $c\tau > 10$ mm. For electrons and muons, this corresponds to leptons after final state radiation.
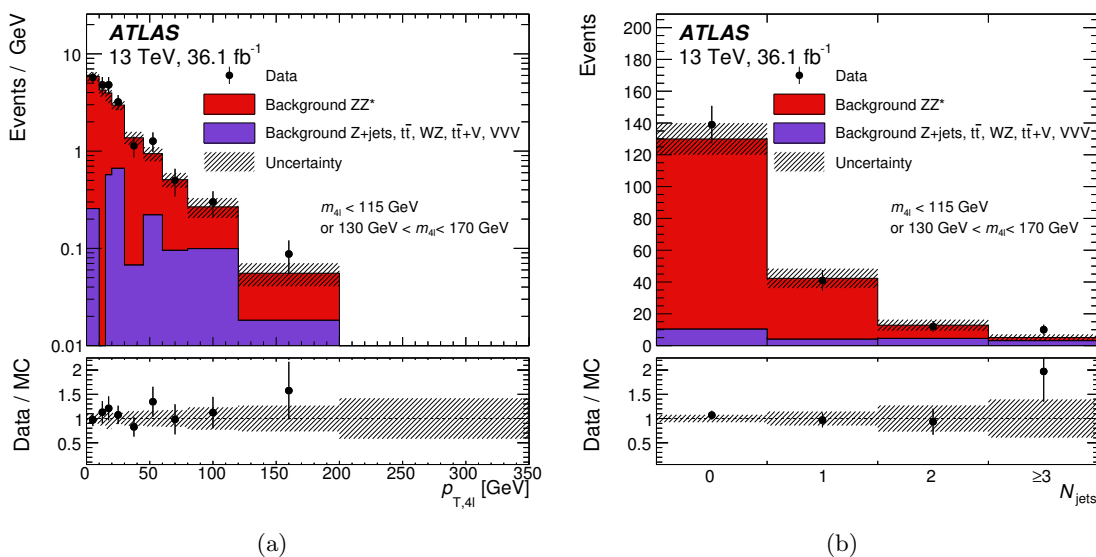
Figure 2. Reconstructed event yields in bins of (a) the transverse momentum of the four leptons $p_{T,4\ell}$ and (b) the number of jets N_{jets}, in a non-resonant ZZ^*-enriched control region, obtained by applying the full event selection except for the $m_{4\ell}$ window, i.e. $m_{4\ell} < 115\,\text{GeV}$ or $130\,\text{GeV} < m_{4\ell} < 170\,\text{GeV}$. The error bars on the data points indicate the statistical uncertainty. The uncertainty in the prediction is shown by the dashed band. The bottom part of the figures shows the ratio of data to the MC expectation.

6 Background estimates

Non-resonant SM ZZ^* production via $q\bar{q}$ annihilation and gluon-gluon fusion can result in four prompt leptons in the final state and constitutes the largest background for this analysis. It is estimated using the SHERPA and gg2VV simulated samples presented in section 3. To cross-check the theoretical modelling of this background, a ZZ^*-enriched control region is formed using almost the full event selection, but requiring that the four-lepton invariant mass not lie within the region $115\,\text{GeV} < m_{4\ell} < 130\,\text{GeV}$. In this control region, good agreement is observed between the simulation and the data for all distributions, as demonstrated for $p_{T,4\ell}$ and N_{jets} in figure 2.

Other processes that contribute to the background, such as Z + jets, $t\bar{t}$, and WZ, contain at least one jet, photon or lepton candidate that is misidentified as a prompt lepton. These backgrounds are significantly smaller than the non-resonant ZZ^* background and are estimated using data where possible, following slightly different approaches for the $\ell\ell\mu\mu$ and $\ell\ell ee$ final states [112].

In the $\ell\ell\mu\mu$ final states, the normalizations for the Z + jets and $t\bar{t}$ backgrounds are determined using fits to the invariant mass of the leading lepton pair in dedicated data control regions. The control regions are formed by relaxing the χ^2 requirement on the vertex fit, and by inverting or relaxing isolation and/or impact-parameter requirements on the subleading muon pair. An additional control region ($e\mu\mu\mu$) is used to improve the $t\bar{t}$ background estimate. Transfer factors to extrapolate from the control regions to the signal

region are obtained separately for $t\bar{t}$ and Z + jets using simulation. The shapes of the Z + jets and $t\bar{t}$ backgrounds for the differential observables are taken from simulation and normalized using the inclusive data-driven estimate. Comparisons in the control regions show good agreement between data and the simulation for the different observables.

The $\ell\ell ee$ control-region selection requires the electrons in the subleading lepton pair to have the same charge, and relaxes the identification and isolation requirements on the electron candidate with the lowest transverse energy. This electron candidate, denoted as X, can be a light-flavour jet, a photon conversion or an electron from heavy-flavour hadron decay. The heavy-flavour background is completely determined from simulation, whereas the light-flavour and photon conversion background is obtained with the sPlot [113] method, based on a fit to the number of hits in the innermost ID layer in the data control region. Transfer factors for the light-flavour jets and converted photons, obtained from simulated samples, are corrected using $Z + X$ control regions and then used to extrapolate the extracted yields to the signal region. Both the extraction of the yield in the control region and the extrapolation are performed in bins of the transverse momentum of the electron candidate and the jet multiplicity. In order to extract the shape of the backgrounds from light-flavour jets and photon conversions in bins of the differential distributions, a similar method is used, except that the extraction and extrapolation is now performed as a function of the transverse momentum of the electron candidate in each bin of the variable of interest.

The $m_{4\ell}$ shapes are extracted from simulation for most background components except for the light-flavour jet + conversion contribution in the $\ell\ell ee$ final state, which is not well described by the simulation and therefore taken from the control region and extrapolated using the data-corrected efficiencies. It was observed that the $m_{4\ell}$ shape of the Z + jets and $t\bar{t}$ backgrounds does not change significantly across the differential distributions, and so the same shape, obtained using all available events, is used for all bins.

The background from WZ production is included in the data-driven estimates for the $\ell\ell ee$ final states, while it is added from simulation for the $\ell\ell\mu\mu$ final states. The contributions from $t\bar{t} + Z$ and triboson processes are very small and taken from simulated samples.

7 Measured data yields

The observed number of events in the four decay channels after the event selection, as well as the expected signal and background yields, is presented in table 2. Figure 3 shows the expected and observed event yields for four of the measured differential spectra. The total observed and predicted event counts agree within 1.3 standard deviations.

8 Signal extraction and correction for detector effects

To extract the number of signal events in each bin of a differential distribution (or for each decay channel for the inclusive fiducial cross section), invariant mass templates for the Higgs boson signal and the background processes are fit to the $m_{4\ell}$ distribution in data.

Final state	SM Higgs	ZZ^*	$Z + $ jets, $t\bar{t}$ WZ, ttV, VVV	Expected	Observed
4μ	20.1 ± 1.6	9.8 ± 0.8	1.3 ± 0.3	31.2 ± 1.8	33
$4e$	10.6 ± 1.0	4.4 ± 0.4	1.3 ± 0.2	16.3 ± 1.1	16
$2e2\mu$	14.2 ± 1.1	7.1 ± 0.5	1.0 ± 0.2	22.3 ± 1.2	32
$2\mu2e$	10.8 ± 1.0	4.6 ± 0.5	1.4 ± 0.3	16.8 ± 1.1	21
Total	56 ± 4	25.9 ± 2.0	5.0 ± 0.7	87 ± 5	102

Table 2. Number of expected and observed events in the four decay channels after the event selection, in the mass range $115\,\mathrm{GeV} < m_{4\ell} < 130\,\mathrm{GeV}$. The sum of the expected number of SM Higgs boson events and the estimated background yields is compared to the data. Combined statistical and systematic uncertainties are included for the predictions (see section 9).

The signal shape is obtained from the simulated samples described in section 3 assuming a Higgs boson mass of 125 GeV. Most of the background shapes are also obtained from the simulated samples described in section 3, while some of the backgrounds in the $\ell\ell ee$ channel are derived from control regions in data, as discussed in section 6. The normalization of the backgrounds is fixed in this fit. Figures 4 and 5 show the data, templates and best fits for the $m_{4\ell}$ distributions in the four decay channels for the extraction of the inclusive fiducial cross section, and two bins of the transverse momentum of the four leptons. For the differential distributions, no split into decay channels is performed, and the SM $ZZ^* \to 4\ell$ decay fractions are assumed.

The fiducial cross section $\sigma_{i,\mathrm{fid}}$ for a given final state or bin of the differential distribution is defined as:

$$\sigma_{i,\mathrm{fid}} = \sigma_i \times A_i \times \mathcal{B} = \frac{N_{i,\mathrm{fit}}}{\mathcal{L} \times C_i}, \quad C_i = \frac{N_{i,\mathrm{reco}}}{N_{i,\mathrm{part}}}, \tag{8.1}$$

where A_i is the acceptance in the fiducial phase space, $\mathcal{B}$ is the branching ratio and σ_i is the total cross section in bin i. The term $N_{i,\mathrm{fit}}$ is the number of extracted signal events in data, $\mathcal{L}$ is the integrated luminosity and C_i is the bin-by-bin correction factor for detector inefficiency and resolution. The term $N_{i,\mathrm{reco}}$ is the number of reconstructed signal events and $N_{i,\mathrm{part}}$ is the number of events at the particle level in the fiducial phase-space. The correction factor is calculated from simulated Higgs boson samples, assuming SM production mode fractions and $ZZ^* \to 4\ell$ decay fractions as discussed in section 3. The systematic uncertainties in this assumption are described in section 9. The correction factors for the different Higgs boson production modes agree within 15%, except for the $t\bar{t}H$ mode, which differs by up to 40%, due to the fact that $t\bar{t}H$ events have more hadronic jets and that no isolation requirements are applied to the leptons at the particle level. The correction factors for the four final states are 0.64 ± 0.04 (4μ), 0.55 ± 0.03 ($2e2\mu$), 0.48 ± 0.05 ($2\mu2e$), and 0.43 ± 0.06 ($4e$). Figure 6 shows the bin-by-bin correction factors for all decay channels combined including systematic uncertainties for the $p_{\mathrm{T},4\ell}$ and N_{jets} distributions. The large uncertainty for $N_{\mathrm{jets}} \geq 3$ is due to the experimental jet reconstruction uncertainties and the variations of the fractions of Higgs boson production modes (see section 9). The same figure also shows the bin purity, defined as the fraction of events in a bin of the
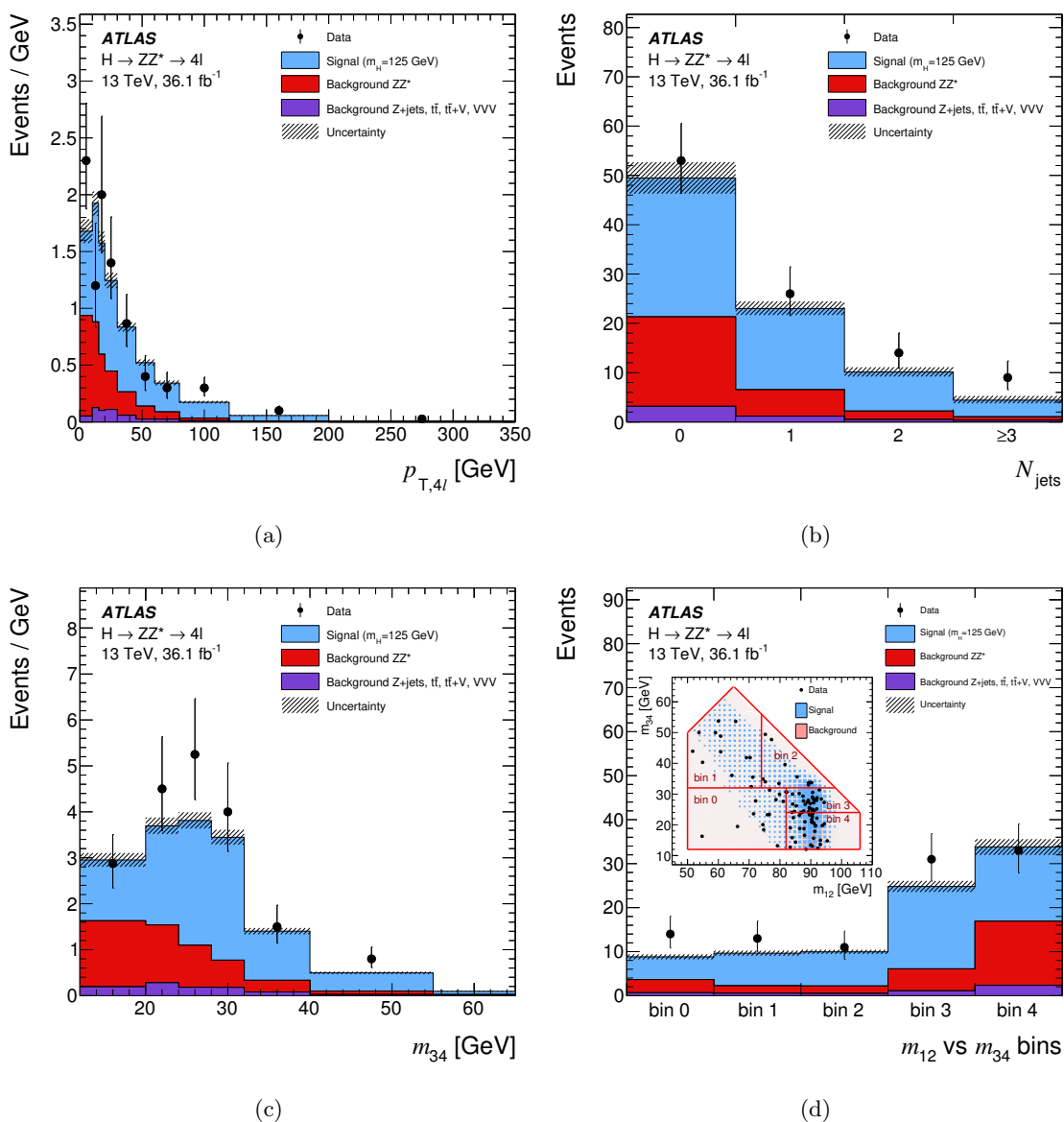
Figure 3. Measured data yields compared to SM Higgs boson signal and background processes for (a) the transverse momentum of the four leptons $p_{T,4\ell}$, (b) the number of jets N_{jets}, (c) the invariant mass of the subleading lepton pair m_{34}, and (d) the invariant mass of the leading vs the subleading pair m_{12} vs m_{34}. Figure (d) also includes an illustration of the chosen bins, as well as the two-dimensional distributions of data and prediction. The error bars on the data points indicate the statistical uncertainty. The uncertainty in the prediction is shown by the dashed band.

reconstructed distribution that are found in the same bin at particle level. The bin purity is greater than 0.75 for the Higgs boson kinematic and decay observables, and typically greater than 0.6 for the jet variables. It can be seen that the narrower bins at low $p_{T,4\ell}$ have a slightly reduced bin purity, as detector resolution effects result in larger bin migration effects, which is enhanced by the presence of a steep slope.
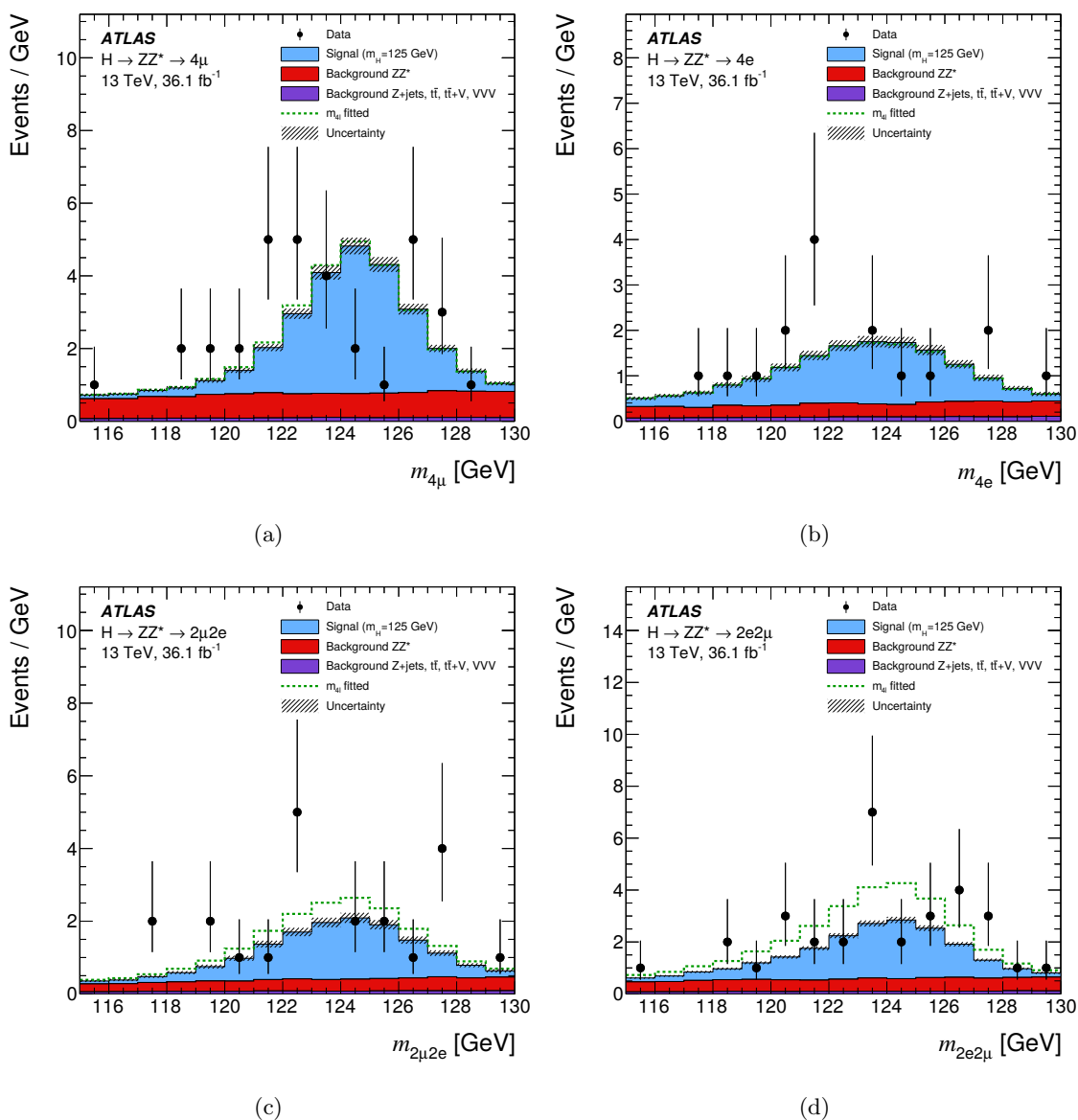
Figure 4. Template fit of SM Higgs boson signal and background to the data for the inclusive distributions for the different decay channels (a) 4μ, (b) $4e$, (c) $2\mu2e$, (d) $2e2\mu$. The error bars on the data points indicate the statistical uncertainty. The SM Higgs boson predictions are normalized to the cross sections discussed in section 3, while the backgrounds are normalized to the estimates described in section 6. The uncertainty in the prediction is shown by the dashed band. The dotted green line illustrates the best fit.

The signal, background, and data $m_{4\ell}$ distributions, as well as the correction factors, are used as input to a profile-likelihood-ratio fit [114], taking into account all bins of a given distribution and all final states for the inclusive measurement. The likelihood includes the shape and normalization uncertainties of the backgrounds and correction factors as nuisance parameters. This allows for correlation of systematic uncertainties between the
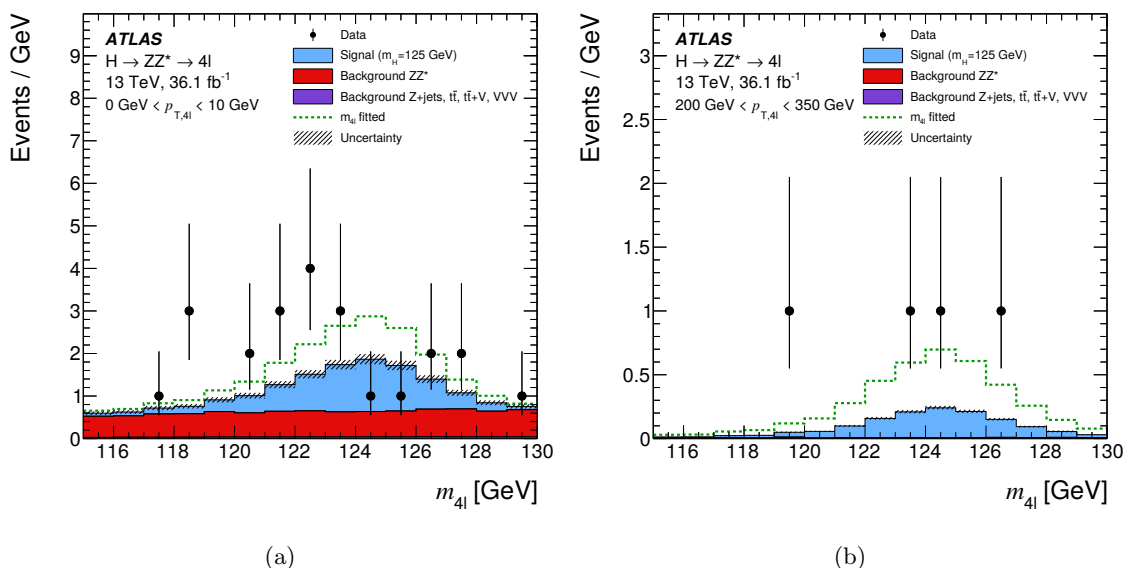
Figure 5. Template fit of SM Higgs boson signal and background to the data for the (a) first and (b) last bins of the distribution of the transverse momentum of the four leptons $p_{\mathrm{T},4\ell}$. The error bars on the data points indicate the statistical uncertainty. The SM Higgs boson predictions are normalized to the cross sections discussed in section 3, while the backgrounds are normalized to the estimates described in section 6. The uncertainty in the prediction is shown by the dashed band. The dotted green line illustrates the best fit.
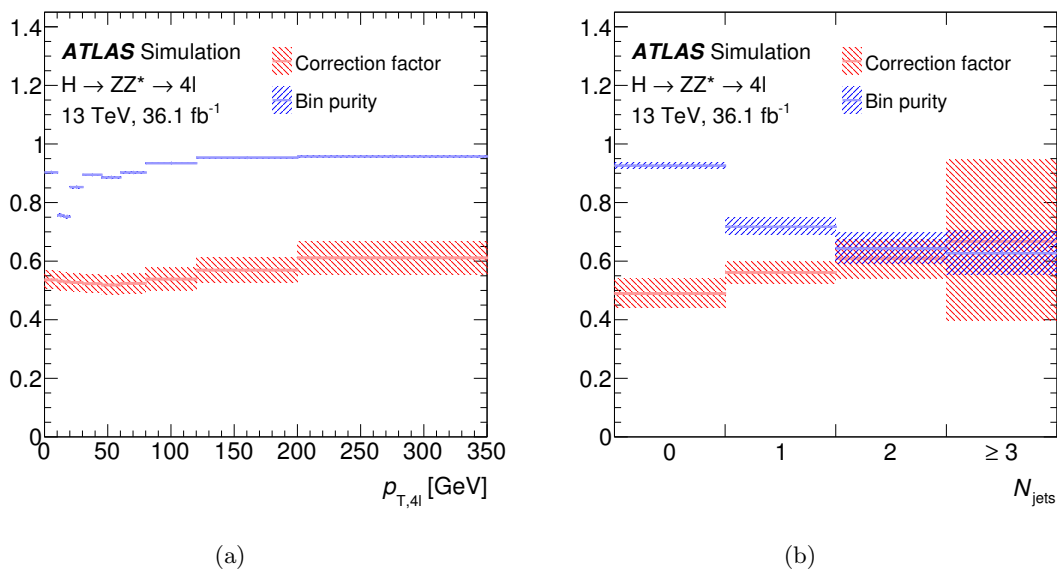

Figure 6. Bin-by-bin correction factors and bin purities for (a) the transverse momentum of the four leptons $p_{\mathrm{T},4\ell}$ and (b) the number of jets N_{jets}. The bands show the systematic uncertainties in the correction factors, which are discussed in section 9. The uncertainties in the bin purity include the detector response and pile-up uncertainties.

background estimates and the correction factors, as well as between bins or decay channels. The cross sections are extracted for each bin, or final state, by minimizing twice the negative logarithm of the profile likelihood ratio, $-2\ln\Lambda$. In the asymptotic assumption, i.e. the large sample limit, $-2\ln\Lambda$ behaves as a χ^2 distribution with one degree of freedom. The compatibility of a measured cross section and a theoretical prediction is evaluated by computing a p-value based on the difference between the value of $-2\ln\Lambda$ at the best-fit value and the value obtained by fixing the cross sections in all bins to the ones predicted by the theory. These p-values do not include the uncertainties in the theoretical predictions, which are significantly smaller than the total data uncertainties. Therefore, they are slightly smaller than they would be with all uncertainties included. For all measured observables the asymptotic assumption is verified with pseudo-experiments, and if necessary, the uncertainties are corrected to the values obtained with the pseudo-experiments. In the case of zero observed events, 95% confidence level (CL) limits on the fiducial cross sections are set using the $\mathrm{CL_s}$ modified frequentist formalism [114, 115].

The inclusive fiducial cross section for each channel is calculated from the fit results following eq. (8.1). The fiducial cross sections of the four final states can either be summed together to obtain an inclusive fiducial cross section, or they can be combined assuming the SM $ZZ^* \to 4\ell$ branching ratios. The latter combination is more model dependent, but benefits from a smaller statistical uncertainty.

9 Systematic uncertainties

Experimental systematic uncertainties affecting both the simulated background and correction factors arise from uncertainties in the efficiencies, resolutions and energy scales of leptons and jets [106, 107, 110, 116], as well as pile-up modelling. These uncertainties can affect both the shape and the normalization of the distributions. For the background estimate and the conversion of the corrected signal yields to cross sections, the luminosity uncertainty needs to be taken into account. The uncertainty in the combined 2015+2016 integrated luminosity is 3.2%, which affects the signal and simulated background estimates. It is derived, following a methodology similar to that detailed in ref. [117], from a preliminary calibration of the luminosity scale using x-y beam-separation scans performed in August 2015 and May 2016.

Uncertainties in the estimation of $Z + \text{jets}$, $t\bar{t}$, and WZ backgrounds are also considered. The dominant systematic uncertainties here arise from difficulties in modelling the extrapolation from the control regions to the signal region, which can affect not only the overall normalization but also the background composition estimates and hence the yields in the bins of the differential distributions.

For the simulated backgrounds and the extrapolation of the inclusive fiducial cross section to the total cross section, theoretical modelling uncertainties associated with PDF, missing higher-order QCD corrections (via variations of the factorization and renormalization scales), as well as underlying event and parton showering uncertainties are considered. For the extrapolation to the total cross section, uncertainties in the $H \to ZZ^* \to 4\ell$ branching ratios are also included [21].

The effect on the fitted event yields of shifting the $m_{4\ell}$ template according to the uncertainties in the measured Higgs boson mass, $0.24\,\mathrm{GeV}$ [1], is smaller than 0.5% and therefore neglected.

The dependence of the correction for detector effects on the theoretical modelling is assessed in a number of ways. For ggF, VBF and VH, the PDF4LHC NLO PDF set is varied according to its eigenvectors, and the envelope of the variations is used as the systematic uncertainty. The renormalization and factorization scales are varied by factors of 2.0 and 0.5. Furthermore, m_H is varied within the uncertainties in the measured Higgs mass. The relative contribution of each Higgs boson production mechanism is varied by an amount consistent with the uncertainties obtained from the combined ATLAS and CMS measurement of the Higgs boson production cross sections [2], except for $t\bar{t}H$ where the allowed variation is inflated to cover the measured value, which is more than two standard deviations away from the SM prediction. The correction factors are cross-checked using the alternative MADGRAPH5 ggF samples (for SM and modified couplings) and the differences with respect to nominal values are found to be well within the statistical uncertainties of the samples. Bias studies and cross-checks with other unfolding methods, such as matrix inversion and Bayesian iterative unfolding [118] show results that agree very well with the bin-by-bin correction factor results. Observed differences are generally much smaller than the statistical uncertainties.

The uncertainties in this analysis are dominated by the limited number of data events. The statistical uncertainty in the fiducial inclusive cross section obtained by combining all decay channels is 14%, while the systematic uncertainty is 7%, dominated by the lepton uncertainties and the uncertainty in the luminosity. For the differential cross sections, the size of the statistical and systematic uncertainties depends on the variable and is shown in table 3. The breakdown of the dominant systematic uncertainties is obtained by performing the fits while fixing groups of nuisance parameters to their best-fit value. The statistical uncertainties are mostly in the range 20–50%, and can be as high as 150%. For the Higgs boson kinematic properties, the most important systematic uncertainties are the experimental lepton uncertainties, 1–5%. The signal composition uncertainty grows with the increase of the fraction of $t\bar{t}H$ in some regions of phase space. Therefore, for observables defined by the jet activity produced in association with the Higgs boson, not only the jet energy scale but also the signal composition uncertainties become increasingly important, especially at high N_{jets} and $p_{\mathrm{T}}^{\mathrm{lead.jet}}$ ($\sim$20% each for $N_{\mathrm{jets}} \geq 3$).

10 Results

The inclusive fiducial cross sections of $H \rightarrow ZZ^* \rightarrow 4\ell$ are presented in table 4 and figure 7. The left panel in figure 7 shows the fiducial cross sections for the four individual decay channels (4μ, $4e$, $2\mu 2e$, $2e2\mu$). The middle panel shows the cross sections for opposite- and same-flavour decays, which can provide a handle on same-flavour interference effects, as well as the fiducial cross sections obtained by either summing all 4ℓ decay channels or combining them assuming SM branching ratios. The data are compared to the LHCXSWG prediction after accounting for the fiducial acceptance as determined from

Observable	Stat unc. [%]	Systematic unc. [%]	Dominant systematic components [%]						
			e	μ	jets	ZZ^* theo	Model	$Z+$jets$+ t\bar{t}$	Lumi
σ_{comb}	14	7	3	3	< 0.5	2	0.8	0.8	4
$\mathrm{d}\sigma$ / $\mathrm{d}p_{\text{T},4\ell}$	30–150	3–11	1–4	1–3	< 0.5	< 7	< 6	1–6	3–5
$\mathrm{d}\sigma$ / $\mathrm{d}p_{\text{T},4\ell}$ (0j)	31–52	10–18	2–5	1–4	3–16	3–8	1	2–3	3–5
$\mathrm{d}\sigma$ / $\mathrm{d}p_{\text{T},4\ell}$ (1j)	35–15	6–30	1–4	1–3	2–29	1–4	1–11	1–2	3–5
$\mathrm{d}\sigma$ / $\mathrm{d}p_{\text{T},4\ell}$ (2j)	30–41	5–21	1–3	1–3	2–19	1–5	1–7	1–2	3–5
$\mathrm{d}\sigma$ / $\mathrm{d}|y_{4\ell}|$	29–120	5–8	2–4	2–3	< 0.5	1–2	< 1	1	3–5
$\mathrm{d}\sigma$ / $\mathrm{d}|\cos\theta^*|$	31–100	5–8	2–4	2–3	< 0.5	1–2	< 2	1–4	3–5
$\mathrm{d}\sigma$ / $\mathrm{d}m_{34}$	26–53	4–13	2–5	1–5	< 0.5	1–6	< 1	1–3	3–5
$\mathrm{d}^2\sigma$ / $\mathrm{d}m_{12}\mathrm{d}m_{34}$	21–40	4–12	2–4	1–4	< 0.5	1–6	< 1	1–4	3–5
$\mathrm{d}\sigma$ / $\mathrm{d}N_{\text{jets}}$	22–44	6–31	1–4	1–3	4–22	2–4	1–22	1–2	3–5
$\mathrm{d}\sigma$ / $\mathrm{d}p_{\text{T}}^{\text{lead.jet}}$	30–53	5–18	1–4	1–3	3–16	2–3	1–8	1–2	3–5
$\mathrm{d}\sigma$ / $\mathrm{d}\Delta\phi_{\text{jj}}$	29–43	9–17	1–3	1–3	8–14	3–4	1–7	1	3–5
$\mathrm{d}\sigma$ / $\mathrm{d}m_{\text{jj}}$	23–100	9–27	1–4	1–4	8–24	3–8	1–7	< 3	3–5

Table 3. Fractional uncertainties for the inclusive fiducial cross section σ_{comb}, obtained by combining all decay channels, and ranges of systematic uncertainties for the differential observables. The columns e, μ, jets represent the experimental uncertainties in lepton and jet reconstruction and identification. The ZZ^* theory uncertainties include the PDF and scale variations. The model uncertainties are dominated by the production mode composition variations in the extraction of the correction factors.

the SM Higgs boson simulated samples (see section 3). The fiducial cross section is extrapolated to the total phase space, as shown in the right panel, using the same fiducial acceptance as well as the branching ratios, with the additional uncertainties described in section 9. The total cross section is also compared to the cross sections predicted by NNLOPS, HRes, and MG5_AMC@NLO_FxFx (see section 3). It can be seen that the MG5_AMC@NLO_FxFx cross section is lower than the other predictions, as it is only accurate to NLO in QCD for inclusive ggF production. All generators predict cross sections that are lower than the LHCXSWG calculation. The observed fiducial cross sections in the $2e2\mu$ and $2\mu2e$ final states are higher than the prediction, which leads to an overall larger observed cross section. The combined fiducial cross section and the LHCXSWG prediction agree well, only differing by 1.3 standard deviations. The p-values, calculated as described in section 8, are also shown in table 4. They indicate good compatibility with the LHCXSWG predictions.

The measured differential cross sections and their comparisons to SM predictions are presented in figures 8–10. The data are compared to SM predictions constructed from the ggF predictions provided by NNLOPS, MG5_AMC@NLO_FxFx, and, for $p_{\text{T},4\ell}$ and $|y_{4\ell}|$, by HRes. All ggF samples are normalized using the LHCXSWG cross section. Predictions for all other Higgs boson production modes are normalized as discussed in section 3. The shaded bands on the expected cross sections indicate the PDF and scale uncertainties. The

Cross section [fb]	Data ($\pm$ (stat) $\pm$ (sys))		LHCXSWG prediction	p-value [%]
$\sigma_{4\mu}$	0.92	$^{+0.25}_{-0.23}$ $^{+0.07}_{-0.05}$	0.880 ± 0.039	88
σ_{4e}	0.67	$^{+0.28}_{-0.23}$ $^{+0.08}_{-0.06}$	0.688 ± 0.031	96
$\sigma_{2\mu2e}$	0.84	$^{+0.28}_{-0.24}$ $^{+0.09}_{-0.06}$	0.625 ± 0.028	39
$\sigma_{2e2\mu}$	1.18	$^{+0.30}_{-0.26}$ $^{+0.07}_{-0.05}$	0.717 ± 0.032	7
$\sigma_{4\mu+4e}$	1.59	$^{+0.37}_{-0.33}$ $^{+0.12}_{-0.10}$	1.57 ± 0.07	65
$\sigma_{2\mu2e+2e2\mu}$	2.02	$^{+0.40}_{-0.36}$ $^{+0.14}_{-0.11}$	1.34 ± 0.06	6
σ_{sum}	3.61 $\pm$ 0.50	$^{+0.26}_{-0.21}$	2.91 ± 0.13	19
σ_{comb}	3.62 $\pm$ 0.50	$^{+0.25}_{-0.20}$	2.91 ± 0.13	18
σ_{tot} [pb]	69 $^{+10}_{-9}$	± 5	55.6 ± 2.5	19

Table 4. The fiducial and total cross sections of Higgs boson production measured in the 4ℓ final state. The fiducial cross sections are given separately for each decay channel, and for same- and opposite-flavour decays. The inclusive fiducial cross section is measured as the sum of all channels, as well as by combining the per-channel measurements assuming SM $ZZ^* \to 4\ell$ branching ratios. The LHCXSWG prediction is accurate to N3LO in QCD for the ggF process. For the fiducial cross-section predictions, the LHCXSWG cross sections are multiplied by the acceptances determined using the NNLOPS sample for ggF and the samples discussed in section 3 for the other production modes. The p-values indicating the compatibility of the measurement and the SM prediction are shown as well. They do not include the systematic uncertainty in the theoretical predictions.

PDF inputs used for each prediction are varied according to the eigenvectors of each PDF set. The renormalization and factorization scales are varied by factors of 2.0 and 0.5. The figures include the p-values quantifying the compatibility of the measurement and the SM predictions.

The observed small excess in the measured inclusive cross section cannot be traced to a particular phase space region. Figure 8 shows differential fiducial cross sections as a function of $p_{\mathrm{T},4\ell}$, $|y_{4\ell}|$, m_{34}, and $|\cos\theta^*|$. The measured cross sections at high $p_{\mathrm{T},4\ell}$ are slightly higher than the predictions, but the distribution is consistent with the SM predictions within the uncertainties. The observation of good agreement between data and SM prediction of the cross sections as a function of m_{34} and $|\cos\theta^*|$ is consistent with dedicated measurements that have shown the Higgs boson to be a scalar particle with even parity [3, 4].

In figure 9, the differential fiducial cross sections as a function of N_{jets}, $p_{\mathrm{T}}^{\mathrm{lead.jet}}$, m_{jj}, and $\Delta\phi_{\mathrm{jj}}$ are shown. Agreement between data and theory is still good, but becomes a bit worse for higher jet multiplicities and higher $p_{\mathrm{T}}^{\mathrm{lead.jet}}$, similarly to what was observed in the ATLAS analyses at $\sqrt{s} = 8\,\mathrm{TeV}$ [7–9]. MG5_AMC@NLO_FxFx describes the jet multiplicities slightly better than NNLOPS. For large values of m_{jj} and the left bin of the $\Delta\phi_{\mathrm{jj}}$ distribution, the measured cross section is more than twice the predicted value ($\sim$2 and $\sim$1.5 standard deviations respectively).

Figure 10 presents the differential fiducial cross sections as a function of $p_{\mathrm{T},4\ell}$ for different jet multiplicities as well as the cross sections measured in regions of the m_{12} vs m_{34}
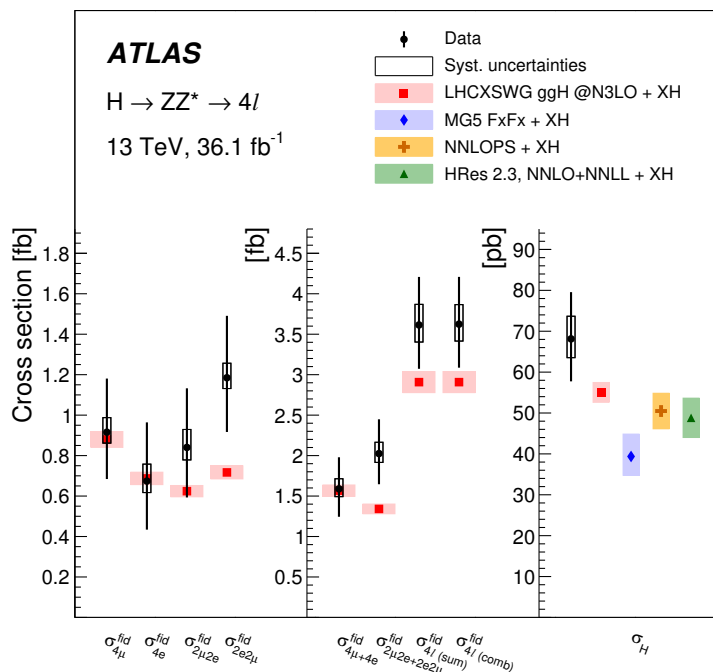
Figure 7. The fiducial cross sections (left two panels) and total cross section (right panel) of Higgs boson production measured in the 4ℓ final state. The fiducial cross sections are shown separately for each decay channel, and for same- and opposite-flavour decays. The inclusive fiducial cross section is measured as the sum of all channels, as well as by combining the per-channel measurements assuming SM $ZZ^* \to 4\ell$ branching ratios. The LHCXSWG prediction is accurate to N3LO in QCD for the ggF process. For the fiducial cross-section predictions, the LHCXSWG cross sections are multiplied by the acceptances determined using the NNLOPS sample for ggF and the samples discussed in section 3 for the other production modes. For the total cross section, the cross-section predictions by the generators NNLOPS, HRES, and MG5_AMC@NLO_FxFx are also shown. The cross sections for all other Higgs boson production modes XH are added. The error bars on the data points show the total uncertainties, while the systematic uncertainties are indicated by the boxes. The shaded bands around the theoretical predictions indicate the PDF and scale uncertainties.

distribution. For the latter, the m_{12} vs m_{34} kinematic plane is divided into five regions and projected onto a one-dimensional distribution, as shown in figure 3(d). The split into different jet multiplicities allows one to probe perturbative QCD calculations for different production modes. The 0-jet bin is dominated by Higgs boson events produced through ggF, while the $\geq$ 2-jet bin is enriched with VBF events. No significant deviation from the predictions is seen, as indicated by the p-values which reflect the level of agreement for the three jet bins together, treating them as a two-dimensional distribution. The higher values of the measured cross sections in the $\geq$ 2-jet bin reflect the observations in figure 9(a). The data and the predictions also agree well for the m_{12} vs m_{34} distribution.

The differential fiducial cross sections can be interpreted in the context of searches for physics beyond the SM. In the absence of significant deviations from the SM predictions, limits are set on modified Higgs boson interactions within the framework of pseudo-
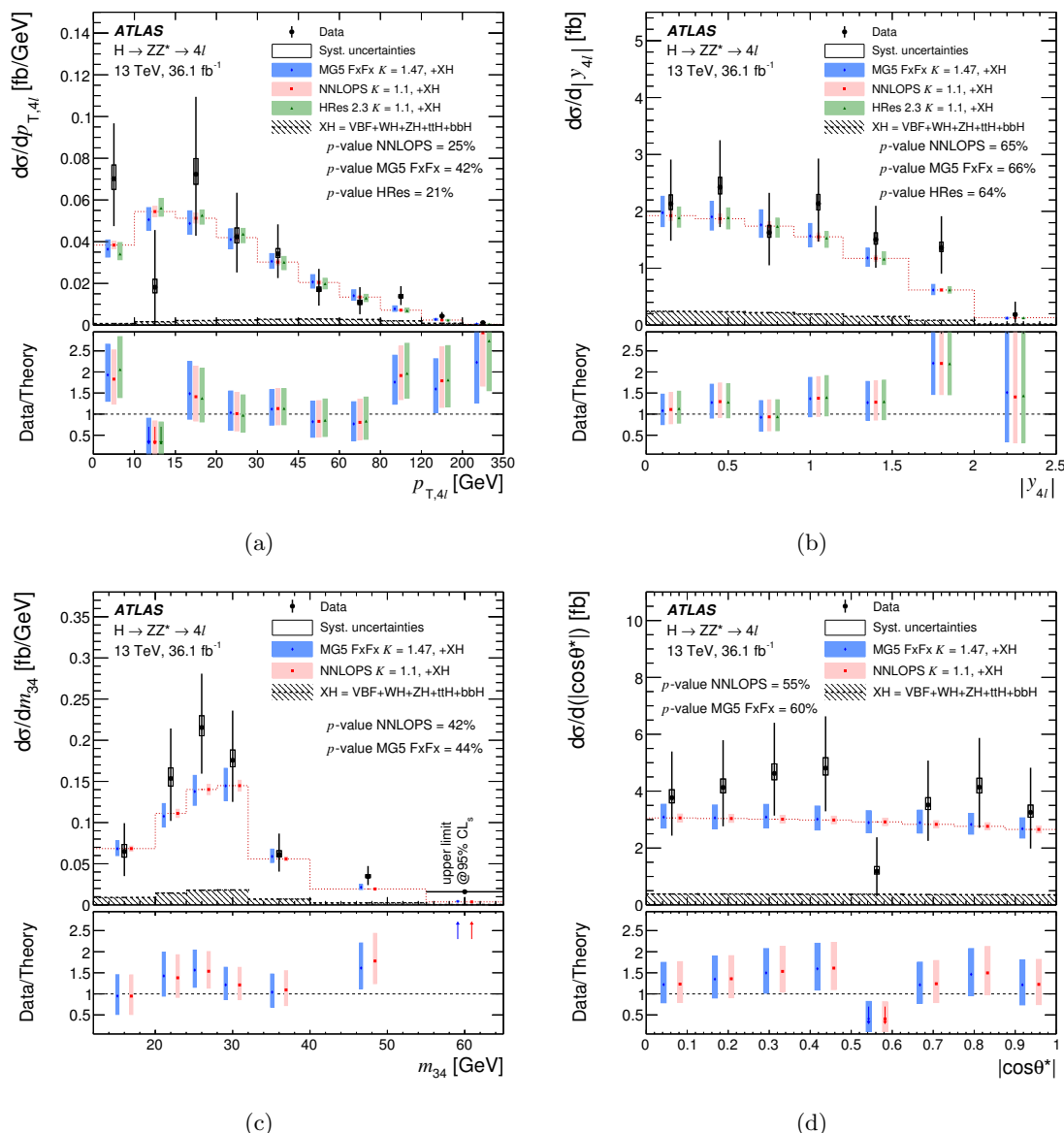
Figure 8. Differential fiducial cross sections, for (a) the transverse momentum $p_{\mathrm{T},4\ell}$ of the Higgs boson, (b) the absolute value of the rapidity $|y_{4\ell}|$ of the Higgs boson, (c) the invariant mass of the subleading lepton pair m_{34}, (d) the magnitude of the cosine of the decay angle of the leading lepton pair in the four-lepton rest frame with respect to the beam axis $|\cos\theta^*|$. The measured cross sections are compared to ggF predictions by NNLOPS, MG5_AMC@NLO_FxFx, and, for $p_{\mathrm{T},4\ell}$ and $|y_{4\ell}|$, by HRES, all normalized to the N3LO cross section with the listed K-factors. Predictions for all other Higgs boson production modes XH are added. The error bars on the data points show the total uncertainties, while the systematic uncertainties are indicated by the boxes. The shaded bands on the expected cross sections indicate the PDF and scale uncertainties. The p-values indicating the compatibility of the measurement and the SM prediction are shown as well. They do not include the systematic uncertainty in the theoretical predictions.
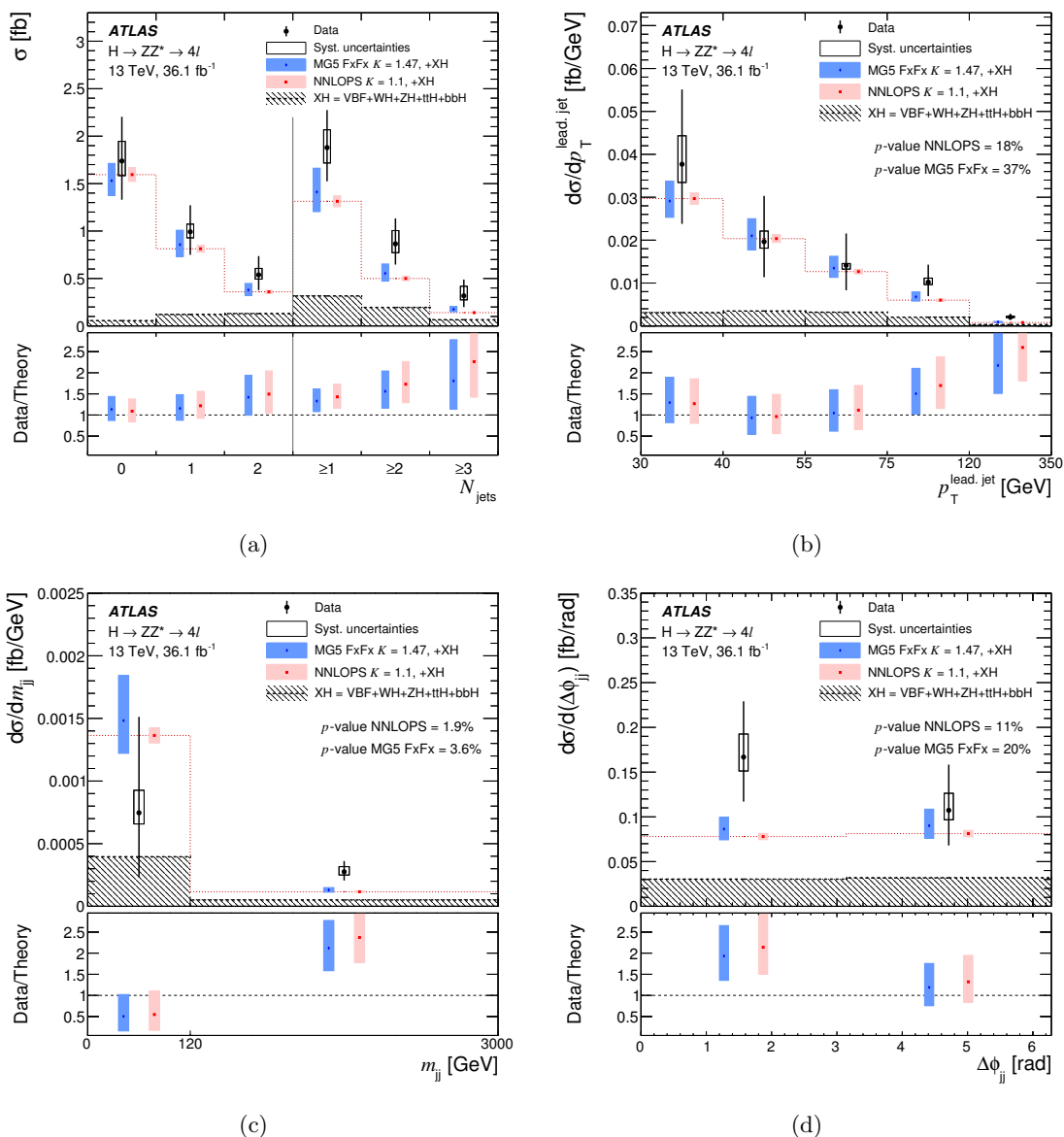
Figure 9. Differential fiducial cross sections, for (a) the number of jets N_{jets}, (b) the transverse momentum $p_T^{lead.jet}$ of the leading jet, (c) the invariant mass of the two leading jets m_{jj}, (d) the angle between the two leading jets in the transverse plane $\Delta\phi_{jj}$. The measured cross sections are compared to ggF predictions by NNLOPS and MG5_AMC@NLO_FxFx, all normalized to the N3LO cross section with the listed K-factors. Predictions for all other Higgs boson production modes XH are added. The error bars on the data points show the total uncertainties, while the systematic uncertainties are indicated by the boxes. The shaded bands on the expected cross sections indicate the PDF and scale uncertainties. The p-values indicating the compatibility of the measurement and the SM prediction are shown as well. They do not include the systematic uncertainty in the theoretical predictions.
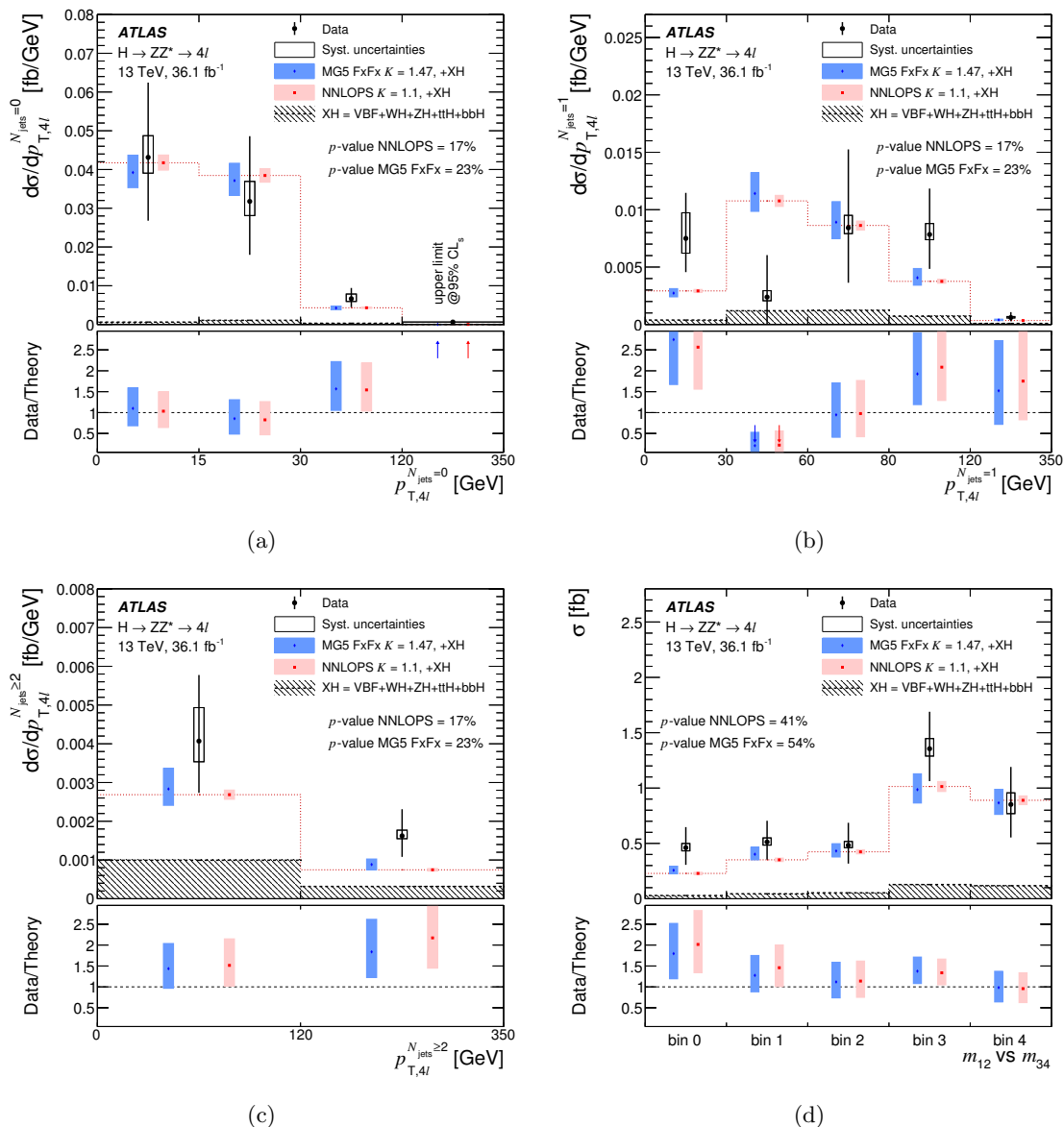
Figure 10. Figures (a)–(c) show differential fiducial cross sections of the transverse momentum $p_{\mathrm{T},4\ell}$ of the Higgs boson for different jet multiplicities N_{jets}, and (d) shows the invariant mass of the leading lepton pair vs that of the subleading pair, m_{12} vs m_{34}. The binning of m_{12} vs m_{34} is the same as presented in figure 3(d). The measured cross sections are compared to ggF predictions by NNLOPS and MG5_AMC@NLO_FxFx, all normalized to the N3LO cross section with the listed K-factors. Predictions for all other Higgs boson production modes XH are added. The error bars on the data points show the total uncertainties, while the systematic uncertainties are indicated by the boxes. The shaded bands on the expected cross sections indicate the PDF and scale uncertainties. For the cross sections as a function of $p_{\mathrm{T},4\ell}$, the p-values reflect the level of agreement for the three jet bins together, treating them as a two-dimensional distribution.
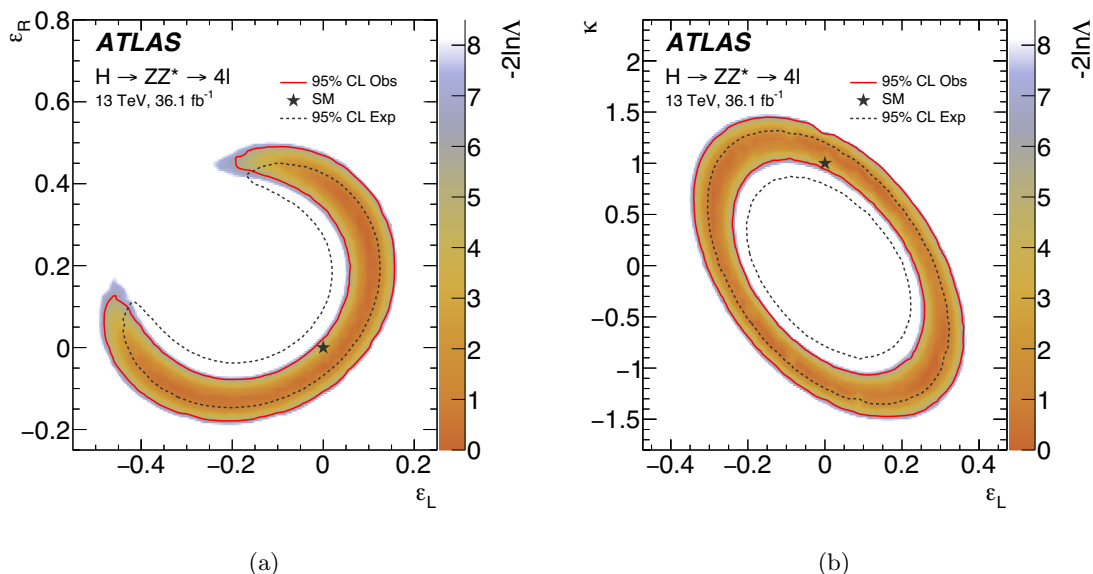
Figure 11. Limits on modified Higgs boson decays within the framework of pseudo-observables [15, 81]. In (a), the limits are extracted in the plane of ε_L and ε_R, which modify the contact terms between the Higgs boson and left- and right-handed leptons, assuming lepton-flavour universality. In (b), the tested parameters are ε_L and κ. The latter modifies the coupling of the Higgs boson to Z bosons. The allowed observed area at the 95% CL is surrounded by the red solid line. This can be compared to the SM prediction, which is indicated by the black star and the black dotted line. The coloured scale indicates the values of $-2\ln\Lambda$.

observables [15, 81]. In this paper, the couplings related to the contact interaction of the Higgs boson decay are considered, ε_L and ε_R, which modify, in a flavour-universal way, the contact terms between the Higgs boson, the Z boson, and left- or right-handed leptons. Since the contact terms have the same Lorentz structure as the SM term, they only affect the dilepton invariant mass spectra, while the lepton angular distributions are not modified. The difference in χ^2 between the measured and predicted cross sections in the m_{12} vs m_{34} observable plane is therefore used to constrain the possible contributions from contact interactions. It was checked with pseudo experiments that the χ^2 distribution agrees with the hypothesis of two degrees of freedom. Assuming the SM values for all but the tested parameters, limits are set on the contact-interaction coupling strength as shown in figure 11. Two parameter planes are considered: ε_L vs ε_R, as well as ε_L vs κ, where κ is the coupling of the Higgs boson to the Z bosons and $\varepsilon_R = 0.48 \cdot \varepsilon_L$ [81]. Since the addition of the contact terms changes the Higgs boson production rate, in principle limits could be set based on the inclusive Higgs boson cross sections alone. In this case, the obtained allowed area in figure 11(a) would be circular, but the addition of the invariant mass spectra improves the sensitivity, especially for negative ε_L and positive ε_R. The addition of the shape information also improves the limit in the ε_L vs κ parameter plane. It can be seen that the expected and observed limits are slightly shifted with respect to each other, but no significant deviation is observed.

11 Conclusion

Measurements of the inclusive and differential fiducial cross sections of Higgs boson production in the $H \to ZZ^* \to 4\ell$ decay channel are presented. They are based on data extracted from $36.1\,\text{fb}^{-1}$ of $\sqrt{s} = 13\,\text{TeV}$ proton-proton collisions recorded by the ATLAS detector at the LHC in 2015 and 2016. The inclusive fiducial cross section in the $H \to ZZ^* \to 4\ell$ decay channel is measured to be $3.62 \pm 0.50\,(\text{stat})\,^{+0.25}_{-0.20}\,(\text{sys})\,\text{fb}$, in agreement with the Standard Model prediction of $2.91 \pm 0.13\,\text{fb}$. The inclusive fiducial cross section is also extrapolated to the total phase space which includes all Standard Model Higgs boson decays. Several differential fiducial cross sections are measured for observables sensitive to the Higgs boson production and decay, including kinematic distributions of the jets produced together with the Higgs boson. Good agreement is found between the data and the predictions of the Standard Model. The extracted cross-section distributions are used to constrain anomalous Higgs boson interactions with Standard Model particles using the pseudo-observable framework.

The crucial computing support from all WLCG partners is acknowledged gratefully, in particular from CERN, the ATLAS Tier-1 facilities at TRIUMF (Canada), NDGF (Denmark, Norway, Sweden), CC-IN2P3 (France), KIT/GridKA (Germany), INFN-CNAF (Italy), NL-T1 (Netherlands), PIC (Spain), ASGC (Taiwan), RAL (U.K.) and BNL (U.S.A.), the Tier-2 facilities worldwide and large non-WLCG resource providers. Major contributors of computing resources are listed in ref. [119].

References

[1] ATLAS, CMS collaborations, *Combined Measurement of the Higgs Boson Mass in pp Collisions at $\sqrt{s} = 7$ and $8\,TeV$ with the ATLAS and CMS Experiments*, *Phys. Rev. Lett.* **114** (2015) 191803 [arXiv:1503.07589] [INSPIRE].

[2] ATLAS, CMS collaborations, *Measurements of the Higgs boson production and decay rates and constraints on its couplings from a combined ATLAS and CMS analysis of the LHC pp collision data at $\sqrt{s} = 7$ and $8\,TeV$*, *JHEP* **08** (2016) 045 [arXiv:1606.02266] [INSPIRE].

[3] ATLAS collaboration, *Evidence for the spin-0 nature of the Higgs boson using ATLAS data*, *Phys. Lett.* **B 726** (2013) 120 [arXiv:1307.1432] [INSPIRE].

[4] ATLAS collaboration, *Study of the spin and parity of the Higgs boson in diboson decays with the ATLAS detector*, *Eur. Phys. J.* **C 75** (2015) 476 [arXiv:1506.05669] [INSPIRE].

[5] CMS collaboration, *Constraints on the spin-parity and anomalous HVV couplings of the Higgs boson in proton collisions at 7 and $8\,TeV$*, *Phys. Rev.* **D 92** (2015) 012004 [arXiv:1411.3441] [INSPIRE].

[6] CMS collaboration, *Combined search for anomalous pseudoscalar HVV couplings in VH(H → b̄b) production and H → VV decay*, *Phys. Lett.* **B 759** (2016) 672 [arXiv:1602.04305] [INSPIRE].

[7] ATLAS collaboration, *Fiducial and differential cross sections of Higgs boson production measured in the four-lepton decay channel in pp collisions at $\sqrt{s} = 8\,TeV$ with the ATLAS detector*, *Phys. Lett.* **B 738** (2014) 234 [arXiv:1408.3226] [INSPIRE].

[8] ATLAS collaboration, *Measurements of fiducial and differential cross sections for Higgs boson production in the diphoton decay channel at $\sqrt{s} = 8\,TeV$ with ATLAS*, *JHEP* **09** (2014) 112 [arXiv:1407.4222] [INSPIRE].

[9] ATLAS collaboration, *Measurements of the Total and Differential Higgs Boson Production Cross Sections Combining the H → γγ and H → ZZ* → 4ℓ Decay Channels at $\sqrt{s} = 8\,TeV$ with the ATLAS Detector*, *Phys. Rev. Lett.* **115** (2015) 091801 [arXiv:1504.05833] [INSPIRE].

[10] ATLAS collaboration, *Measurement of fiducial differential cross sections of gluon-fusion production of Higgs bosons decaying to WW* → eνμν with the ATLAS detector at $\sqrt{s} = 8\,TeV$*, *JHEP* **08** (2016) 104 [arXiv:1604.02997] [INSPIRE].

[11] CMS collaboration, *Measurement of differential and integrated fiducial cross sections for Higgs boson production in the four-lepton decay channel in pp collisions at $\sqrt{s} = 7$ and $8\,TeV$*, *JHEP* **04** (2016) 005 [arXiv:1512.08377] [INSPIRE].

[12] CMS collaboration, *Measurement of differential cross sections for Higgs boson production in the diphoton decay channel in pp collisions at $\sqrt{s} = 8$ TeV*, *Eur. Phys. J.* **C 76** (2016) 13 [arXiv:1508.07819] [INSPIRE].

[13] M. Grazzini, A. Ilnicka, M. Spira and M. Wiesemann, *Modeling BSM effects on the Higgs transverse-momentum spectrum in an EFT approach*, *JHEP* **03** (2017) 115 [arXiv:1612.00283] [INSPIRE].

[14] J.M. Campbell, R.K. Ellis and G. Zanderighi, *Next-to-Leading order Higgs + 2 jet production via gluon fusion*, *JHEP* **10** (2006) 028 [hep-ph/0608194] [INSPIRE].

[15] M. Gonzalez-Alonso, A. Greljo, G. Isidori and D. Marzocca, *Pseudo-observables in Higgs decays*, *Eur. Phys. J.* **C 75** (2015) 128 [arXiv:1412.6038] [INSPIRE].

[16] LHC HIGGS CROSS SECTION Working Group, J.R. Andersen et al., *Handbook of LHC Higgs Cross Sections: 3. Higgs Properties*, CERN-2013-004 [arXiv:1307.1347] [INSPIRE].

[17] ATLAS collaboration, *The ATLAS Experiment at the CERN Large Hadron Collider*, 2008 *JINST* **3** S08003 [INSPIRE].

[18] ATLAS collaboration, *ATLAS Insertable B-Layer Technical Design Report*, ATLAS-TDR-19.

[19] ATLAS collaboration, *ATLAS Insertable B-Layer Technical Design Report Addendum*, ATLAS-TDR-19-ADD-1.

[20] ATLAS collaboration, *Performance of the ATLAS Trigger System in 2015*, *Eur. Phys. J.* **C 77** (2017) 317 [arXiv:1611.09661] [INSPIRE].

[21] LHC HIGGS CROSS SECTION Working Group, S. Dittmaier et al., *Handbook of LHC Higgs Cross Sections: 1. Inclusive Observables*, CERN-2011-002 [arXiv:1101.0593] [INSPIRE].

[22] LHC HIGGS CROSS SECTION Working Group, S. Dittmaier et al., *Handbook of LHC Higgs Cross Sections: 2. Differential Distributions*, CERN-2012-002 [arXiv:1201.3084] [INSPIRE].

[23] LHC HIGGS CROSS SECTION Working Group, D. de Florian et al., *Handbook of LHC Higgs Cross Sections: 4. Deciphering the Nature of the Higgs Sector*, CERN-2017-002 [arXiv:1610.07922] [INSPIRE].

[24] A. Djouadi, M. Spira and P.M. Zerwas, *Production of Higgs bosons in proton colliders: QCD corrections*, *Phys. Lett.* **B 264** (1991) 440 [INSPIRE].

[25] S. Dawson, *Radiative corrections to Higgs boson production*, *Nucl. Phys.* **B 359** (1991) 283 [INSPIRE].

[26] M. Spira, A. Djouadi, D. Graudenz and P.M. Zerwas, *Higgs boson production at the LHC*, *Nucl. Phys.* **B 453** (1995) 17 [hep-ph/9504378] [INSPIRE].

[27] R.V. Harlander and W.B. Kilgore, *Next-to-next-to-leading order Higgs production at hadron colliders*, *Phys. Rev. Lett.* **88** (2002) 201801 [hep-ph/0201206] [INSPIRE].

[28] C. Anastasiou and K. Melnikov, *Higgs boson production at hadron colliders in NNLO QCD*, *Nucl. Phys.* **B 646** (2002) 220 [hep-ph/0207004] [INSPIRE].

[29] V. Ravindran, J. Smith and W.L. van Neerven, *NNLO corrections to the total cross-section for Higgs boson production in hadron hadron collisions*, *Nucl. Phys.* **B 665** (2003) 325 [hep-ph/0302135] [INSPIRE].

[30] C. Anastasiou et al., *Higgs boson gluon-fusion production at threshold in N^3LO QCD*, *Phys. Lett.* **B 737** (2014) 325 [arXiv:1403.4616] [INSPIRE].

[31] C. Anastasiou et al., *Higgs boson gluon-fusion production beyond threshold in N^3LO QCD*, *JHEP* **03** (2015) 091 [arXiv:1411.3584] [InSPIRE].

[32] C. Anastasiou et al., *High precision determination of the gluon fusion Higgs boson cross-section at the LHC*, *JHEP* **05** (2016) 058 [arXiv:1602.00695] [InSPIRE].

[33] U. Aglietti, R. Bonciani, G. Degrassi and A. Vicini, *Two loop light fermion contribution to Higgs production and decays*, *Phys. Lett.* **B 595** (2004) 432 [hep-ph/0404071] [InSPIRE].

[34] S. Actis, G. Passarino, C. Sturm and S. Uccirati, *NLO Electroweak Corrections to Higgs Boson Production at Hadron Colliders*, *Phys. Lett.* **B 670** (2008) 12 [arXiv:0809.1301] [InSPIRE].

[35] D. de Florian and M. Grazzini, *Higgs production at the LHC: updated cross sections at $\sqrt{s} = 8\,TeV$*, *Phys. Lett.* **B 718** (2012) 117 [arXiv:1206.4133] [InSPIRE].

[36] C. Anastasiou, S. Buehler, F. Herzog and A. Lazopoulos, *Inclusive Higgs boson cross-section for the LHC at $8\,TeV$*, *JHEP* **04** (2012) 004 [arXiv:1202.3638] [InSPIRE].

[37] J. Baglio and A. Djouadi, *Higgs production at the LHC*, *JHEP* **03** (2011) 055 [arXiv:1012.0530] [InSPIRE].

[38] M. Ciccolini, A. Denner and S. Dittmaier, *Strong and electroweak corrections to the production of Higgs + 2-jets via weak interactions at the LHC*, *Phys. Rev. Lett.* **99** (2007) 161803 [arXiv:0707.0381] [InSPIRE].

[39] M. Ciccolini, A. Denner and S. Dittmaier, *Electroweak and QCD corrections to Higgs production via vector-boson fusion at the LHC*, *Phys. Rev.* **D 77** (2008) 013002 [arXiv:0710.4749] [InSPIRE].

[40] K. Arnold et al., *VBFNLO: A Parton level Monte Carlo for processes with electroweak bosons*, *Comput. Phys. Commun.* **180** (2009) 1661 [arXiv:0811.4559] [InSPIRE].

[41] P. Bolzoni, F. Maltoni, S.-O. Moch and M. Zaro, *Higgs production via vector-boson fusion at NNLO in QCD*, *Phys. Rev. Lett.* **105** (2010) 011801 [arXiv:1003.4451] [InSPIRE].

[42] T. Han and S. Willenbrock, *QCD correction to the $pp \to WH$ and ZH total cross-sections*, *Phys. Lett.* **B 273** (1991) 167 [InSPIRE].

[43] O. Brein, A. Djouadi and R. Harlander, *NNLO QCD corrections to the Higgs-strahlung processes at hadron colliders*, *Phys. Lett.* **B 579** (2004) 149 [hep-ph/0307206] [InSPIRE].

[44] M.L. Ciccolini, S. Dittmaier and M. Krämer, *Electroweak radiative corrections to associated WH and ZH production at hadron colliders*, *Phys. Rev.* **D 68** (2003) 073003 [hep-ph/0306234] [InSPIRE].

[45] W. Beenakker, S. Dittmaier, M. Krämer, B. Plumper, M. Spira and P.M. Zerwas, *Higgs radiation off top quarks at the Tevatron and the LHC*, *Phys. Rev. Lett.* **87** (2001) 201805 [hep-ph/0107081] [InSPIRE].

[46] W. Beenakker, S. Dittmaier, M. Krämer, B. Plumper, M. Spira and P.M. Zerwas, *NLO QCD corrections to $t\bar{t}H$ production in hadron collisions*, *Nucl. Phys.* **B 653** (2003) 151 [hep-ph/0211352] [InSPIRE].

[47] S. Dawson, L.H. Orr, L. Reina and D. Wackeroth, *Next-to-leading order QCD corrections to $pp \to t\bar{t}h$ at the CERN Large Hadron Collider*, *Phys. Rev.* **D 67** (2003) 071503 [hep-ph/0211438] [InSPIRE].

[48] S. Dawson, C. Jackson, L.H. Orr, L. Reina and D. Wackeroth, *Associated Higgs production with top quarks at the large hadron collider: NLO QCD corrections*, *Phys. Rev.* **D 68** (2003) 034022 [hep-ph/0305087] [InSPIRE].

[49] R. Harlander, M. Krämer and M. Schumacher, *Bottom-quark associated Higgs-boson production: reconciling the four- and five-flavour scheme approach*, arXiv:1112.3478 [INSPIRE].

[50] A. Djouadi, J. Kalinowski and M. Spira, *HDECAY: A program for Higgs boson decays in the standard model and its supersymmetric extension*, *Comput. Phys. Commun.* **108** (1998) 56 [hep-ph/9704448] [INSPIRE].

[51] A. Bredenstein, A. Denner, S. Dittmaier and M.M. Weber, *Precise predictions for the Higgs-boson decay $H \to WW/ZZ \to 4$ leptons*, *Phys. Rev.* **D 74** (2006) 013004 [hep-ph/0604011] [INSPIRE].

[52] A. Bredenstein, A. Denner, S. Dittmaier and M.M. Weber, *Radiative corrections to the semileptonic and hadronic Higgs-boson decays $H \to WW/ZZ \to 4$ fermions*, *JHEP* **02** (2007) 080 [hep-ph/0611234] [INSPIRE].

[53] P. Nason, *A new method for combining NLO QCD with shower Monte Carlo algorithms*, *JHEP* **11** (2004) 040 [hep-ph/0409146] [INSPIRE].

[54] S. Frixione, P. Nason and C. Oleari, *Matching NLO QCD computations with Parton Shower simulations: the POWHEG method*, *JHEP* **11** (2007) 070 [arXiv:0709.2092] [INSPIRE].

[55] S. Alioli, P. Nason, C. Oleari and E. Re, *A general framework for implementing NLO calculations in shower Monte Carlo programs: the POWHEG BOX*, *JHEP* **06** (2010) 043 [arXiv:1002.2581] [INSPIRE].

[56] J.M. Campbell, R.K. Ellis, R. Frederix, P. Nason, C. Oleari and C. Williams, *NLO Higgs Boson Production Plus One and Two Jets Using the POWHEG BOX, MadGraph4 and MCFM*, *JHEP* **07** (2012) 092 [arXiv:1202.5475] [INSPIRE].

[57] P. Nason and C. Oleari, *NLO Higgs boson production via vector-boson fusion matched with shower in POWHEG*, *JHEP* **02** (2010) 037 [arXiv:0911.5299] [INSPIRE].

[58] G. Luisoni, P. Nason, C. Oleari and F. Tramontano, *$HW^{\pm}/HZ + 0$ and 1 jet at NLO with the POWHEG BOX interfaced to GoSam and their merging within MiNLO*, *JHEP* **10** (2013) 083 [arXiv:1306.2542] [INSPIRE].

[59] J. Butterworth et al., *PDF4LHC recommendations for LHC Run II*, *J. Phys.* **G 43** (2016) 023001 [arXiv:1510.03865] [INSPIRE].

[60] K. Hamilton, P. Nason and G. Zanderighi, *MINLO: Multi-Scale Improved NLO*, *JHEP* **10** (2012) 155 [arXiv:1206.3572] [INSPIRE].

[61] K. Hamilton, P. Nason, C. Oleari and G. Zanderighi, *Merging $H/W/Z + 0$ and 1 jet at NLO with no merging scale: a path to parton shower + NNLO matching*, *JHEP* **05** (2013) 082 [arXiv:1212.4504] [INSPIRE].

[62] S. Catani and M. Grazzini, *An NNLO subtraction formalism in hadron collisions and its application to Higgs boson production at the LHC*, *Phys. Rev. Lett.* **98** (2007) 222002 [hep-ph/0703012] [INSPIRE].

[63] M. Grazzini, *NNLO predictions for the Higgs boson signal in the $H \to WW \to \ell\nu\ell\nu$ and $H \to ZZ \to 4\ell$ decay channels*, *JHEP* **02** (2008) 043 [arXiv:0801.3232] [INSPIRE].

[64] M. Grazzini and H. Sargsyan, *Heavy-quark mass effects in Higgs boson production at the LHC*, *JHEP* **09** (2013) 129 [arXiv:1306.4581] [INSPIRE].

[65] K. Hamilton, P. Nason, E. Re and G. Zanderighi, *NNLOPS simulation of Higgs boson production*, *JHEP* **10** (2013) 222 [arXiv:1309.0017] [INSPIRE].

[66] M. Wiesemann, R. Frederix, S. Frixione, V. Hirschi, F. Maltoni and P. Torrielli, *Higgs production in association with bottom quarks*, *JHEP* **02** (2015) 132 [arXiv:1409.5301] [INSPIRE].

[67] J. Alwall et al., *The automated computation of tree-level and next-to-leading order differential cross sections and their matching to parton shower simulations*, *JHEP* **07** (2014) 079 [arXiv:1405.0301] [INSPIRE].

[68] H.-L. Lai et al., *New parton distributions for collider physics*, *Phys. Rev.* **D 82** (2010) 074024 [arXiv:1007.2241] [INSPIRE].

[69] R.D. Ball et al., *Parton distributions with LHC data*, *Nucl. Phys.* **B 867** (2013) 244 [arXiv:1207.1303] [INSPIRE].

[70] T. Sjöstrand, S. Mrenna and P.Z. Skands, *PYTHIA 6.4 Physics and Manual*, *JHEP* **05** (2006) 026 [hep-ph/0603175] [INSPIRE].

[71] T. Sjöstrand, S. Mrenna and P.Z. Skands, *A Brief Introduction to PYTHIA 8.1*, *Comput. Phys. Commun.* **178** (2008) 852 [arXiv:0710.3820] [INSPIRE].

[72] ATLAS collaboration, *Measurement of the Z/γ^* boson transverse momentum distribution in pp collisions at $\sqrt{s} = 7$ TeV with the ATLAS detector*, *JHEP* **09** (2014) 145 [arXiv:1406.3660] [INSPIRE].

[73] M. Bahr et al., *HERWIG++ Physics and Manual*, *Eur. Phys. J.* **C 58** (2008) 639 [arXiv:0803.0883] [INSPIRE].

[74] J. Bellm et al., *HERWIG++ 2.7 Release Note*, arXiv:1310.6877 [INSPIRE].

[75] M.H. Seymour and A. Siodmok, *Constraining MPI models using $\sigma_{\rm eff}$ and recent Tevatron and LHC Underlying Event data*, *JHEP* **10** (2013) 113 [arXiv:1307.5015] [INSPIRE].

[76] R. Frederix and S. Frixione, *Merging meets matching in MC@NLO*, *JHEP* **12** (2012) 061 [arXiv:1209.6215] [INSPIRE].

[77] NNPDF collaboration, R.D. Ball et al., *Parton distributions for the LHC Run II*, *JHEP* **04** (2015) 040 [arXiv:1410.8849] [INSPIRE].

[78] ATLAS collaboration, *ATLAS Run 1 PYTHIA8 tunes*, ATL-PHYS-PUB-2014-021.

[79] D. de Florian, G. Ferrera, M. Grazzini and D. Tommasini, *Higgs boson production at the LHC: transverse momentum resummation effects in the $H \to 2\gamma, H \to WW \to \ell\nu\ell\nu$ and $H \to ZZ \to 4\ell$ decay modes*, *JHEP* **06** (2012) 132 [arXiv:1203.6321] [INSPIRE].

[80] A.D. Martin, W.J. Stirling, R.S. Thorne and G. Watt, *Parton distributions for the LHC*, *Eur. Phys. J.* **C 63** (2009) 189 [arXiv:0901.0002] [INSPIRE].

[81] M. Gonzalez-Alonso, A. Greljo, G. Isidori and D. Marzocca, *Electroweak bounds on Higgs pseudo-observables and $h \to 4\ell$ decays*, *Eur. Phys. J.* **C 75** (2015) 341 [arXiv:1504.04018] [INSPIRE].

[82] A. Alloul, N.D. Christensen, C. Degrande, C. Duhr and B. Fuks, *FeynRules 2.0 — A complete toolbox for tree-level phenomenology*, *Comput. Phys. Commun.* **185** (2014) 2250 [arXiv:1310.1921] [INSPIRE].

[83] T. Gleisberg et al., *Event generation with SHERPA 1.1*, *JHEP* **02** (2009) 007 [arXiv:0811.4622] [INSPIRE].

[84] T. Gleisberg and S. Hoeche, *Comix, a new matrix element generator*, *JHEP* **12** (2008) 039 [arXiv:0808.3674] [INSPIRE].

[85] F. Cascioli, P. Maierhofer and S. Pozzorini, *Scattering Amplitudes with Open Loops*, *Phys. Rev. Lett.* **108** (2012) 111601 [arXiv:1111.5206] [INSPIRE].

[86] S. Schumann and F. Krauss, *A parton shower algorithm based on Catani-Seymour dipole factorisation*, *JHEP* **03** (2008) 038 [arXiv:0709.1027] [INSPIRE].

[87] S. Hoeche, F. Krauss, M. Schonherr and F. Siegert, *QCD matrix elements + parton showers: The NLO case*, *JHEP* **04** (2013) 027 [arXiv:1207.5030] [INSPIRE].

[88] B. Biedermann, A. Denner, S. Dittmaier, L. Hofer and B. Jäger, *Electroweak corrections to* $pp \to \mu^+\mu^- e^+e^- + X$ *at the LHC: a Higgs background study*, *Phys. Rev. Lett.* **116** (2016) 161803 [arXiv:1601.07787] [INSPIRE].

[89] B. Biedermann, A. Denner, S. Dittmaier, L. Hofer and B. Jager, *Next-to-leading-order electroweak corrections to the production of four charged leptons at the LHC*, *JHEP* **01** (2017) 033 [arXiv:1611.05338] [INSPIRE].

[90] N. Kauer, C. O'Brien and E. Vryonidou, *Interference effects for* $H \to W W \to \ell\nu q\overline{q}'$ *and* $H \to ZZ \to \ell\ell q\overline{q}$ *searches in gluon fusion at the LHC*, *JHEP* **10** (2015) 074 [arXiv:1506.01694] [INSPIRE].

[91] F. Caola, K. Melnikov, R. Röntsch and L. Tancredi, *QCD corrections to ZZ production in gluon fusion at the LHC*, *Phys. Rev.* **D 92** (2015) 094028 [arXiv:1509.06734] [INSPIRE].

[92] F. Caola, K. Melnikov, R. Röntsch and L. Tancredi, *QCD corrections to* W^+W^- *production through gluon fusion*, *Phys. Lett.* **B 754** (2016) 275 [arXiv:1511.08617] [INSPIRE].

[93] J.M. Campbell, R.K. Ellis, M. Czakon and S. Kirchner, *Two loop correction to interference in* $gg \to ZZ$, *JHEP* **08** (2016) 011 [arXiv:1605.01380] [INSPIRE].

[94] M. Bonvini, F. Caola, S. Forte, K. Melnikov and G. Ridolfi, *Signal-background interference effects for* $gg \to H \to W^+W^-$ *beyond leading order*, *Phys. Rev.* **D 88** (2013) 034032 [arXiv:1304.3053] [INSPIRE].

[95] C.S. Li, H.T. Li, D.Y. Shao and J. Wang, *Soft gluon resummation in the signal-background interference process of* $gg(\to h^*) \to ZZ$, *JHEP* **08** (2015) 065 [arXiv:1504.02388] [INSPIRE].

[96] S. Alioli, F. Caola, G. Luisoni and R. Röntsch, *ZZ production in gluon fusion at NLO matched to parton-shower*, *Phys. Rev.* **D 95** (2017) 034042 [arXiv:1609.09719] [INSPIRE].

[97] K. Melnikov and F. Petriello, *Electroweak gauge boson production at hadron colliders through* $O(\alpha_s^2)$, *Phys. Rev.* **D 74** (2006) 114017 [hep-ph/0609070] [INSPIRE].

[98] C. Anastasiou, L.J. Dixon, K. Melnikov and F. Petriello, *High precision QCD at hadron colliders: Electroweak gauge boson rapidity distributions at NNLO*, *Phys. Rev.* **D 69** (2004) 094008 [hep-ph/0312266] [INSPIRE].

[99] P. Golonka and Z. Was, *PHOTOS Monte Carlo: A Precision tool for QED corrections in Z and W decays*, *Eur. Phys. J.* **C 45** (2006) 97 [hep-ph/0506026] [INSPIRE].

[100] S. Jadach, Z. Was, R. Decker and J.H. Kuhn, *The* τ *decay library TAUOLA: Version 2.4*, *Comput. Phys. Commun.* **76** (1993) 361 [INSPIRE].

[101] P. Golonka, B. Kersevan, T. Pierzchala, E. Richter-Was, Z. Was and M. Worek, *The Tauola photos F environment for the TAUOLA and PHOTOS packages: Release II*, *Comput. Phys. Commun.* **174** (2006) 818 [hep-ph/0312240] [INSPIRE].

[102] D.J. Lange, *The EvtGen particle decay simulation package*, *Nucl. Instrum. Meth.* **A 462** (2001) 152 [INSPIRE].

[103] P.Z. Skands, *Tuning Monte Carlo Generators: The Perugia Tunes*, *Phys. Rev.* **D 82** (2010) 074018 [arXiv:1005.3457] [INSPIRE].

[104] GEANT4 collaboration, S. Agostinelli et al., *GEANT4: A simulation toolkit*, *Nucl. Instrum. Meth.* **A 506** (2003) 250 [INSPIRE].

[105] ATLAS collaboration, *The ATLAS Simulation Infrastructure*, *Eur. Phys. J.* **C 70** (2010) 823 [arXiv:1005.4568] [INSPIRE].

[106] ATLAS collaboration, *Electron efficiency measurements with the ATLAS detector using the 2015 LHC proton-proton collision data*, ATLAS-CONF-2016-024.

[107] ATLAS collaboration, *Muon reconstruction performance of the ATLAS detector in proton-proton collision data at $\sqrt{s} = 13$ TeV*, *Eur. Phys. J.* **C 76** (2016) 292 [arXiv:1603.05598] [INSPIRE].

[108] M. Cacciari, G.P. Salam and G. Soyez, *The anti-k_t jet clustering algorithm*, *JHEP* **04** (2008) 063 [arXiv:0802.1189] [INSPIRE].

[109] M. Cacciari, G.P. Salam and G. Soyez, *FastJet User Manual*, *Eur. Phys. J.* **C 72** (2012) 1896 [arXiv:1111.6097] [INSPIRE].

[110] ATLAS collaboration, *Jet energy scale measurements and their systematic uncertainties in proton-proton collisions at $\sqrt{s} = 13$ TeV with the ATLAS detector*, arXiv:1703.09665 [INSPIRE].

[111] ATLAS collaboration, *Jet Calibration and Systematic Uncertainties for Jets Reconstructed in the ATLAS Detector at $\sqrt{s} = 13$ TeV*, ATL-PHYS-PUB-2015-015.

[112] ATLAS collaboration, *Measurements of Higgs boson production and couplings in the four-lepton channel in pp collisions at center-of-mass energies of 7 and 8 TeV with the ATLAS detector*, *Phys. Rev.* **D 91** (2015) 012006 [arXiv:1408.5191] [INSPIRE].

[113] M. Pivk and F.R. Le Diberder, *SPlot: A statistical tool to unfold data distributions*, *Nucl. Instrum. Meth.* **A 555** (2005) 356 [physics/0402083] [INSPIRE].

[114] G. Cowan, K. Cranmer, E. Gross and O. Vitells, *Asymptotic formulae for likelihood-based tests of new physics*, *Eur. Phys. J.* **C 71** (2011) 1554 [*Erratum ibid.* **C 73** (2013) 2501] [arXiv:1007.1727] [INSPIRE].

[115] A.L. Read, *Presentation of search results: The CL_S technique*, *J. Phys.* **G 28** (2002) 2693 [INSPIRE].

[116] ATLAS collaboration, *Electron and photon energy calibration with the ATLAS detector using LHC Run 1 data*, *Eur. Phys. J.* **C 74** (2014) 3071 [arXiv:1407.5063] [INSPIRE].

[117] ATLAS collaboration, *Luminosity determination in pp collisions at $\sqrt{s} = 8$ TeV using the ATLAS detector at the LHC*, *Eur. Phys. J.* **C 76** (2016) 653 [arXiv:1608.03953] [INSPIRE].

[118] G. D'Agostini, *A multidimensional unfolding method based on Bayes' theorem*, *Nucl. Instrum. Meth.* **A 362** (1995) 487 [INSPIRE].

[119] ATLAS collaboration, *ATLAS Computing Acknowledgements 2016–2017*, ATL-GEN-PUB-2016-002.

The ATLAS collaboration

M. Aaboud[137d], G. Aad[88], B. Abbott[115], O. Abdinov[12,*], B. Abeloos[119], S.H. Abidi[161],
O.S. AbouZeid[139], N.L. Abraham[151], H. Abramowicz[155], H. Abreu[154], R. Abreu[118],
Y. Abulaiti[148a,148b], B.S. Acharya[167a,167b,a], S. Adachi[157], L. Adamczyk[41a], J. Adelman[110],
M. Adersberger[102], T. Adye[133], A.A. Affolder[139], Y. Afik[154], T. Agatonovic-Jovin[14],
C. Agheorghiesei[28c], J.A. Aguilar-Saavedra[128a,128f], S.P. Ahlen[24], F. Ahmadov[68,b],
G. Aielli[135a,135b], S. Akatsuka[71], H. Akerstedt[148a,148b], T.P.A. Åkesson[84], E. Akilli[52],
A.V. Akimov[98], G.L. Alberghi[22a,22b], J. Albert[172], P. Albicocco[50], M.J. Alconada Verzini[74],
S.C. Alderweireldt[108], M. Aleksa[32], I.N. Aleksandrov[68], C. Alexa[28b], G. Alexander[155],
T. Alexopoulos[10], M. Alhroob[115], B. Ali[130], M. Aliev[76a,76b], G. Alimonti[94a], J. Alison[33],
S.P. Alkire[38], B.M.M. Allbrooke[151], B.W. Allen[118], P.P. Allport[19], A. Aloisio[106a,106b],
A. Alonso[39], F. Alonso[74], C. Alpigiani[140], A.A. Alshehri[56], M.I. Alstaty[88], B. Alvarez Gonzalez[32],
D. Álvarez Piqueras[170], M.G. Alviggi[106a,106b], B.T. Amadio[16], Y. Amaral Coutinho[26a],
C. Amelung[25], D. Amidei[92], S.P. Amor Dos Santos[128a,128c], S. Amoroso[32], G. Amundsen[25],
C. Anastopoulos[141], L.S. Ancu[52], N. Andari[19], T. Andeen[11], C.F. Anders[60b], J.K. Anders[77],
K.J. Anderson[33], A. Andreazza[94a,94b], V. Andrei[60a], S. Angelidakis[37], I. Angelozzi[109],
A. Angerami[38], A.V. Anisenkov[111,c], N. Anjos[13], A. Annovi[126a,126b], C. Antel[60a], M. Antonelli[50],
A. Antonov[100,*], D.J. Antrim[166], F. Anulli[134a], M. Aoki[69], L. Aperio Bella[32], G. Arabidze[93],
Y. Arai[69], J.P. Araque[128a], V. Araujo Ferraz[26a], A.T.H. Arce[48], R.E. Ardell[80], F.A. Arduh[74],
J-F. Arguin[97], S. Argyropoulos[66], M. Arik[20a], A.J. Armbruster[32], L.J. Armitage[79], O. Arnaez[161],
H. Arnold[51], M. Arratia[30], O. Arslan[23], A. Artamonov[99,*], G. Artoni[122], S. Artz[86], S. Asai[157],
N. Asbah[45], A. Ashkenazi[155], L. Asquith[151], K. Assamagan[27], R. Astalos[146a], M. Atkinson[169],
N.B. Atlay[143], K. Augsten[130], G. Avolio[32], B. Axen[16], M.K. Ayoub[35a], G. Azuelos[97,d],
A.E. Baas[60a], M.J. Baca[19], H. Bachacou[138], K. Bachas[76a,76b], M. Backes[122], P. Bagnaia[134a,134b],
M. Bahmani[42], H. Bahrasemani[144], J.T. Baines[133], M. Bajic[39], O.K. Baker[179], E.M. Baldin[111,c],
P. Balek[175], F. Balli[138], W.K. Balunas[124], E. Banas[42], A. Bandyopadhyay[23], Sw. Banerjee[176,e],
A.A.E. Bannoura[178], L. Barak[155], E.L. Barberio[91], D. Barberis[53a,53b], M. Barbero[88],
T. Barillari[103], M-S Barisits[32], J.T. Barkeloo[118], T. Barklow[145], N. Barlow[30], S.L. Barnes[36c],
B.M. Barnett[133], R.M. Barnett[16], Z. Barnovska-Blenessy[36a], A. Baroncelli[136a], G. Barone[25],
A.J. Barr[122], L. Barranco Navarro[170], F. Barreiro[85], J. Barreiro Guimarães da Costa[35a],
R. Bartoldus[145], A.E. Barton[75], P. Bartos[146a], A. Basalaev[125], A. Bassalat[119,f], R.L. Bates[56],
S.J. Batista[161], J.R. Batley[30], M. Battaglia[139], M. Bauce[134a,134b], F. Bauer[138], H.S. Bawa[145,g],
J.B. Beacham[113], M.D. Beattie[75], T. Beau[83], P.H. Beauchemin[165], P. Bechtle[23], H.P. Beck[18,h],
H.C. Beck[57], K. Becker[122], M. Becker[86], C. Becot[112], A.J. Beddall[20e], A. Beddall[20b],
V.A. Bednyakov[68], M. Bedognetti[109], C.P. Bee[150], T.A. Beermann[32], M. Begalli[26a], M. Begel[27],
J.K. Behr[45], A.S. Bell[81], G. Bella[155], L. Bellagamba[22a], A. Bellerive[31], M. Bellomo[154],
K. Belotskiy[100], O. Beltramello[32], N.L. Belyaev[100], O. Benary[155,*], D. Benchekroun[137a],
M. Bender[102], N. Benekos[10], Y. Benhammou[155], E. Benhar Noccioli[179], J. Benitez[66],
D.P. Benjamin[48], M. Benoit[52], J.R. Bensinger[25], S. Bentvelsen[109], L. Beresford[122], M. Beretta[50],
D. Berge[109], E. Bergeaas Kuutmann[168], N. Berger[5], J. Beringer[16], S. Berlendis[58],
N.R. Bernard[89], G. Bernardi[83], C. Bernius[145], F.U. Bernlochner[23], T. Berry[80], P. Berta[86],
C. Bertella[35a], G. Bertoli[148a,148b], I.A. Bertram[75], C. Bertsche[45], D. Bertsche[115], G.J. Besjes[39],
O. Bessidskaia Bylund[148a,148b], M. Bessner[45], N. Besson[138], A. Bethani[87], S. Bethke[103],
A.J. Bevan[79], J. Beyer[103], R.M. Bianchi[127], O. Biebel[102], D. Biedermann[17], R. Bielski[87],
K. Bierwagen[86], N.V. Biesuz[126a,126b], M. Biglietti[136a], T.R.V. Billoud[97], H. Bilokon[50],
M. Bindi[57], A. Bingul[20b], C. Bini[134a,134b], S. Biondi[22a,22b], T. Bisanz[57], C. Bittrich[47],
D.M. Bjergaard[48], J.E. Black[145], K.M. Black[24], R.E. Blair[6], T. Blazek[146a], I. Bloch[45],

C. Blocker[25], A. Blue[56], W. Blum[86,*], U. Blumenschein[79], S. Blunier[34a], G.J. Bobbink[109],
V.S. Bobrovnikov[111,c], S.S. Bocchetta[84], A. Bocci[48], C. Bock[102], M. Boehler[51], D. Boerner[178],
D. Bogavac[102], A.G. Bogdanchikov[111], C. Bohm[148a], V. Boisvert[80], P. Bokan[168,i], T. Bold[41a],
A.S. Boldyrev[101], A.E. Bolz[60b], M. Bomben[83], M. Bona[79], M. Boonekamp[138], A. Borisov[132],
G. Borissov[75], J. Bortfeldt[32], D. Bortoletto[122], V. Bortolotto[62a,62b,62c], D. Boscherini[22a],
M. Bosman[13], J.D. Bossio Sola[29], J. Boudreau[127], J. Bouffard[2], E.V. Bouhova-Thacker[75],
D. Boumediene[37], C. Bourdarios[119], S.K. Boutle[56], A. Boveia[113], J. Boyd[32], I.R. Boyko[68],
J. Bracinik[19], A. Brandt[8], G. Brandt[57], O. Brandt[60a], F. Braren[45], U. Bratzler[158], B. Brau[89],
J.E. Brau[118], W.D. Breaden Madden[56], K. Brendlinger[45], A.J. Brennan[91], L. Brenner[109],
R. Brenner[168], S. Bressler[175], D.L. Briglin[19], T.M. Bristow[49], D. Britton[56], D. Britzger[45],
F.M. Brochu[30], I. Brock[23], R. Brock[93], G. Brooijmans[38], T. Brooks[80], W.K. Brooks[34b],
J. Brosamer[16], E. Brost[110], J.H Broughton[19], P.A. Bruckman de Renstrom[42], D. Bruncko[146b],
A. Bruni[22a], G. Bruni[22a], L.S. Bruni[109], S. Bruno[135a,135b], BH Brunt[30], M. Bruschi[22a],
N. Bruscino[127], P. Bryant[33], L. Bryngemark[45], T. Buanes[15], Q. Buat[144], P. Buchholz[143],
A.G. Buckley[56], I.A. Budagov[68], F. Buehrer[51], M.K. Bugge[121], O. Bulekov[100], D. Bullock[8],
T.J. Burch[110], S. Burdin[77], C.D. Burgard[51], A.M. Burger[5], B. Burghgrave[110], K. Burka[42],
S. Burke[133], I. Burmeister[46], J.T.P. Burr[122], E. Busato[37], D. Büscher[51], V. Büscher[86],
P. Bussey[56], J.M. Butler[24], C.M. Buttar[56], J.M. Butterworth[81], P. Butti[32], W. Buttinger[27],
A. Buzatu[153], A.R. Buzykaev[111,c], S. Cabrera Urbán[170], D. Caforio[130], V.M. Cairo[40a,40b],
O. Cakir[4a], N. Calace[52], P. Calafiura[16], A. Calandri[88], G. Calderini[83], P. Calfayan[64],
G. Callea[40a,40b], L.P. Caloba[26a], S. Calvente Lopez[85], D. Calvet[37], S. Calvet[37], T.P. Calvet[88],
R. Camacho Toro[33], S. Camarda[32], P. Camarri[135a,135b], D. Cameron[121],
R. Caminal Armadans[169], C. Camincher[58], S. Campana[32], M. Campanelli[81], A. Camplani[94a,94b],
A. Campoverde[143], V. Canale[106a,106b], M. Cano Bret[36c], J. Cantero[116], T. Cao[155],
M.D.M. Capeans Garrido[32], I. Caprini[28b], M. Caprini[28b], M. Capua[40a,40b], R.M. Carbone[38],
R. Cardarelli[135a], F. Cardillo[51], I. Carli[131], T. Carli[32], G. Carlino[106a], B.T. Carlson[127],
L. Carminati[94a,94b], R.M.D. Carney[148a,148b], S. Caron[108], E. Carquin[34b], S. Carrá[94a,94b],
G.D. Carrillo-Montoya[32], D. Casadei[19], M.P. Casado[13,j], M. Casolino[13], D.W. Casper[166],
R. Castelijn[109], V. Castillo Gimenez[170], N.F. Castro[128a,k], A. Catinaccio[32], J.R. Catmore[121],
A. Cattai[32], J. Caudron[23], V. Cavaliere[169], E. Cavallaro[13], D. Cavalli[94a], M. Cavalli-Sforza[13],
V. Cavasinni[126a,126b], E. Celebi[20d], F. Ceradini[136a,136b], L. Cerda Alberich[170], A.S. Cerqueira[26b],
A. Cerri[151], L. Cerrito[135a,135b], F. Cerutti[16], A. Cervelli[22a,22b], S.A. Cetin[20d], A. Chafaq[137a],
D. Chakraborty[110], S.K. Chan[59], W.S. Chan[109], Y.L. Chan[62a], P. Chang[169], J.D. Chapman[30],
D.G. Charlton[19], C.C. Chau[31], C.A. Chavez Barajas[151], S. Che[113], S. Cheatham[167a,167c],
A. Chegwidden[93], S. Chekanov[6], S.V. Chekulaev[163a], G.A. Chelkov[68,l], M.A. Chelstowska[32],
C. Chen[36a], C. Chen[67], H. Chen[27], J. Chen[36a], S. Chen[35b], S. Chen[157], X. Chen[35c,m],
Y. Chen[70], H.C. Cheng[92], H.J. Cheng[35a], A. Cheplakov[68], E. Cheremushkina[132],
R. Cherkaoui El Moursli[137e], E. Cheu[7], K. Cheung[63], L. Chevalier[138], V. Chiarella[50],
G. Chiarelli[126a,126b], G. Chiodini[76a], A.S. Chisholm[32], A. Chitan[28b], Y.H. Chiu[172],
M.V. Chizhov[68], K. Choi[64], A.R. Chomont[37], S. Chouridou[156], Y.S. Chow[62a],
V. Christodoulou[81], M.C. Chu[62a], J. Chudoba[129], A.J. Chuinard[90], J.J. Chwastowski[42],
L. Chytka[117], A.K. Ciftci[4a], D. Cinca[46], V. Cindro[78], I.A. Cioara[23], A. Ciocio[16],
F. Cirotto[106a,106b], Z.H. Citron[175], M. Citterio[94a], M. Ciubancan[28b], A. Clark[52], B.L. Clark[59],
M.R. Clark[38], P.J. Clark[49], R.N. Clarke[16], C. Clement[148a,148b], Y. Coadou[88], M. Cobal[167a,167c],
A. Coccaro[52], J. Cochran[67], L. Colasurdo[108], B. Cole[38], A.P. Colijn[109], J. Collot[58],
T. Colombo[166], P. Conde Muiño[128a,128b], E. Coniavitis[51], S.H. Connell[147b], I.A. Connelly[87],
S. Constantinescu[28b], G. Conti[32], F. Conventi[106a,n], M. Cooke[16], A.M. Cooper-Sarkar[122],
F. Cormier[171], K.J.R. Cormier[161], M. Corradi[134a,134b], F. Corriveau[90,o], A. Cortes-Gonzalez[32],

G. Costa[94a], M.J. Costa[170], D. Costanzo[141], G. Cottin[30], G. Cowan[80], B.E. Cox[87],
K. Cranmer[112], S.J. Crawley[56], R.A. Creager[124], G. Cree[31], S. Crépé-Renaudin[58], F. Crescioli[83],
W.A. Cribbs[148a,148b], M. Cristinziani[23], V. Croft[112], G. Crosetti[40a,40b], A. Cueto[85],
T. Cuhadar Donszelmann[141], A.R. Cukierman[145], J. Cummings[179], M. Curatolo[50], J. Cúth[86],
S. Czekierda[42], P. Czodrowski[32], G. D'amen[22a,22b], S. D'Auria[56], L. D'eramo[83], M. D'Onofrio[77],
M.J. Da Cunha Sargedas De Sousa[128a,128b], C. Da Via[87], W. Dabrowski[41a], T. Dado[146a],
T. Dai[92], O. Dale[15], F. Dallaire[97], C. Dallapiccola[89], M. Dam[39], J.R. Dandoy[124], M.F. Daneri[29],
N.P. Dang[176], A.C. Daniells[19], N.S. Dann[87], M. Danninger[171], M. Dano Hoffmann[138], V. Dao[150],
G. Darbo[53a], S. Darmora[8], J. Dassoulas[3], A. Dattagupta[118], T. Daubney[45], W. Davey[23],
C. David[45], T. Davidek[131], D.R. Davis[48], P. Davison[81], E. Dawe[91], I. Dawson[141], K. De[8],
R. de Asmundis[106a], A. De Benedetti[115], S. De Castro[22a,22b], S. De Cecco[83], N. De Groot[108],
P. de Jong[109], H. De la Torre[93], F. De Lorenzi[67], A. De Maria[57], D. De Pedis[134a],
A. De Salvo[134a], U. De Sanctis[135a,135b], A. De Santo[151], K. De Vasconcelos Corga[88],
J.B. De Vivie De Regie[119], R. Debbe[27], C. Debenedetti[139], D.V. Dedovich[68], N. Dehghanian[3],
I. Deigaard[109], M. Del Gaudio[40a,40b], J. Del Peso[85], D. Delgove[119], F. Deliot[138], C.M. Delitzsch[7],
A. Dell'Acqua[32], L. Dell'Asta[24], M. Dell'Orso[126a,126b], M. Della Pietra[106a,106b], D. della Volpe[52],
M. Delmastro[5], C. Delporte[119], P.A. Delsart[58], D.A. DeMarco[161], S. Demers[179], M. Demichev[68],
A. Demilly[83], S.P. Denisov[132], D. Denysiuk[138], D. Derendarz[42], J.E. Derkaoui[137d], F. Derue[83],
P. Dervan[77], K. Desch[23], C. Deterre[45], K. Dette[161], M.R. Devesa[29], P.O. Deviveiros[32],
A. Dewhurst[133], S. Dhaliwal[25], F.A. Di Bello[52], A. Di Ciaccio[135a,135b], L. Di Ciaccio[5],
W.K. Di Clemente[124], C. Di Donato[106a,106b], A. Di Girolamo[32], B. Di Girolamo[32],
B. Di Micco[136a,136b], R. Di Nardo[32], K.F. Di Petrillo[59], A. Di Simone[51], R. Di Sipio[161],
D. Di Valentino[31], C. Diaconu[88], M. Diamond[161], F.A. Dias[39], M.A. Diaz[34a], E.B. Diehl[92],
J. Dietrich[17], S. Díez Cornell[45], A. Dimitrievska[14], J. Dingfelder[23], P. Dita[28b], S. Dita[28b],
F. Dittus[32], F. Djama[88], T. Djobava[54b], J.I. Djuvsland[60a], M.A.B. do Vale[26c], D. Dobos[32],
M. Dobre[28b], C. Doglioni[84], J. Dolejsi[131], Z. Dolezal[131], M. Donadelli[26d], S. Donati[126a,126b],
P. Dondero[123a,123b], J. Donini[37], J. Dopke[133], A. Doria[106a], M.T. Dova[74], A.T. Doyle[56],
E. Drechsler[57], M. Dris[10], Y. Du[36b], J. Duarte-Campderros[155], A. Dubreuil[52], E. Duchovni[175],
G. Duckeck[102], A. Ducourthial[83], O.A. Ducu[97,p], D. Duda[109], A. Dudarev[32], A.Chr. Dudder[86],
E.M. Duffield[16], L. Duflot[119], M. Dührssen[32], M. Dumancic[175], A.E. Dumitriu[28b],
A.K. Duncan[56], M. Dunford[60a], H. Duran Yildiz[4a], M. Düren[55], A. Durglishvili[54b],
D. Duschinger[47], B. Dutta[45], D. Duvnjak[1], M. Dyndal[45], B.S. Dziedzic[42], C. Eckardt[45],
K.M. Ecker[103], R.C. Edgar[92], T. Eifert[32], G. Eigen[15], K. Einsweiler[16], T. Ekelof[168],
M. El Kacimi[137c], R. El Kosseifi[88], V. Ellajosyula[88], M. Ellert[168], S. Elles[5], F. Ellinghaus[178],
A.A. Elliot[172], N. Ellis[32], J. Elmsheuser[27], M. Elsing[32], D. Emeliyanov[133], Y. Enari[157],
O.C. Endner[86], J.S. Ennis[173], J. Erdmann[46], A. Ereditato[18], M. Ernst[27], S. Errede[169],
M. Escalier[119], C. Escobar[170], B. Esposito[50], O. Estrada Pastor[170], A.I. Etienvre[138], E. Etzion[155],
H. Evans[64], A. Ezhilov[125], M. Ezzi[137e], F. Fabbri[22a,22b], L. Fabbri[22a,22b], V. Fabiani[108],
G. Facini[81], R.M. Fakhrutdinov[132], S. Falciano[134a], R.J. Falla[81], J. Faltova[32], Y. Fang[35a],
M. Fanti[94a,94b], A. Farbin[8], A. Farilla[136a], C. Farina[127], E.M. Farina[123a,123b], T. Farooque[93],
S. Farrell[16], S.M. Farrington[173], P. Farthouat[32], F. Fassi[137e], P. Fassnacht[32], D. Fassouliotis[9],
M. Faucci Giannelli[49], A. Favareto[53a,53b], W.J. Fawcett[122], L. Fayard[119], O.L. Fedin[125,q],
W. Fedorko[171], S. Feigl[121], L. Feligioni[88], C. Feng[36b], E.J. Feng[32], M.J. Fenton[56],
A.B. Fenyuk[132], L. Feremenga[8], P. Fernandez Martinez[170], S. Fernandez Perez[13], J. Ferrando[45],
A. Ferrari[168], P. Ferrari[109], R. Ferrari[123a], D.E. Ferreira de Lima[60b], A. Ferrer[170], D. Ferrere[52],
C. Ferretti[92], F. Fiedler[86], A. Filipčič[78], M. Filipuzzi[45], F. Filthaut[108], M. Fincke-Keeler[172],
K.D. Finelli[152], M.C.N. Fiolhais[128a,128c,r], L. Fiorini[170], A. Fischer[2], C. Fischer[13], J. Fischer[178],
W.C. Fisher[93], N. Flaschel[45], I. Fleck[143], P. Fleischmann[92], R.R.M. Fletcher[124], T. Flick[178],

B.M. Flierl[102], L.R. Flores Castillo[62a], M.J. Flowerdew[103], G.T. Forcolin[87], A. Formica[138],
F.A. Förster[13], A. Forti[87], A.G. Foster[19], D. Fournier[119], H. Fox[75], S. Fracchia[141],
P. Francavilla[83], M. Franchini[22a,22b], S. Franchino[60a], D. Francis[32], L. Franconi[121],
M. Franklin[59], M. Frate[166], M. Fraternali[123a,123b], D. Freeborn[81], S.M. Fressard-Batraneanu[32],
B. Freund[97], D. Froidevaux[32], J.A. Frost[122], C. Fukunaga[158], T. Fusayasu[104], J. Fuster[170],
O. Gabizon[154], A. Gabrielli[22a,22b], A. Gabrielli[16], G.P. Gach[41a], S. Gadatsch[32], S. Gadomski[80],
G. Gagliardi[53a,53b], L.G. Gagnon[97], C. Galea[108], B. Galhardo[128a,128c], E.J. Gallas[122],
B.J. Gallop[133], P. Gallus[130], G. Galster[39], K.K. Gan[113], S. Ganguly[37], Y. Gao[77], Y.S. Gao[145,g],
F.M. Garay Walls[34a], C. García[170], J.E. García Navarro[170], J.A. García Pascual[35a],
M. Garcia-Sciveres[16], R.W. Gardner[33], N. Garelli[145], V. Garonne[121], A. Gascon Bravo[45],
K. Gasnikova[45], C. Gatti[50], A. Gaudiello[53a,53b], G. Gaudio[123a], I.L. Gavrilenko[98], C. Gay[171],
G. Gaycken[23], E.N. Gazis[10], C.N.P. Gee[133], J. Geisen[57], M. Geisen[86], M.P. Geisler[60a],
K. Gellerstedt[148a,148b], C. Gemme[53a], M.H. Genest[58], C. Geng[92], S. Gentile[134a,134b],
C. Gentsos[156], S. George[80], D. Gerbaudo[13], G. Geßner[46], S. Ghasemi[143], M. Ghneimat[23],
B. Giacobbe[22a], S. Giagu[134a,134b], N. Giangiacomi[22a,22b], P. Giannetti[126a,126b], S.M. Gibson[80],
M. Gignac[171], M. Gilchriese[16], D. Gillberg[31], G. Gilles[178], D.M. Gingrich[3,d],
M.P. Giordani[167a,167c], F.M. Giorgi[22a], P.F. Giraud[138], P. Giromini[59], G. Giugliarelli[167a,167c],
D. Giugni[94a], F. Giuli[122], C. Giuliani[103], M. Giulini[60b], B.K. Gjelsten[121], S. Gkaitatzis[156],
I. Gkialas[9,s], E.L. Gkougkousis[13], P. Gkountoumis[10], L.K. Gladilin[101], C. Glasman[85],
J. Glatzer[13], P.C.F. Glaysher[45], A. Glazov[45], M. Goblirsch-Kolb[25], J. Godlewski[42], S. Goldfarb[91],
T. Golling[52], D. Golubkov[132], A. Gomes[128a,128b,128d], R. Gonçalo[128a], R. Goncalves Gama[26a],
J. Goncalves Pinto Firmino Da Costa[138], G. Gonella[51], L. Gonella[19], A. Gongadze[68],
S. González de la Hoz[170], S. Gonzalez-Sevilla[52], L. Goossens[32], P.A. Gorbounov[99],
H.A. Gordon[27], I. Gorelov[107], B. Gorini[32], E. Gorini[76a,76b], A. Gorišek[78], A.T. Goshaw[48],
C. Gössling[46], M.I. Gostkin[68], C.A. Gottardo[23], C.R. Goudet[119], D. Goujdami[137c],
A.G. Goussiou[140], N. Govender[147b,t], E. Gozani[154], I. Grabowska-Bold[41a], P.O.J. Gradin[168],
J. Gramling[166], E. Gramstad[121], S. Grancagnolo[17], V. Gratchev[125], P.M. Gravila[28f], C. Gray[56],
H.M. Gray[16], Z.D. Greenwood[82,u], C. Grefe[23], K. Gregersen[81], I.M. Gregor[45], P. Grenier[145],
K. Grevtsov[5], J. Griffiths[8], A.A. Grillo[139], K. Grimm[75], S. Grinstein[13,v], Ph. Gris[37],
J.-F. Grivaz[119], S. Groh[86], E. Gross[175], J. Grosse-Knetter[57], G.C. Grossi[82], Z.J. Grout[81],
A. Grummer[107], L. Guan[92], W. Guan[176], J. Guenther[32], F. Guescini[163a], D. Guest[166],
O. Gueta[155], B. Gui[113], E. Guido[53a,53b], T. Guillemin[5], S. Guindon[32], U. Gul[56], C. Gumpert[32],
J. Guo[36c], W. Guo[92], Y. Guo[36a], R. Gupta[43], S. Gupta[122], S. Gurbuz[20a], G. Gustavino[115],
B.J. Gutelman[154], P. Gutierrez[115], N.G. Gutierrez Ortiz[81], C. Gutschow[81], C. Guyot[138],
M.P. Guzik[41a], C. Gwenlan[122], C.B. Gwilliam[77], A. Haas[112], C. Haber[16], H.K. Hadavand[8],
N. Haddad[137e], A. Hadef[88], S. Hageböck[23], M. Hagihara[164], H. Hakobyan[180,*], M. Haleem[45],
J. Haley[116], G. Halladjian[93], G.D. Hallewell[88], K. Hamacher[178], P. Hamal[117], K. Hamano[172],
A. Hamilton[147a], G.N. Hamity[141], P.G. Hamnett[45], L. Han[36a], S. Han[35a], K. Hanagaki[69,w],
K. Hanawa[157], M. Hance[139], B. Haney[124], P. Hanke[60a], J.B. Hansen[39], J.D. Hansen[39],
M.C. Hansen[23], P.H. Hansen[39], K. Hara[164], A.S. Hard[176], T. Harenberg[178], F. Hariri[119],
S. Harkusha[95], P.F. Harrison[173], N.M. Hartmann[102], Y. Hasegawa[142], A. Hasib[49], S. Hassani[138],
S. Haug[18], R. Hauser[93], L. Hauswald[47], L.B. Havener[38], M. Havranek[130], C.M. Hawkes[19],
R.J. Hawkings[32], D. Hayakawa[159], D. Hayden[93], C.P. Hays[122], J.M. Hays[79], H.S. Hayward[77],
S.J. Haywood[133], S.J. Head[19], T. Heck[86], V. Hedberg[84], L. Heelan[8], S. Heer[23], K.K. Heidegger[51],
S. Heim[45], T. Heim[16], B. Heinemann[45,x], J.J. Heinrich[102], L. Heinrich[112], C. Heinz[55],
J. Hejbal[129], L. Helary[32], A. Held[171], S. Hellman[148a,148b], C. Helsens[32], R.C.W. Henderson[75],
Y. Heng[176], S. Henkelmann[171], A.M. Henriques Correia[32], S. Henrot-Versille[119], G.H. Herbert[17],
H. Herde[25], V. Herget[177], Y. Hernández Jiménez[147c], H. Herr[86], G. Herten[51], R. Hertenberger[102],

L. Hervas[32], T.C. Herwig[124], G.G. Hesketh[81], N.P. Hessey[163a], J.W. Hetherly[43], S. Higashino[69],
E. Higón-Rodriguez[170], K. Hildebrand[33], E. Hill[172], J.C. Hill[30], K.H. Hiller[45], S.J. Hillier[19],
M. Hils[47], I. Hinchliffe[16], M. Hirose[51], D. Hirschbuehl[178], B. Hiti[78], O. Hladik[129], X. Hoad[49],
J. Hobbs[150], N. Hod[163a], M.C. Hodgkinson[141], P. Hodgson[141], A. Hoecker[32],
M.R. Hoeferkamp[107], F. Hoenig[102], D. Hohn[23], T.R. Holmes[33], M. Homann[46], S. Honda[164],
T. Honda[69], T.M. Hong[127], B.H. Hooberman[169], W.H. Hopkins[118], Y. Horii[105], A.J. Horton[144],
J-Y. Hostachy[58], S. Hou[153], A. Hoummada[137a], J. Howarth[87], J. Hoya[74], M. Hrabovsky[117],
J. Hrdinka[32], I. Hristova[17], J. Hrivnac[119], T. Hryn'ova[5], A. Hrynevich[96], P.J. Hsu[63],
S.-C. Hsu[140], Q. Hu[36a], S. Hu[36c], Y. Huang[35a], Z. Hubacek[130], F. Hubaut[88], F. Huegging[23],
T.B. Huffman[122], E.W. Hughes[38], G. Hughes[75], M. Huhtinen[32], P. Huo[150], N. Huseynov[68,b],
J. Huston[93], J. Huth[59], R. Hyneman[92], G. Iacobucci[52], G. Iakovidis[27], I. Ibragimov[143],
L. Iconomidou-Fayard[119], Z. Idrissi[137e], P. Iengo[32], O. Igonkina[109,y], T. Iizawa[174], Y. Ikegami[69],
M. Ikeno[69], Y. Ilchenko[11,z], D. Iliadis[156], N. Ilic[145], G. Introzzi[123a,123b], P. Ioannou[9,*],
M. Iodice[136a], K. Iordanidou[38], V. Ippolito[59], M.F. Isacson[168], N. Ishijima[120], M. Ishino[157],
M. Ishitsuka[159], C. Issever[122], S. Istin[20a], F. Ito[164], J.M. Iturbe Ponce[62a], R. Iuppa[162a,162b],
H. Iwasaki[69], J.M. Izen[44], V. Izzo[106a], S. Jabbar[3], P. Jackson[1], R.M. Jacobs[23], V. Jain[2],
K.B. Jakobi[86], K. Jakobs[51], S. Jakobsen[65], T. Jakoubek[129], D.O. Jamin[116], D.K. Jana[82],
R. Jansky[52], J. Janssen[23], M. Janus[57], P.A. Janus[41a], G. Jarlskog[84], N. Javadov[68,b],
T. Javůrek[51], M. Javurkova[51], F. Jeanneau[138], L. Jeanty[16], J. Jejelava[54a,aa], A. Jelinskas[173],
P. Jenni[51,ab], C. Jeske[173], S. Jézéquel[5], H. Ji[176], J. Jia[150], H. Jiang[67], Y. Jiang[36a], Z. Jiang[145],
S. Jiggins[81], J. Jimenez Pena[170], S. Jin[35a], A. Jinaru[28b], O. Jinnouchi[159], H. Jivan[147c],
P. Johansson[141], K.A. Johns[7], C.A. Johnson[64], W.J. Johnson[140], K. Jon-And[148a,148b],
R.W.L. Jones[75], S.D. Jones[151], S. Jones[7], T.J. Jones[77], J. Jongmanns[60a], P.M. Jorge[128a,128b],
J. Jovicevic[163a], X. Ju[176], A. Juste Rozas[13,v], M.K. Köhler[175], A. Kaczmarska[42], M. Kado[119],
H. Kagan[113], M. Kagan[145], S.J. Kahn[88], T. Kaji[174], E. Kajomovitz[154], C.W. Kalderon[84],
A. Kaluza[86], S. Kama[43], A. Kamenshchikov[132], N. Kanaya[157], L. Kanjir[78], V.A. Kantserov[100],
J. Kanzaki[69], B. Kaplan[112], L.S. Kaplan[176], D. Kar[147c], K. Karakostas[10], N. Karastathis[10],
M.J. Kareem[57], E. Karentzos[10], S.N. Karpov[68], Z.M. Karpova[68], K. Karthik[112],
V. Kartvelishvili[75], A.N. Karyukhin[132], K. Kasahara[164], L. Kashif[176], R.D. Kass[113],
A. Kastanas[149], Y. Kataoka[157], C. Kato[157], A. Katre[52], J. Katzy[45], K. Kawade[70], K. Kawagoe[73],
T. Kawamoto[157], G. Kawamura[57], E.F. Kay[77], V.F. Kazanin[111,c], R. Keeler[172], R. Kehoe[43],
J.S. Keller[31], E. Kellermann[84], J.J. Kempster[80], J Kendrick[19], H. Keoshkerian[161], O. Kepka[129],
B.P. Kerševan[78], S. Kersten[178], R.A. Keyes[90], M. Khader[169], F. Khalil-zada[12], A. Khanov[116],
A.G. Kharlamov[111,c], T. Kharlamova[111,c], A. Khodinov[160], T.J. Khoo[52], V. Khovanskiy[99,*],
E. Khramov[68], J. Khubua[54b,ac], S. Kido[70], C.R. Kilby[80], H.Y. Kim[8], S.H. Kim[164], Y.K. Kim[33],
N. Kimura[156], O.M. Kind[17], B.T. King[77], D. Kirchmeier[47], J. Kirk[133], A.E. Kiryunin[103],
T. Kishimoto[157], D. Kisielewska[41a], V. Kitali[45], O. Kivernyk[5], E. Kladiva[146b],
T. Klapdor-Kleingrothaus[51], M.H. Klein[92], M. Klein[77], U. Klein[77], K. Kleinknecht[86],
P. Klimek[110], A. Klimentov[27], R. Klingenberg[46], T. Klingl[23], T. Klioutchnikova[32],
E.-E. Kluge[60a], P. Kluit[109], S. Kluth[103], E. Kneringer[65], E.B.F.G. Knoops[88], A. Knue[103],
A. Kobayashi[157], D. Kobayashi[159], T. Kobayashi[157], M. Kobel[47], M. Kocian[145], P. Kodys[131],
T. Koffas[31], E. Koffeman[109], N.M. Köhler[103], T. Koi[145], M. Kolb[60b], I. Koletsou[5],
A.A. Komar[98,*], T. Kondo[69], N. Kondrashova[36c], K. Köneke[51], A.C. König[108], T. Kono[69,ad],
R. Konoplich[112,ae], N. Konstantinidis[81], R. Kopeliansky[64], S. Koperny[41a], A.K. Kopp[51],
K. Korcyl[42], K. Kordas[156], A. Korn[81], A.A. Korol[111,c], I. Korolkov[13], E.V. Korolkova[141],
O. Kortner[103], S. Kortner[103], T. Kosek[131], V.V. Kostyukhin[23], A. Kotwal[48], A. Koulouris[10],
A. Kourkoumeli-Charalampidi[123a,123b], C. Kourkoumelis[9], E. Kourlitis[141], V. Kouskoura[27],
A.B. Kowalewska[42], R. Kowalewski[172], T.Z. Kowalski[41a], C. Kozakai[157], W. Kozanecki[138],

A.S. Kozhin[132], V.A. Kramarenko[101], G. Kramberger[78], D. Krasnopevtsev[100], M.W. Krasny[83],
A. Krasznahorkay[32], D. Krauss[103], J.A. Kremer[41a], J. Kretzschmar[77], K. Kreutzfeldt[55],
P. Krieger[161], K. Krizka[16], K. Kroeninger[46], H. Kroha[103], J. Kroll[129], J. Kroll[124], J. Kroseberg[23],
J. Krstic[14], U. Kruchonak[68], H. Krüger[23], N. Krumnack[67], M.C. Kruse[48], T. Kubota[91],
H. Kucuk[81], S. Kuday[4b], J.T. Kuechler[178], S. Kuehn[32], A. Kugel[60a], F. Kuger[177], T. Kuhl[45],
V. Kukhtin[68], R. Kukla[88], Y. Kulchitsky[95], S. Kuleshov[34b], Y.P. Kulinich[169], M. Kuna[134a,134b],
T. Kunigo[71], A. Kupco[129], T. Kupfer[46], O. Kuprash[155], H. Kurashige[70], L.L. Kurchaninov[163a],
Y.A. Kurochkin[95], M.G. Kurth[35a], V. Kus[129], E.S. Kuwertz[172], M. Kuze[159], J. Kvita[117],
T. Kwan[172], D. Kyriazopoulos[141], A. La Rosa[103], J.L. La Rosa Navarro[26d], L. La Rotonda[40a,40b],
F. La Ruffa[40a,40b], C. Lacasta[170], F. Lacava[134a,134b], J. Lacey[45], D.P.J. Lack[87], H. Lacker[17],
D. Lacour[83], E. Ladygin[68], R. Lafaye[5], B. Laforge[83], T. Lagouri[179], S. Lai[57], S. Lammers[64],
W. Lampl[7], E. Lançon[27], U. Landgraf[51], M.P.J. Landon[79], M.C. Lanfermann[52], V.S. Lang[45],
J.C. Lange[13], R.J. Langenberg[32], A.J. Lankford[166], F. Lanni[27], K. Lantzsch[23], A. Lanza[123a],
A. Lapertosa[53a,53b], S. Laplace[83], J.F. Laporte[138], T. Lari[94a], F. Lasagni Manghi[22a,22b],
M. Lassnig[32], T.S. Lau[62a], P. Laurelli[50], W. Lavrijsen[16], A.T. Law[139], P. Laycock[77],
T. Lazovich[59], M. Lazzaroni[94a,94b], B. Le[91], O. Le Dortz[83], E. Le Guirriec[88], E.P. Le Quilleuc[138],
M. LeBlanc[172], T. LeCompte[6], F. Ledroit-Guillon[58], C.A. Lee[27], G.R. Lee[34a], S.C. Lee[153],
L. Lee[59], B. Lefebvre[90], G. Lefebvre[83], M. Lefebvre[172], F. Legger[102], C. Leggett[16],
G. Lehmann Miotto[32], X. Lei[7], W.A. Leight[45], M.A.L. Leite[26d], R. Leitner[131], D. Lellouch[175],
B. Lemmer[57], K.J.C. Leney[81], T. Lenz[23], B. Lenzi[32], R. Leone[7], S. Leone[126a,126b],
C. Leonidopoulos[49], G. Lerner[151], C. Leroy[97], A.A.J. Lesage[138], C.G. Lester[30], M. Levchenko[125],
J. Levêque[5], D. Levin[92], L.J. Levinson[175], M. Levy[19], D. Lewis[79], B. Li[36a,af], Changqiao Li[36a],
H. Li[150], L. Li[36c], Q. Li[35a], Q. Li[36a], S. Li[48], X. Li[36c], Y. Li[143], Z. Liang[35a], B. Liberti[135a],
A. Liblong[161], K. Lie[62c], J. Liebal[23], W. Liebig[15], A. Limosani[152], K. Lin[93], S.C. Lin[182],
T.H. Lin[86], R.A. Linck[64], B.E. Lindquist[150], A.E. Lionti[52], E. Lipeles[124], A. Lipniacka[15],
M. Lisovyi[60b], T.M. Liss[169,ag], A. Lister[171], A.M. Litke[139], B. Liu[67], H. Liu[92], H. Liu[27],
J.K.K. Liu[122], J. Liu[36b], J.B. Liu[36a], K. Liu[88], L. Liu[169], M. Liu[36a], Y.L. Liu[36a], Y. Liu[36a],
M. Livan[123a,123b], A. Lleres[58], J. Llorente Merino[35a], S.L. Lloyd[79], C.Y. Lo[62b], F. Lo Sterzo[43],
E.M. Lobodzinska[45], P. Loch[7], F.K. Loebinger[87], A. Loesle[51], K.M. Loew[25], T. Lohse[17],
K. Lohwasser[141], M. Lokajicek[129], B.A. Long[24], J.D. Long[169], R.E. Long[75], L. Longo[76a,76b],
K.A. Looper[113], J.A. Lopez[34b], D. Lopez Mateos[59], I. Lopez Paz[13], A. Lopez Solis[83],
J. Lorenz[102], N. Lorenzo Martinez[5], M. Losada[21], P.J. Lösel[102], X. Lou[35a], A. Lounis[119],
J. Love[6], P.A. Love[75], H. Lu[62a], N. Lu[92], Y.J. Lu[63], H.J. Lubatti[140], C. Luci[134a,134b],
A. Lucotte[58], C. Luedtke[51], F. Luehring[64], W. Lukas[65], L. Luminari[134a], O. Lundberg[148a,148b],
B. Lund-Jensen[149], M.S. Lutz[89], P.M. Luzi[83], D. Lynn[27], R. Lysak[129], E. Lytken[84], F. Lyu[35a],
V. Lyubushkin[68], H. Ma[27], L.L. Ma[36b], Y. Ma[36b], G. Maccarrone[50], A. Macchiolo[103],
C.M. Macdonald[141], B. Maček[78], J. Machado Miguens[124,128b], D. Madaffari[170], R. Madar[37],
W.F. Mader[47], A. Madsen[45], J. Maeda[70], S. Maeland[15], T. Maeno[27], A.S. Maevskiy[101],
V. Magerl[51], C. Maiani[119], C. Maidantchik[26a], T. Maier[102], A. Maio[128a,128b,128d],
O. Majersky[146a], S. Majewski[118], Y. Makida[69], N. Makovec[119], B. Malaescu[83], Pa. Malecki[42],
V.P. Maleev[125], F. Malek[58], U. Mallik[66], D. Malon[6], C. Malone[30], S. Maltezos[10], S. Malyukov[32],
J. Mamuzic[170], G. Mancini[50], I. Mandić[78], J. Maneira[128a,128b], L. Manhaes de Andrade Filho[26b],
J. Manjarres Ramos[47], K.H. Mankinen[84], A. Mann[102], A. Manousos[32], B. Mansoulie[138],
J.D. Mansour[35a], R. Mantifel[90], M. Mantoani[57], S. Manzoni[94a,94b], L. Mapelli[32], G. Marceca[29],
L. March[52], L. Marchese[122], G. Marchiori[83], M. Marcisovsky[129], C.A. Marin Tobon[32],
M. Marjanovic[37], D.E. Marley[92], F. Marroquim[26a], S.P. Marsden[87], Z. Marshall[16],
M.U.F Martensson[168], S. Marti-Garcia[170], C.B. Martin[113], T.A. Martin[173], V.J. Martin[49],
B. Martin dit Latour[15], M. Martinez[13,v], V.I. Martinez Outschoorn[169], S. Martin-Haugh[133],

V.S. Martoiu[28b], A.C. Martyniuk[81], A. Marzin[32], L. Masetti[86], T. Mashimo[157],
R. Mashinistov[98], J. Masik[87], A.L. Maslennikov[111,c], L.H. Mason[91], L. Massa[135a,135b],
P. Mastrandrea[5], A. Mastroberardino[40a,40b], T. Masubuchi[157], P. Mättig[178], J. Maurer[28b],
S.J. Maxfield[77], D.A. Maximov[111,c], R. Mazini[153], I. Maznas[156], S.M. Mazza[94a,94b],
N.C. Mc Fadden[107], G. Mc Goldrick[161], S.P. Mc Kee[92], A. McCarn[92], R.L. McCarthy[150],
T.G. McCarthy[103], L.I. McClymont[81], E.F. McDonald[91], J.A. Mcfayden[32], G. Mchedlidze[57],
S.J. McMahon[133], P.C. McNamara[91], C.J. McNicol[173], R.A. McPherson[172,o], S. Meehan[140],
T.J. Megy[51], S. Mehlhase[102], A. Mehta[77], T. Meideck[58], K. Meier[60a], B. Meirose[44],
D. Melini[170,ah], B.R. Mellado Garcia[147c], J.D. Mellenthin[57], M. Melo[146a], F. Meloni[18],
A. Melzer[23], S.B. Menary[87], L. Meng[77], X.T. Meng[92], A. Mengarelli[22a,22b], S. Menke[103],
E. Meoni[40a,40b], S. Mergelmeyer[17], C. Merlassino[18], P. Mermod[52], L. Merola[106a,106b],
C. Meroni[94a], F.S. Merritt[33], A. Messina[134a,134b], J. Metcalfe[6], A.S. Mete[166], C. Meyer[124],
J-P. Meyer[138], J. Meyer[109], H. Meyer Zu Theenhausen[60a], F. Miano[151], R.P. Middleton[133],
S. Miglioranzi[53a,53b], L. Mijović[49], G. Mikenberg[175], M. Mikestikova[129], M. Mikuž[78], M. Milesi[91],
A. Milic[161], D.A. Millar[79], D.W. Miller[33], C. Mills[49], A. Milov[175], D.A. Milstead[148a,148b],
A.A. Minaenko[132], Y. Minami[157], I.A. Minashvili[54b], A.I. Mincer[112], B. Mindur[41a], M. Mineev[68],
Y. Minegishi[157], Y. Ming[176], L.M. Mir[13], A. Mirto[76a,76b], K.P. Mistry[124], T. Mitani[174],
J. Mitrevski[102], V.A. Mitsou[170], A. Miucci[18], P.S. Miyagawa[141], A. Mizukami[69],
J.U. Mjörnmark[84], T. Mkrtchyan[180], M. Mlynarikova[131], T. Moa[148a,148b], K. Mochizuki[97],
P. Mogg[51], S. Mohapatra[38], S. Molander[148a,148b], R. Moles-Valls[23], M.C. Mondragon[93],
K. Mönig[45], J. Monk[39], E. Monnier[88], A. Montalbano[150], J. Montejo Berlingen[32],
F. Monticelli[74], S. Monzani[94a,94b], R.W. Moore[3], N. Morange[119], D. Moreno[21],
M. Moreno Llácer[32], P. Morettini[53a], S. Morgenstern[32], D. Mori[144], T. Mori[157], M. Morii[59],
M. Morinaga[174], V. Morisbak[121], A.K. Morley[32], G. Mornacchi[32], J.D. Morris[79], L. Morvaj[150],
P. Moschovakos[10], M. Mosidze[54b], H.J. Moss[141], J. Moss[145,ai], K. Motohashi[159], R. Mount[145],
E. Mountricha[27], E.J.W. Moyse[89], S. Muanza[88], F. Mueller[103], J. Mueller[127], R.S.P. Mueller[102],
D. Muenstermann[75], P. Mullen[56], G.A. Mullier[18], F.J. Munoz Sanchez[87], W.J. Murray[173,133],
H. Musheghyan[32], M. Muškinja[78], A.G. Myagkov[132,aj], M. Myska[130], B.P. Nachman[16],
O. Nackenhorst[52], K. Nagai[122], R. Nagai[69,ad], K. Nagano[69], Y. Nagasaka[61], K. Nagata[164],
M. Nagel[51], E. Nagy[88], A.M. Nairz[32], Y. Nakahama[105], K. Nakamura[69], T. Nakamura[157],
I. Nakano[114], R.F. Naranjo Garcia[45], R. Narayan[11], D.I. Narrias Villar[60a], I. Naryshkin[125],
T. Naumann[45], G. Navarro[21], R. Nayyar[7], H.A. Neal[92], P.Yu. Nechaeva[98], T.J. Neep[138],
A. Negri[123a,123b], M. Negrini[22a], S. Nektarijevic[108], C. Nellist[57], A. Nelson[166], M.E. Nelson[122],
S. Nemecek[129], P. Nemethy[112], M. Nessi[32,ak], M.S. Neubauer[169], M. Neumann[178],
P.R. Newman[19], T.Y. Ng[62c], T. Nguyen Manh[97], R.B. Nickerson[122], R. Nicolaidou[138],
J. Nielsen[139], N. Nikiforou[11], V. Nikolaenko[132,aj], I. Nikolic-Audit[83], K. Nikolopoulos[19],
J.K. Nilsen[121], P. Nilsson[27], Y. Ninomiya[157], A. Nisati[134a], N. Nishu[36c], R. Nisius[103],
I. Nitsche[46], T. Nitta[174], T. Nobe[157], Y. Noguchi[71], M. Nomachi[120], I. Nomidis[31],
M.A. Nomura[27], T. Nooney[79], M. Nordberg[32], N. Norjoharuddeen[122], O. Novgorodova[47],
M. Nozaki[69], L. Nozka[117], K. Ntekas[166], E. Nurse[81], F. Nuti[91], K. O'connor[25], D.C. O'Neil[144],
A.A. O'Rourke[45], V. O'Shea[56], F.G. Oakham[31,d], H. Oberlack[103], T. Obermann[23], J. Ocariz[83],
A. Ochi[70], I. Ochoa[38], J.P. Ochoa-Ricoux[34a], S. Oda[73], S. Odaka[69], A. Oh[87], S.H. Oh[48],
C.C. Ohm[149], H. Ohman[168], H. Oide[53a,53b], H. Okawa[164], Y. Okumura[157], T. Okuyama[69],
A. Olariu[28b], L.F. Oleiro Seabra[128a], S.A. Olivares Pino[34a], D. Oliveira Damazio[27],
A. Olszewski[42], J. Olszowska[42], A. Onofre[128a,128e], K. Onogi[105], P.U.E. Onyisi[11,z], H. Oppen[121],
M.J. Oreglia[33], Y. Oren[155], D. Orestano[136a,136b], N. Orlando[62b], R.S. Orr[161],
B. Osculati[53a,53b,*], R. Ospanov[36a], G. Otero y Garzon[29], H. Otono[73], M. Ouchrif[137d],
F. Ould-Saada[121], A. Ouraou[138], K.P. Oussoren[109], Q. Ouyang[35a], M. Owen[56], R.E. Owen[19],

V.E. Ozcan[20a], N. Ozturk[8], K. Pachal[144], A. Pacheco Pages[13], L. Pacheco Rodriguez[138],
C. Padilla Aranda[13], S. Pagan Griso[16], M. Paganini[179], F. Paige[27], G. Palacino[64],
S. Palazzo[40a,40b], S. Palestini[32], M. Palka[41b], D. Pallin[37], E.St. Panagiotopoulou[10],
I. Panagoulias[10], C.E. Pandini[52], J.G. Panduro Vazquez[80], P. Pani[32], S. Panitkin[27],
D. Pantea[28b], L. Paolozzi[52], Th.D. Papadopoulou[10], K. Papageorgiou[9,s], A. Paramonov[6],
D. Paredes Hernandez[179], A.J. Parker[75], M.A. Parker[30], K.A. Parker[45], F. Parodi[53a,53b],
J.A. Parsons[38], U. Parzefall[51], V.R. Pascuzzi[161], J.M. Pasner[139], E. Pasqualucci[134a],
S. Passaggio[53a], Fr. Pastore[80], S. Pataraia[86], J.R. Pater[87], T. Pauly[32], B. Pearson[103],
S. Pedraza Lopez[170], R. Pedro[128a,128b], S.V. Peleganchuk[111,c], O. Penc[129], C. Peng[35a],
H. Peng[36a], J. Penwell[64], B.S. Peralva[26b], M.M. Perego[138], D.V. Perepelitsa[27], F. Peri[17],
L. Perini[94a,94b], H. Pernegger[32], S. Perrella[106a,106b], R. Peschke[45], V.D. Peshekhonov[68,*],
K. Peters[45], R.F.Y. Peters[87], B.A. Petersen[32], T.C. Petersen[39], E. Petit[58], A. Petridis[1],
C. Petridou[156], P. Petroff[119], E. Petrolo[134a], M. Petrov[122], F. Petrucci[136a,136b],
N.E. Pettersson[89], A. Peyaud[138], R. Pezoa[34b], F.H. Phillips[93], P.W. Phillips[133],
G. Piacquadio[150], E. Pianori[173], A. Picazio[89], E. Piccaro[79], M.A. Pickering[122], R. Piegaia[29],
J.E. Pilcher[33], A.D. Pilkington[87], M. Pinamonti[135a,135b], J.L. Pinfold[3], H. Pirumov[45],
M. Pitt[175], L. Plazak[146a], M.-A. Pleier[27], V. Pleskot[86], E. Plotnikova[68], D. Pluth[67],
P. Podberezko[111], R. Poettgen[84], R. Poggi[123a,123b], L. Poggioli[119], I. Pogrebnyak[93], D. Pohl[23],
I. Pokharel[57], G. Polesello[123a], A. Poley[45], A. Policicchio[40a,40b], R. Polifka[32], A. Polini[22a],
C.S. Pollard[56], V. Polychronakos[27], K. Pommès[32], D. Ponomarenko[100], L. Pontecorvo[134a],
G.A. Popeneciu[28d], S. Pospisil[130], K. Potamianos[16], I.N. Potrap[68], C.J. Potter[30], H. Potti[11],
T. Poulsen[84], J. Poveda[32], M.E. Pozo Astigarraga[32], P. Pralavorio[88], A. Pranko[16], S. Prell[67],
D. Price[87], M. Primavera[76a], S. Prince[90], N. Proklova[100], K. Prokofiev[62c], F. Prokoshin[34b],
S. Protopopescu[27], J. Proudfoot[6], M. Przybycien[41a], A. Puri[169], P. Puzo[119], J. Qian[92], G. Qin[56],
Y. Qin[87], A. Quadt[57], M. Queitsch-Maitland[45], D. Quilty[56], S. Raddum[121], V. Radeka[27],
V. Radescu[122], S.K. Radhakrishnan[150], P. Radloff[118], P. Rados[91], F. Ragusa[94a,94b], G. Rahal[181],
J.A. Raine[87], S. Rajagopalan[27], C. Rangel-Smith[168], T. Rashid[119], S. Raspopov[5],
M.G. Ratti[94a,94b], D.M. Rauch[45], F. Rauscher[102], S. Rave[86], I. Ravinovich[175], J.H. Rawling[87],
M. Raymond[32], A.L. Read[121], N.P. Readioff[58], M. Reale[76a,76b], D.M. Rebuzzi[123a,123b],
A. Redelbach[177], G. Redlinger[27], R. Reece[139], R.G. Reed[147c], K. Reeves[44], L. Rehnisch[17],
J. Reichert[124], A. Reiss[86], C. Rembser[32], H. Ren[35a], M. Rescigno[134a], S. Resconi[94a],
E.D. Resseguie[124], S. Rettie[171], E. Reynolds[19], O.L. Rezanova[111,c], P. Reznicek[131], R. Rezvani[97],
R. Richter[103], S. Richter[81], E. Richter-Was[41b], O. Ricken[23], M. Ridel[83], P. Rieck[103],
C.J. Riegel[178], J. Rieger[57], O. Rifki[115], M. Rijssenbeek[150], A. Rimoldi[123a,123b], M. Rimoldi[18],
L. Rinaldi[22a], G. Ripellino[149], B. Ristić[32], E. Ritsch[32], I. Riu[13], F. Rizatdinova[116], E. Rizvi[79],
C. Rizzi[13], R.T. Roberts[87], S.H. Robertson[90,o], A. Robichaud-Veronneau[90], D. Robinson[30],
J.E.M. Robinson[45], A. Robson[56], E. Rocco[86], C. Roda[126a,126b], Y. Rodina[88,al],
S. Rodriguez Bosca[170], A. Rodriguez Perez[13], D. Rodriguez Rodriguez[170], S. Roe[32],
C.S. Rogan[59], O. Røhne[121], J. Roloff[59], A. Romaniouk[100], M. Romano[22a,22b],
S.M. Romano Saez[37], E. Romero Adam[170], N. Rompotis[77], M. Ronzani[51], L. Roos[83],
S. Rosati[134a], K. Rosbach[51], P. Rose[139], N.-A. Rosien[57], E. Rossi[106a,106b], L.P. Rossi[53a],
J.H.N. Rosten[30], R. Rosten[140], M. Rotaru[28b], J. Rothberg[140], D. Rousseau[119], A. Rozanov[88],
Y. Rozen[154], X. Ruan[147c], F. Rubbo[145], F. Rühr[51], A. Ruiz-Martinez[31], Z. Rurikova[51],
N.A. Rusakovich[68], H.L. Russell[90], J.P. Rutherfoord[7], N. Ruthmann[32], Y.F. Ryabov[125],
M. Rybar[169], G. Rybkin[119], S. Ryu[6], A. Ryzhov[132], G.F. Rzehorz[57], A.F. Saavedra[152],
G. Sabato[109], S. Sacerdoti[29], H.F-W. Sadrozinski[139], R. Sadykov[68], F. Safai Tehrani[134a],
P. Saha[110], M. Sahinsoy[60a], M. Saimpert[45], M. Saito[157], T. Saito[157], H. Sakamoto[157],
Y. Sakurai[174], G. Salamanna[136a,136b], J.E. Salazar Loyola[34b], D. Salek[109],

P.H. Sales De Bruin[168], D. Salihagic[103], A. Salnikov[145], J. Salt[170], D. Salvatore[40a,40b],
F. Salvatore[151], A. Salvucci[62a,62b,62c], A. Salzburger[32], D. Sammel[51], D. Sampsonidis[156],
D. Sampsonidou[156], J. Sánchez[170], V. Sanchez Martinez[170], A. Sanchez Pineda[167a,167c],
H. Sandaker[121], R.L. Sandbach[79], C.O. Sander[45], M. Sandhoff[178], C. Sandoval[21],
D.P.C. Sankey[133], M. Sannino[53a,53b], Y. Sano[105], A. Sansoni[50], C. Santoni[37], H. Santos[128a],
I. Santoyo Castillo[151], A. Sapronov[68], J.G. Saraiva[128a,128d], B. Sarrazin[23], O. Sasaki[69],
K. Sato[164], E. Sauvan[5], G. Savage[80], P. Savard[161,d], N. Savic[103], C. Sawyer[133], L. Sawyer[82,u],
J. Saxon[33], C. Sbarra[22a], A. Sbrizzi[22a,22b], T. Scanlon[81], D.A. Scannicchio[166],
J. Schaarschmidt[140], P. Schacht[103], B.M. Schachtner[102], D. Schaefer[33], L. Schaefer[124],
R. Schaefer[45], J. Schaeffer[86], S. Schaepe[23], S. Schaetzel[60b], U. Schäfer[86], A.C. Schaffer[119],
D. Schaile[102], R.D. Schamberger[150], V.A. Schegelsky[125], D. Scheirich[131], M. Schernau[166],
C. Schiavi[53a,53b], S. Schier[139], L.K. Schildgen[23], C. Schillo[51], M. Schioppa[40a,40b], S. Schlenker[32],
K.R. Schmidt-Sommerfeld[103], K. Schmieden[32], C. Schmitt[86], S. Schmitt[45], S. Schmitz[86],
U. Schnoor[51], L. Schoeffel[138], A. Schoening[60b], B.D. Schoenrock[93], E. Schopf[23], M. Schott[86],
J.F.P. Schouwenberg[108], J. Schovancova[32], S. Schramm[52], N. Schuh[86], A. Schulte[86],
M.J. Schultens[23], H.-C. Schultz-Coulon[60a], H. Schulz[17], M. Schumacher[51], B.A. Schumm[139],
Ph. Schune[138], A. Schwartzman[145], T.A. Schwarz[92], H. Schweiger[87], Ph. Schwemling[138],
R. Schwienhorst[93], J. Schwindling[138], A. Sciandra[23], G. Sciolla[25], M. Scornajenghi[40a,40b],
F. Scuri[126a,126b], F. Scutti[91], J. Searcy[92], P. Seema[23], S.C. Seidel[107], A. Seiden[139],
J.M. Seixas[26a], G. Sekhniaidze[106a], K. Sekhon[92], S.J. Sekula[43], N. Semprini-Cesari[22a,22b],
S. Senkin[37], C. Serfon[121], L. Serin[119], L. Serkin[167a,167b], M. Sessa[136a,136b], R. Seuster[172],
H. Severini[115], T. Sfiligoj[78], F. Sforza[165], A. Sfyrla[52], E. Shabalina[57], N.W. Shaikh[148a,148b],
L.Y. Shan[35a], R. Shang[169], J.T. Shank[24], M. Shapiro[16], P.B. Shatalov[99], K. Shaw[167a,167b],
S.M. Shaw[87], A. Shcherbakova[148a,148b], C.Y. Shehu[151], Y. Shen[115], N. Sherafati[31],
P. Sherwood[81], L. Shi[153,am], S. Shimizu[70], C.O. Shimmin[179], M. Shimojima[104], I.P.J. Shipsey[122],
S. Shirabe[73], M. Shiyakova[68,an], J. Shlomi[175], A. Shmeleva[98], D. Shoaleh Saadi[97],
M.J. Shochet[33], S. Shojaii[94a,94b], D.R. Shope[115], S. Shrestha[113], E. Shulga[100], M.A. Shupe[7],
P. Sicho[129], A.M. Sickles[169], P.E. Sidebo[149], E. Sideras Haddad[147c], O. Sidiropoulou[177],
A. Sidoti[22a,22b], F. Siegert[47], Dj. Sijacki[14], J. Silva[128a,128d], S.B. Silverstein[148a], V. Simak[130],
Lj. Simic[14], S. Simion[119], E. Simioni[86], B. Simmons[81], M. Simon[86], P. Sinervo[161], N.B. Sinev[118],
M. Sioli[22a,22b], G. Siragusa[177], I. Siral[92], S.Yu. Sivoklokov[101], J. Sjölin[148a,148b], M.B. Skinner[75],
P. Skubic[115], M. Slater[19], T. Slavicek[130], M. Slawinska[42], K. Sliwa[165], R. Slovak[131],
V. Smakhtin[175], B.H. Smart[5], J. Smiesko[146a], N. Smirnov[100], S.Yu. Smirnov[100], Y. Smirnov[100],
L.N. Smirnova[101,ao], O. Smirnova[84], J.W. Smith[57], M.N.K. Smith[38], R.W. Smith[38],
M. Smizanska[75], K. Smolek[130], A.A. Snesarev[98], I.M. Snyder[118], S. Snyder[27], R. Sobie[172,o],
F. Socher[47], A. Soffer[155], A. Søgaard[49], D.A. Soh[153], G. Sokhrannyi[78], C.A. Solans Sanchez[32],
M. Solar[130], E.Yu. Soldatov[100], U. Soldevila[170], A.A. Solodkov[132], A. Soloshenko[68],
O.V. Solovyanov[132], V. Solovyev[125], P. Sommer[51], H. Son[165], A. Sopczak[130], D. Sosa[60b],
C.L. Sotiropoulou[126a,126b], R. Soualah[167a,167c], A.M. Soukharev[111,c], D. South[45], B.C. Sowden[80],
S. Spagnolo[76a,76b], M. Spalla[126a,126b], M. Spangenberg[173], F. Spanò[80], D. Sperlich[17],
F. Spettel[103], T.M. Spieker[60a], R. Spighi[22a], G. Spigo[32], L.A. Spiller[91], M. Spousta[131],
R.D. St. Denis[56,*], A. Stabile[94a], R. Stamen[60a], S. Stamm[17], E. Stanecka[42], R.W. Stanek[6],
C. Stanescu[136a], M.M. Stanitzki[45], B.S. Stapf[109], S. Stapnes[121], E.A. Starchenko[132],
G.H. Stark[33], J. Stark[58], S.H Stark[39], P. Staroba[129], P. Starovoitov[60a], S. Stärz[32],
R. Staszewski[42], M. Stegler[45], P. Steinberg[27], B. Stelzer[144], H.J. Stelzer[32], O. Stelzer-Chilton[163a],
H. Stenzel[55], G.A. Stewart[56], M.C. Stockton[118], M. Stoebe[90], G. Stoicea[28b], P. Stolte[57],
S. Stonjek[103], A.R. Stradling[8], A. Straessner[47], M.E. Stramaglia[18], J. Strandberg[149],
S. Strandberg[148a,148b], M. Strauss[115], P. Strizenec[146b], R. Ströhmer[177], D.M. Strom[118],

R. Stroynowski[43], A. Strubig[49], S.A. Stucci[27], B. Stugu[15], N.A. Styles[45], D. Su[145], J. Su[127],
S. Suchek[60a], Y. Sugaya[120], M. Suk[130], V.V. Sulin[98], DMS Sultan[162a,162b], S. Sultansoy[4c],
T. Sumida[71], S. Sun[59], X. Sun[3], K. Suruliz[151], C.J.E. Suster[152], M.R. Sutton[151], S. Suzuki[69],
M. Svatos[129], M. Swiatlowski[33], S.P. Swift[2], I. Sykora[146a], T. Sykora[131], D. Ta[51],
K. Tackmann[45], J. Taenzer[155], A. Taffard[166], R. Tafirout[163a], E. Tahirovic[79], N. Taiblum[155],
H. Takai[27], R. Takashima[72], E.H. Takasugi[103], T. Takeshita[142], Y. Takubo[69], M. Talby[88],
A.A. Talyshev[111,c], J. Tanaka[157], M. Tanaka[159], R. Tanaka[119], S. Tanaka[69], R. Tanioka[70],
B.B. Tannenwald[113], S. Tapia Araya[34b], S. Tapprogge[86], S. Tarem[154], G.F. Tartarelli[94a],
P. Tas[131], M. Tasevsky[129], T. Tashiro[71], E. Tassi[40a,40b], A. Tavares Delgado[128a,128b],
Y. Tayalati[137e], A.C. Taylor[107], A.J. Taylor[49], G.N. Taylor[91], P.T.E. Taylor[91], W. Taylor[163b],
P. Teixeira-Dias[80], D. Temple[144], H. Ten Kate[32], P.K. Teng[153], J.J. Teoh[120], F. Tepel[178],
S. Terada[69], K. Terashi[157], J. Terron[85], S. Terzo[13], M. Testa[50], R.J. Teuscher[161,o],
T. Theveneaux-Pelzer[88], F. Thiele[39], J.P. Thomas[19], J. Thomas-Wilsker[80], P.D. Thompson[19],
A.S. Thompson[56], L.A. Thomsen[179], E. Thomson[124], M.J. Tibbetts[16], R.E. Ticse Torres[88],
V.O. Tikhomirov[98,ap], Yu.A. Tikhonov[111,c], S. Timoshenko[100], P. Tipton[179], S. Tisserant[88],
K. Todome[159], S. Todorova-Nova[5], S. Todt[47], J. Tojo[73], S. Tokár[146a], K. Tokushuku[69],
E. Tolley[59], L. Tomlinson[87], M. Tomoto[105], L. Tompkins[145,aq], K. Toms[107], B. Tong[59],
P. Tornambe[51], E. Torrence[118], H. Torres[47], E. Torró Pastor[140], J. Toth[88,ar], F. Touchard[88],
D.R. Tovey[141], C.J. Treado[112], T. Trefzger[177], F. Tresoldi[151], A. Tricoli[27], I.M. Trigger[163a],
S. Trincaz-Duvoid[83], M.F. Tripiana[13], W. Trischuk[161], B. Trocmé[58], A. Trofymov[45],
C. Troncon[94a], M. Trottier-McDonald[16], M. Trovatelli[172], L. Truong[147b], M. Trzebinski[42],
A. Trzupek[42], K.W. Tsang[62a], J.C-L. Tseng[122], P.V. Tsiareshka[95], G. Tsipolitis[10],
N. Tsirintanis[9], S. Tsiskaridze[13], V. Tsiskaridze[51], E.G. Tskhadadze[54a], K.M. Tsui[62a],
I.I. Tsukerman[99], V. Tsulaia[16], S. Tsuno[69], D. Tsybychev[150], Y. Tu[62b], A. Tudorache[28b],
V. Tudorache[28b], T.T. Tulbure[28a], A.N. Tuna[59], S.A. Tupputi[22a,22b], S. Turchikhin[68],
D. Turgeman[175], I. Turk Cakir[4b,as], R. Turra[94a], P.M. Tuts[38], G. Ucchielli[22a,22b], I. Ueda[69],
M. Ughetto[148a,148b], F. Ukegawa[164], G. Unal[32], A. Undrus[27], G. Unel[166], F.C. Ungaro[91],
Y. Unno[69], C. Unverdorben[102], J. Urban[146b], P. Urquijo[91], P. Urrejola[86], G. Usai[8], J. Usui[69],
L. Vacavant[88], V. Vacek[130], B. Vachon[90], K.O.H. Vadla[121], A. Vaidya[81], C. Valderanis[102],
E. Valdes Santurio[148a,148b], M. Valente[52], S. Valentinetti[22a,22b], A. Valero[170], L. Valéry[13],
S. Valkar[131], A. Vallier[5], J.A. Valls Ferrer[170], W. Van Den Wollenberg[109], H. van der Graaf[109],
P. van Gemmeren[6], J. Van Nieuwkoop[144], I. van Vulpen[109], M.C. van Woerden[109],
M. Vanadia[135a,135b], W. Vandelli[32], A. Vaniachine[160], P. Vankov[109], G. Vardanyan[180],
R. Vari[134a], E.W. Varnes[7], C. Varni[53a,53b], T. Varol[43], D. Varouchas[119], A. Vartapetian[8],
K.E. Varvell[152], J.G. Vasquez[179], G.A. Vasquez[34b], F. Vazeille[37], D. Vazquez Furelos[13],
T. Vazquez Schroeder[90], J. Veatch[57], V. Veeraraghavan[7], L.M. Veloce[161], F. Veloso[128a,128c],
S. Veneziano[134a], A. Ventura[76a,76b], M. Venturi[172], N. Venturi[32], A. Venturini[25], V. Vercesi[123a],
M. Verducci[136a,136b], W. Verkerke[109], A.T. Vermeulen[109], J.C. Vermeulen[109], M.C. Vetterli[144,d],
N. Viaux Maira[34b], O. Viazlo[84], I. Vichou[169,*], T. Vickey[141], O.E. Vickey Boeriu[141],
G.H.A. Viehhauser[122], S. Viel[16], L. Vigani[122], M. Villa[22a,22b], M. Villaplana Perez[94a,94b],
E. Vilucchi[50], M.G. Vincter[31], V.B. Vinogradov[68], A. Vishwakarma[45], C. Vittori[22a,22b],
I. Vivarelli[151], S. Vlachos[10], M. Vogel[178], P. Vokac[130], G. Volpi[13], H. von der Schmitt[103],
E. von Toerne[23], V. Vorobel[131], K. Vorobev[100], M. Vos[170], R. Voss[32], J.H. Vossebeld[77],
N. Vranjes[14], M. Vranjes Milosavljevic[14], V. Vrba[130], M. Vreeswijk[109], R. Vuillermet[32],
I. Vukotic[33], P. Wagner[23], W. Wagner[178], J. Wagner-Kuhr[102], H. Wahlberg[74], S. Wahrmund[47],
J. Walder[75], R. Walker[102], W. Walkowiak[143], V. Wallangen[148a,148b], C. Wang[35b], C. Wang[36b,at],
F. Wang[176], H. Wang[16], H. Wang[3], J. Wang[45], J. Wang[152], Q. Wang[115], R.-J. Wang[83],
R. Wang[6], S.M. Wang[153], T. Wang[38], W. Wang[153,au], W. Wang[36a], Z. Wang[36c],

C. Wanotayaroj[45], A. Warburton[90], C.P. Ward[30], D.R. Wardrope[81], A. Washbrook[49],
P.M. Watkins[19], A.T. Watson[19], M.F. Watson[19], G. Watts[140], S. Watts[87], B.M. Waugh[81],
A.F. Webb[11], S. Webb[86], M.S. Weber[18], S.W. Weber[177], S.A. Weber[31], J.S. Webster[6],
A.R. Weidberg[122], B. Weinert[64], J. Weingarten[57], M. Weirich[86], C. Weiser[51], H. Weits[109],
P.S. Wells[32], T. Wenaus[27], T. Wengler[32], S. Wenig[32], N. Wermes[23], M.D. Werner[67], P. Werner[32],
M. Wessels[60a], T.D. Weston[18], K. Whalen[118], N.L. Whallon[140], A.M. Wharton[75], A.S. White[92],
A. White[8], M.J. White[1], R. White[34b], D. Whiteson[166], B.W. Whitmore[75], F.J. Wickens[133],
W. Wiedenmann[176], M. Wielers[133], C. Wiglesworth[39], L.A.M. Wiik-Fuchs[51], A. Wildauer[103],
F. Wilk[87], H.G. Wilkens[32], H.H. Williams[124], S. Williams[109], C. Willis[93], S. Willocq[89],
J.A. Wilson[19], I. Wingerter-Seez[5], E. Winkels[151], F. Winklmeier[118], O.J. Winston[151],
B.T. Winter[23], M. Wittgen[145], M. Wobisch[82,u], T.M.H. Wolf[109], R. Wolff[88], M.W. Wolter[42],
H. Wolters[128a,128c], V.W.S. Wong[171], S.D. Worm[19], B.K. Wosiek[42], J. Wotschack[32],
K.W. Wozniak[42], M. Wu[33], S.L. Wu[176], X. Wu[52], Y. Wu[92], T.R. Wyatt[87], B.M. Wynne[49],
S. Xella[39], Z. Xi[92], L. Xia[35c], D. Xu[35a], L. Xu[27], T. Xu[138], B. Yabsley[152], S. Yacoob[147a],
D. Yamaguchi[159], Y. Yamaguchi[159], A. Yamamoto[69], S. Yamamoto[157], T. Yamanaka[157],
F. Yamane[70], M. Yamatani[157], Y. Yamazaki[70], Z. Yan[24], H. Yang[36c], H. Yang[16], Y. Yang[153],
Z. Yang[15], W-M. Yao[16], Y.C. Yap[45], Y. Yasu[69], E. Yatsenko[5], K.H. Yau Wong[23], J. Ye[43],
S. Ye[27], I. Yeletskikh[68], E. Yigitbasi[24], E. Yildirim[86], K. Yorita[174], K. Yoshihara[124], C. Young[145],
C.J.S. Young[32], J. Yu[8], J. Yu[67], S.P.Y. Yuen[23], I. Yusuff[30,av], B. Zabinski[42], G. Zacharis[10],
R. Zaidan[13], A.M. Zaitsev[132,aj], N. Zakharchuk[45], J. Zalieckas[15], A. Zaman[150], S. Zambito[59],
D. Zanzi[91], C. Zeitnitz[178], G. Zemaityte[122], A. Zemla[41a], J.C. Zeng[169], Q. Zeng[145], O. Zenin[132],
T. Ženiš[146a], D. Zerwas[119], D. Zhang[36b], D. Zhang[92], F. Zhang[176], G. Zhang[36a,aw], H. Zhang[119],
J. Zhang[6], L. Zhang[51], L. Zhang[36a], M. Zhang[169], P. Zhang[35b], R. Zhang[23], R. Zhang[36a,at],
X. Zhang[36b], Y. Zhang[35a], Z. Zhang[119], X. Zhao[43], Y. Zhao[36b,ax], Z. Zhao[36a], A. Zhemchugov[68],
B. Zhou[92], C. Zhou[176], L. Zhou[43], M. Zhou[35a], M. Zhou[150], N. Zhou[35c], C.G. Zhu[36b], H. Zhu[35a],
J. Zhu[92], Y. Zhu[36a], X. Zhuang[35a], K. Zhukov[98], A. Zibell[177], D. Zieminska[64], N.I. Zimine[68],
C. Zimmermann[86], S. Zimmermann[51], Z. Zinonos[103], M. Zinser[86], M. Ziolkowski[143],
L. Živković[14], G. Zobernig[176], A. Zoccoli[22a,22b], R. Zou[33], M. zur Nedden[17], L. Zwalinski[32]

1   Department of Physics, University of Adelaide, Adelaide, Australia
2   Physics Department, SUNY Albany, Albany NY, United States of America
3   Department of Physics, University of Alberta, Edmonton AB, Canada
4   (a) Department of Physics, Ankara University, Ankara; (b) Istanbul Aydin University, Istanbul; (c)
    Division of Physics, TOBB University of Economics and Technology, Ankara, Turkey
5   LAPP, CNRS/IN2P3 and Université Savoie Mont Blanc, Annecy-le-Vieux, France
6   High Energy Physics Division, Argonne National Laboratory, Argonne IL, United States of America
7   Department of Physics, University of Arizona, Tucson AZ, United States of America
8   Department of Physics, The University of Texas at Arlington, Arlington TX, United States of
    America
9   Physics Department, National and Kapodistrian University of Athens, Athens, Greece
10 Physics Department, National Technical University of Athens, Zografou, Greece
11 Department of Physics, The University of Texas at Austin, Austin TX, United States of America
12 Institute of Physics, Azerbaijan Academy of Sciences, Baku, Azerbaijan
13 Institut de Física d'Altes Energies (IFAE), The Barcelona Institute of Science and Technology,
    Barcelona, Spain
14 Institute of Physics, University of Belgrade, Belgrade, Serbia
15 Department for Physics and Technology, University of Bergen, Bergen, Norway
16 Physics Division, Lawrence Berkeley National Laboratory and University of California, Berkeley
    CA, United States of America

17 Department of Physics, Humboldt University, Berlin, Germany

18 Albert Einstein Center for Fundamental Physics and Laboratory for High Energy Physics, University of Bern, Bern, Switzerland

19 School of Physics and Astronomy, University of Birmingham, Birmingham, United Kingdom

20 (a) Department of Physics, Bogazici University, Istanbul; (b) Department of Physics Engineering, Gaziantep University, Gaziantep; (d) Istanbul Bilgi University, Faculty of Engineering and Natural Sciences, Istanbul; (e) Bahcesehir University, Faculty of Engineering and Natural Sciences, Istanbul, Turkey

21 Centro de Investigaciones, Universidad Antonio Narino, Bogota, Colombia

22 (a) INFN Sezione di Bologna; (b) Dipartimento di Fisica e Astronomia, Università di Bologna, Bologna, Italy

23 Physikalisches Institut, University of Bonn, Bonn, Germany

24 Department of Physics, Boston University, Boston MA, United States of America

25 Department of Physics, Brandeis University, Waltham MA, United States of America

26 (a) Universidade Federal do Rio De Janeiro COPPE/EE/IF, Rio de Janeiro; (b) Electrical Circuits Department, Federal University of Juiz de Fora (UFJF), Juiz de Fora; (c) Federal University of Sao Joao del Rei (UFSJ), Sao Joao del Rei; (d) Instituto de Fisica, Universidade de Sao Paulo, Sao Paulo, Brazil

27 Physics Department, Brookhaven National Laboratory, Upton NY, United States of America

28 (a) Transilvania University of Brasov, Brasov; (b) Horia Hulubei National Institute of Physics and Nuclear Engineering, Bucharest; (c) Department of Physics, Alexandru Ioan Cuza University of Iasi, Iasi; (d) National Institute for Research and Development of Isotopic and Molecular Technologies, Physics Department, Cluj Napoca; (e) University Politehnica Bucharest, Bucharest; (f) West University in Timisoara, Timisoara, Romania

29 Departamento de Física, Universidad de Buenos Aires, Buenos Aires, Argentina

30 Cavendish Laboratory, University of Cambridge, Cambridge, United Kingdom

31 Department of Physics, Carleton University, Ottawa ON, Canada

32 CERN, Geneva, Switzerland

33 Enrico Fermi Institute, University of Chicago, Chicago IL, United States of America

34 (a) Departamento de Física, Pontificia Universidad Católica de Chile, Santiago; (b) Departamento de Física, Universidad Técnica Federico Santa María, Valparaíso, Chile

35 (a) Institute of High Energy Physics, Chinese Academy of Sciences, Beijing; (b) Department of Physics, Nanjing University, Jiangsu; (c) Physics Department, Tsinghua University, Beijing 100084, China

36 (a) Department of Modern Physics and State Key Laboratory of Particle Detection and Electronics, University of Science and Technology of China, Anhui; (b) School of Physics, Shandong University, Shandong; (c) Department of Physics and Astronomy, Key Laboratory for Particle Physics, Astrophysics and Cosmology, Ministry of Education; Shanghai Key Laboratory for Particle Physics and Cosmology, Shanghai Jiao Tong University, Shanghai(also at PKU-CHEP), China

37 Université Clermont Auvergne, CNRS/IN2P3, LPC, Clermont-Ferrand, France

38 Nevis Laboratory, Columbia University, Irvington NY, United States of America

39 Niels Bohr Institute, University of Copenhagen, Kobenhavn, Denmark

40 (a) INFN Gruppo Collegato di Cosenza, Laboratori Nazionali di Frascati; (b) Dipartimento di Fisica, Università della Calabria, Rende, Italy

41 (a) AGH University of Science and Technology, Faculty of Physics and Applied Computer Science, Krakow; (b) Marian Smoluchowski Institute of Physics, Jagiellonian University, Krakow, Poland

42 Institute of Nuclear Physics Polish Academy of Sciences, Krakow, Poland

43 Physics Department, Southern Methodist University, Dallas TX, United States of America

44 Physics Department, University of Texas at Dallas, Richardson TX, United States of America

45 DESY, Hamburg and Zeuthen, Germany

46 Lehrstuhl für Experimentelle Physik IV, Technische Universität Dortmund, Dortmund, Germany

47 Institut für Kern- und Teilchenphysik, Technische Universität Dresden, Dresden, Germany

48 *Department of Physics, Duke University, Durham NC, United States of America*

49 *SUPA - School of Physics and Astronomy, University of Edinburgh, Edinburgh, United Kingdom*

50 *INFN e Laboratori Nazionali di Frascati, Frascati, Italy*

51 *Fakultät für Mathematik und Physik, Albert-Ludwigs-Universität, Freiburg, Germany*

52 *Departement de Physique Nucleaire et Corpusculaire, Université de Genève, Geneva, Switzerland*

53 [a] *INFN Sezione di Genova;* [b] *Dipartimento di Fisica, Università di Genova, Genova, Italy*

54 [a] *E. Andronikashvili Institute of Physics, Iv. Javakhishvili Tbilisi State University, Tbilisi;* [b] *High Energy Physics Institute, Tbilisi State University, Tbilisi, Georgia*

55 *II Physikalisches Institut, Justus-Liebig-Universität Giessen, Giessen, Germany*

56 *SUPA - School of Physics and Astronomy, University of Glasgow, Glasgow, United Kingdom*

57 *II Physikalisches Institut, Georg-August-Universität, Göttingen, Germany*

58 *Laboratoire de Physique Subatomique et de Cosmologie, Université Grenoble-Alpes, CNRS/IN2P3, Grenoble, France*

59 *Laboratory for Particle Physics and Cosmology, Harvard University, Cambridge MA, United States of America*

60 [a] *Kirchhoff-Institut für Physik, Ruprecht-Karls-Universität Heidelberg, Heidelberg;* [b] *Physikalisches Institut, Ruprecht-Karls-Universität Heidelberg, Heidelberg, Germany*

61 *Faculty of Applied Information Science, Hiroshima Institute of Technology, Hiroshima, Japan*

62 [a] *Department of Physics, The Chinese University of Hong Kong, Shatin, N.T., Hong Kong;* [b] *Department of Physics, The University of Hong Kong, Hong Kong;* [c] *Department of Physics and Institute for Advanced Study, The Hong Kong University of Science and Technology, Clear Water Bay, Kowloon, Hong Kong, China*

63 *Department of Physics, National Tsing Hua University, Taiwan*

64 *Department of Physics, Indiana University, Bloomington IN, United States of America*

65 *Institut für Astro- und Teilchenphysik, Leopold-Franzens-Universität, Innsbruck, Austria*

66 *University of Iowa, Iowa City IA, United States of America*

67 *Department of Physics and Astronomy, Iowa State University, Ames IA, United States of America*

68 *Joint Institute for Nuclear Research, JINR Dubna, Dubna, Russia*

69 *KEK, High Energy Accelerator Research Organization, Tsukuba, Japan*

70 *Graduate School of Science, Kobe University, Kobe, Japan*

71 *Faculty of Science, Kyoto University, Kyoto, Japan*

72 *Kyoto University of Education, Kyoto, Japan*

73 *Research Center for Advanced Particle Physics and Department of Physics, Kyushu University, Fukuoka, Japan*

74 *Instituto de Física La Plata, Universidad Nacional de La Plata and CONICET, La Plata, Argentina*

75 *Physics Department, Lancaster University, Lancaster, United Kingdom*

76 [a] *INFN Sezione di Lecce;* [b] *Dipartimento di Matematica e Fisica, Università del Salento, Lecce, Italy*

77 *Oliver Lodge Laboratory, University of Liverpool, Liverpool, United Kingdom*

78 *Department of Experimental Particle Physics, Jožef Stefan Institute and Department of Physics, University of Ljubljana, Ljubljana, Slovenia*

79 *School of Physics and Astronomy, Queen Mary University of London, London, United Kingdom*

80 *Department of Physics, Royal Holloway University of London, Surrey, United Kingdom*

81 *Department of Physics and Astronomy, University College London, London, United Kingdom*

82 *Louisiana Tech University, Ruston LA, United States of America*

83 *Laboratoire de Physique Nucléaire et de Hautes Energies, UPMC and Université Paris-Diderot and CNRS/IN2P3, Paris, France*

84 *Fysiska institutionen, Lunds universitet, Lund, Sweden*

85 *Departamento de Fisica Teorica C-15, Universidad Autonoma de Madrid, Madrid, Spain*

86 *Institut für Physik, Universität Mainz, Mainz, Germany*

87 *School of Physics and Astronomy, University of Manchester, Manchester, United Kingdom*

[88] *CPPM, Aix-Marseille Université and CNRS/IN2P3, Marseille, France*

[89] *Department of Physics, University of Massachusetts, Amherst MA, United States of America*

[90] *Department of Physics, McGill University, Montreal QC, Canada*

[91] *School of Physics, University of Melbourne, Victoria, Australia*

[92] *Department of Physics, The University of Michigan, Ann Arbor MI, United States of America*

[93] *Department of Physics and Astronomy, Michigan State University, East Lansing MI, United States of America*

[94] *[(a)] INFN Sezione di Milano; [(b)] Dipartimento di Fisica, Università di Milano, Milano, Italy*

[95] *B.I. Stepanov Institute of Physics, National Academy of Sciences of Belarus, Minsk, Republic of Belarus*

[96] *Research Institute for Nuclear Problems of Byelorussian State University, Minsk, Republic of Belarus*

[97] *Group of Particle Physics, University of Montreal, Montreal QC, Canada*

[98] *P.N. Lebedev Physical Institute of the Russian Academy of Sciences, Moscow, Russia*

[99] *Institute for Theoretical and Experimental Physics (ITEP), Moscow, Russia*

[100] *National Research Nuclear University MEPhI, Moscow, Russia*

[101] *D.V. Skobeltsyn Institute of Nuclear Physics, M.V. Lomonosov Moscow State University, Moscow, Russia*

[102] *Fakultät für Physik, Ludwig-Maximilians-Universität München, München, Germany*

[103] *Max-Planck-Institut für Physik (Werner-Heisenberg-Institut), München, Germany*

[104] *Nagasaki Institute of Applied Science, Nagasaki, Japan*

[105] *Graduate School of Science and Kobayashi-Maskawa Institute, Nagoya University, Nagoya, Japan*

[106] *[(a)] INFN Sezione di Napoli; [(b)] Dipartimento di Fisica, Università di Napoli, Napoli, Italy*

[107] *Department of Physics and Astronomy, University of New Mexico, Albuquerque NM, United States of America*

[108] *Institute for Mathematics, Astrophysics and Particle Physics, Radboud University Nijmegen/Nikhef, Nijmegen, Netherlands*

[109] *Nikhef National Institute for Subatomic Physics and University of Amsterdam, Amsterdam, Netherlands*

[110] *Department of Physics, Northern Illinois University, DeKalb IL, United States of America*

[111] *Budker Institute of Nuclear Physics, SB RAS, Novosibirsk, Russia*

[112] *Department of Physics, New York University, New York NY, United States of America*

[113] *Ohio State University, Columbus OH, United States of America*

[114] *Faculty of Science, Okayama University, Okayama, Japan*

[115] *Homer L. Dodge Department of Physics and Astronomy, University of Oklahoma, Norman OK, United States of America*

[116] *Department of Physics, Oklahoma State University, Stillwater OK, United States of America*

[117] *Palacký University, RCPTM, Olomouc, Czech Republic*

[118] *Center for High Energy Physics, University of Oregon, Eugene OR, United States of America*

[119] *LAL, Univ. Paris-Sud, CNRS/IN2P3, Université Paris-Saclay, Orsay, France*

[120] *Graduate School of Science, Osaka University, Osaka, Japan*

[121] *Department of Physics, University of Oslo, Oslo, Norway*

[122] *Department of Physics, Oxford University, Oxford, United Kingdom*

[123] *[(a)] INFN Sezione di Pavia; [(b)] Dipartimento di Fisica, Università di Pavia, Pavia, Italy*

[124] *Department of Physics, University of Pennsylvania, Philadelphia PA, United States of America*

[125] *National Research Centre "Kurchatov Institute" B.P.Konstantinov Petersburg Nuclear Physics Institute, St. Petersburg, Russia*

[126] *[(a)] INFN Sezione di Pisa; [(b)] Dipartimento di Fisica E. Fermi, Università di Pisa, Pisa, Italy*

[127] *Department of Physics and Astronomy, University of Pittsburgh, Pittsburgh PA, United States of America*

128 (a) *Laboratório de Instrumentação e Física Experimental de Partículas - LIP, Lisboa;* (b) *Faculdade de Ciências, Universidade de Lisboa, Lisboa;* (c) *Department of Physics, University of Coimbra, Coimbra;* (d) *Centro de Física Nuclear da Universidade de Lisboa, Lisboa;* (e) *Departamento de Fisica, Universidade do Minho, Braga;* (f) *Departamento de Fisica Teorica y del Cosmos, Universidad de Granada, Granada;* (g) *Dep Fisica and CEFITEC of Faculdade de Ciencias e Tecnologia, Universidade Nova de Lisboa, Caparica, Portugal*

129 *Institute of Physics, Academy of Sciences of the Czech Republic, Praha, Czech Republic*

130 *Czech Technical University in Prague, Praha, Czech Republic*

131 *Charles University, Faculty of Mathematics and Physics, Prague, Czech Republic*

132 *State Research Center Institute for High Energy Physics (Protvino), NRC KI, Russia*

133 *Particle Physics Department, Rutherford Appleton Laboratory, Didcot, United Kingdom*

134 (a) *INFN Sezione di Roma;* (b) *Dipartimento di Fisica, Sapienza Università di Roma, Roma, Italy*

135 (a) *INFN Sezione di Roma Tor Vergata;* (b) *Dipartimento di Fisica, Università di Roma Tor Vergata, Roma, Italy*

136 (a) *INFN Sezione di Roma Tre;* (b) *Dipartimento di Matematica e Fisica, Università Roma Tre, Roma, Italy*

137 (a) *Faculté des Sciences Ain Chock, Réseau Universitaire de Physique des Hautes Energies - Université Hassan II, Casablanca;* (b) *Centre National de l'Energie des Sciences Techniques Nucleaires, Rabat;* (c) *Faculté des Sciences Semlalia, Université Cadi Ayyad, LPHEA-Marrakech;* (d) *Faculté des Sciences, Université Mohamed Premier and LPTPM, Oujda;* (e) *Faculté des sciences, Université Mohammed V, Rabat, Morocco*

138 *DSM/IRFU (Institut de Recherches sur les Lois Fondamentales de l'Univers), CEA Saclay (Commissariat à l'Energie Atomique et aux Energies Alternatives), Gif-sur-Yvette, France*

139 *Santa Cruz Institute for Particle Physics, University of California Santa Cruz, Santa Cruz CA, United States of America*

140 *Department of Physics, University of Washington, Seattle WA, United States of America*

141 *Department of Physics and Astronomy, University of Sheffield, Sheffield, United Kingdom*

142 *Department of Physics, Shinshu University, Nagano, Japan*

143 *Department Physik, Universität Siegen, Siegen, Germany*

144 *Department of Physics, Simon Fraser University, Burnaby BC, Canada*

145 *SLAC National Accelerator Laboratory, Stanford CA, United States of America*

146 (a) *Faculty of Mathematics, Physics & Informatics, Comenius University, Bratislava;* (b) *Department of Subnuclear Physics, Institute of Experimental Physics of the Slovak Academy of Sciences, Kosice, Slovak Republic*

147 (a) *Department of Physics, University of Cape Town, Cape Town;* (b) *Department of Physics, University of Johannesburg, Johannesburg;* (c) *School of Physics, University of the Witwatersrand, Johannesburg, South Africa*

148 (a) *Department of Physics, Stockholm University;* (b) *The Oskar Klein Centre, Stockholm, Sweden*

149 *Physics Department, Royal Institute of Technology, Stockholm, Sweden*

150 *Departments of Physics & Astronomy and Chemistry, Stony Brook University, Stony Brook NY, United States of America*

151 *Department of Physics and Astronomy, University of Sussex, Brighton, United Kingdom*

152 *School of Physics, University of Sydney, Sydney, Australia*

153 *Institute of Physics, Academia Sinica, Taipei, Taiwan*

154 *Department of Physics, Technion: Israel Institute of Technology, Haifa, Israel*

155 *Raymond and Beverly Sackler School of Physics and Astronomy, Tel Aviv University, Tel Aviv, Israel*

156 *Department of Physics, Aristotle University of Thessaloniki, Thessaloniki, Greece*

157 *International Center for Elementary Particle Physics and Department of Physics, The University of Tokyo, Tokyo, Japan*

158 *Graduate School of Science and Technology, Tokyo Metropolitan University, Tokyo, Japan*

159 *Department of Physics, Tokyo Institute of Technology, Tokyo, Japan*

160   *Tomsk State University, Tomsk, Russia*

161   *Department of Physics, University of Toronto, Toronto ON, Canada*

162   *(a) INFN-TIFPA; (b) University of Trento, Trento, Italy*

163   *(a) TRIUMF, Vancouver BC; (b) Department of Physics and Astronomy, York University, Toronto ON, Canada*

164   *Faculty of Pure and Applied Sciences, and Center for Integrated Research in Fundamental Science and Engineering, University of Tsukuba, Tsukuba, Japan*

165   *Department of Physics and Astronomy, Tufts University, Medford MA, United States of America*

166   *Department of Physics and Astronomy, University of California Irvine, Irvine CA, United States of America*

167   *(a) INFN Gruppo Collegato di Udine, Sezione di Trieste, Udine; (b) ICTP, Trieste; (c) Dipartimento di Chimica, Fisica e Ambiente, Università di Udine, Udine, Italy*

168   *Department of Physics and Astronomy, University of Uppsala, Uppsala, Sweden*

169   *Department of Physics, University of Illinois, Urbana IL, United States of America*

170   *Instituto de Fisica Corpuscular (IFIC), Centro Mixto Universidad de Valencia - CSIC, Spain*

171   *Department of Physics, University of British Columbia, Vancouver BC, Canada*

172   *Department of Physics and Astronomy, University of Victoria, Victoria BC, Canada*

173   *Department of Physics, University of Warwick, Coventry, United Kingdom*

174   *Waseda University, Tokyo, Japan*

175   *Department of Particle Physics, The Weizmann Institute of Science, Rehovot, Israel*

176   *Department of Physics, University of Wisconsin, Madison WI, United States of America*

177   *Fakultät für Physik und Astronomie, Julius-Maximilians-Universität, Würzburg, Germany*

178   *Fakultät für Mathematik und Naturwissenschaften, Fachgruppe Physik, Bergische Universität Wuppertal, Wuppertal, Germany*

179   *Department of Physics, Yale University, New Haven CT, United States of America*

180   *Yerevan Physics Institute, Yerevan, Armenia*

181   *Centre de Calcul de l'Institut National de Physique Nucléaire et de Physique des Particules (IN2P3), Villeurbanne, France*

182   *Academia Sinica Grid Computing, Institute of Physics, Academia Sinica, Taipei, Taiwan*

[a]   *Also at Department of Physics, King's College London, London, United Kingdom*

[b]   *Also at Institute of Physics, Azerbaijan Academy of Sciences, Baku, Azerbaijan*

[c]   *Also at Novosibirsk State University, Novosibirsk, Russia*

[d]   *Also at TRIUMF, Vancouver BC, Canada*

[e]   *Also at Department of Physics & Astronomy, University of Louisville, Louisville, KY, United States of America*

[f]   *Also at Physics Department, An-Najah National University, Nablus, Palestine*

[g]   *Also at Department of Physics, California State University, Fresno CA, United States of America*

[h]   *Also at Department of Physics, University of Fribourg, Fribourg, Switzerland*

[i]   *Also at II Physikalisches Institut, Georg-August-Universität, Göttingen, Germany*

[j]   *Also at Departament de Fisica de la Universitat Autonoma de Barcelona, Barcelona, Spain*

[k]   *Also at Departamento de Fisica e Astronomia, Faculdade de Ciencias, Universidade do Porto, Portugal*

[l]   *Also at Tomsk State University, Tomsk, and Moscow Institute of Physics and Technology State University, Dolgoprudny, Russia*

[m]   *Also at The Collaborative Innovation Center of Quantum Matter (CICQM), Beijing, China*

[n]   *Also at Universita di Napoli Parthenope, Napoli, Italy*

[o]   *Also at Institute of Particle Physics (IPP), Canada*

[p]   *Also at Horia Hulubei National Institute of Physics and Nuclear Engineering, Bucharest, Romania*

[q]   *Also at Department of Physics, St. Petersburg State Polytechnical University, St. Petersburg, Russia*

[r] Also at Borough of Manhattan Community College, City University of New York, New York City, United States of America

[s] Also at Department of Financial and Management Engineering, University of the Aegean, Chios, Greece

[t] Also at Centre for High Performance Computing, CSIR Campus, Rosebank, Cape Town, South Africa

[u] Also at Louisiana Tech University, Ruston LA, United States of America

[v] Also at Institucio Catalana de Recerca i Estudis Avancats, ICREA, Barcelona, Spain

[w] Also at Graduate School of Science, Osaka University, Osaka, Japan

[x] Also at Fakultät für Mathematik und Physik, Albert-Ludwigs-Universität, Freiburg, Germany

[y] Also at Institute for Mathematics, Astrophysics and Particle Physics, Radboud University Nijmegen/Nikhef, Nijmegen, Netherlands

[z] Also at Department of Physics, The University of Texas at Austin, Austin TX, United States of America

[aa] Also at Institute of Theoretical Physics, Ilia State University, Tbilisi, Georgia

[ab] Also at CERN, Geneva, Switzerland

[ac] Also at Georgian Technical University (GTU),Tbilisi, Georgia

[ad] Also at Ochadai Academic Production, Ochanomizu University, Tokyo, Japan

[ae] Also at Manhattan College, New York NY, United States of America

[af] Also at Department of Physics, The University of Michigan, Ann Arbor MI, United States of America

[ag] Also at The City College of New York, New York NY, United States of America

[ah] Also at Departamento de Fisica Teorica y del Cosmos, Universidad de Granada, Granada, Portugal

[ai] Also at Department of Physics, California State University, Sacramento CA, United States of America

[aj] Also at Moscow Institute of Physics and Technology State University, Dolgoprudny, Russia

[ak] Also at Departement de Physique Nucleaire et Corpusculaire, Université de Genève, Geneva, Switzerland

[al] Also at Institut de Física d'Altes Energies (IFAE), The Barcelona Institute of Science and Technology, Barcelona, Spain

[am] Also at School of Physics, Sun Yat-sen University, Guangzhou, China

[an] Also at Institute for Nuclear Research and Nuclear Energy (INRNE) of the Bulgarian Academy of Sciences, Sofia, Bulgaria

[ao] Also at Faculty of Physics, M.V.Lomonosov Moscow State University, Moscow, Russia

[ap] Also at National Research Nuclear University MEPhI, Moscow, Russia

[aq] Also at Department of Physics, Stanford University, Stanford CA, United States of America

[ar] Also at Institute for Particle and Nuclear Physics, Wigner Research Centre for Physics, Budapest, Hungary

[as] Also at Giresun University, Faculty of Engineering, Turkey

[at] Also at CPPM, Aix-Marseille Université and CNRS/IN2P3, Marseille, France

[au] Also at Department of Physics, Nanjing University, Jiangsu, China

[av] Also at University of Malaya, Department of Physics, Kuala Lumpur, Malaysia

[aw] Also at Institute of Physics, Academia Sinica, Taipei, Taiwan

[ax] Also at LAL, Univ. Paris-Sud, CNRS/IN2P3, Université Paris-Saclay, Orsay, France

[*] Deceased